Isotopic and Geochemical Tracers for Fingerprinting Process-Affected Waters in the Oil Sands Industry: A Pilot Study

J.J. Gibson, S.J. Birks, M. Moncur, Y. Yi, K. Tattrie, S. Jasechko, K. Richardson and P. Eby

Alberta Innovates – Technology Futures

April 2011

Oil Sands Research and Information Network

OSRIN is a university-based, independent organization that compiles, interprets and analyses available knowledge about returning landscapes and water impacted by oil sands mining to a natural state and gets that knowledge into the hands of those who can use it to drive breakthrough improvements in reclamation regulations and practices. OSRIN is a project of the University of Alberta's School of Energy and the Environment (SEE). OSRIN was launched with a start-up grant of $4.5 million from Alberta Environment and a $250,000 grant from the Canada School of Energy and Environment Ltd.

OSRIN provides:

- **Governments** with the independent, objective, credible information and analysis required to put appropriate regulatory and policy frameworks in place
- **Media, opinion leaders and the general public** with the facts about oil sands development, its environmental and social impacts, and landscape/water reclamation activities – so that public dialogue and policy is informed by solid evidence
- **Industry** with ready access to an integrated view of research that will help them make and execute reclamation plans – a view that crosses disciplines and organizational boundaries

OSRIN recognizes that much research has been done in these areas by a variety of players over 40 years of oil sands development. OSRIN synthesizes this collective knowledge and presents it in a form that allows others to use it to solve pressing problems. Where we identify knowledge gaps, we seek research partners to help fill them.

Citation

This report may be cited as:

Gibson, J.J., S.J. Birks, M. Moncur, Y. Yi, K. Tattrie, S. Jasechko, K. Richardson and P. Eby, 2011. *Isotopic and Geochemical Tracers for Fingerprinting Process-Affected Waters in the Oil Sands Industry: A Pilot Study*. Oil Sands Research and Information Network, University of Alberta, School of Energy and the Environment, Edmonton, Alberta. OSRIN Report No. TR-12. 109 pp.

Copies of this report may be obtained from OSRIN at osrin@ualberta.ca or through the OSRIN website at http://www.osrin.ualberta.ca/en/OSRINPublications.aspx or directly from the University of Alberta's Education & Research Archive at http://hdl.handle.net/10402/era.17507.

Table of Contents

LIST OF TABLES

LIST OF FIGURES

REPORT SUMMARY

A pilot study was conducted by Alberta Innovates – Technology Futures during 2009 and 2010 to assess potential for labelling process-affected water from oil sands operations using a suite of isotopic and geochemical tracers, including inorganic and organic compounds in water. The study was initiated in response to a request from Alberta Environment and grant funds for the project were obtained from the Oil Sands Research and Information Network, University of Alberta. Three oil sands operators participated in the study, providing logistical support and/or personnel to assist with on-lease water sampling. Alberta Environment and its consultants also provided support for sampling of groundwater. At the outset of the study, Worley Parsons was subcontracted to carry out a detailed electromagnetic survey of the Athabasca River from Fort McMurray to the confluence of the Firebag River, to map high conductivity seeps as potential targets for water sampling. While the priority of this first phase of the study was fingerprinting of water sources (i.e., tailings ponds vs. natural groundwater, lakes, and river water), the survey also sampled a selection of river bed seeps to test application of the methods to identify the origin of these waters near the point of discharge to the Athabasca River.

In total 39 samples were collected for this study. These included 8 process-affected water samples, 6 groundwater samples, 8 river bed seepage samples, and 15 river samples. A variety of isotope tracers were measured including oxygen-18 ($\delta^{18}O_{H2O}$) and deuterium ($\delta^{2}H_{H2O}$) in water, enriched tritium ($e^{3}H$) in water, carbon-13 in dissolved organic carbon ($\delta^{13}C_{DOC}$), carbon-13 and carbon-14 in dissolved inorganic carbon ($\delta^{13}C_{DIC}$, ^{14}C), sulfur-34 in dissolved sulfate ($\delta^{34}S_{SO4}$), chlorine-37 in dissolved chloride ($\delta^{37}Cl$), and strontium-87 versus strontium-86 ($^{87}Sr/^{86}Sr$) and boron-11 ($\delta^{11}B$) in dissolved solids. Geochemical analyses included major-, minor- and trace elements, a range of metals, nutrients and total organic carbon, as well as 113 priority pollutants and naphthenic acids. Fourier transform ion cyclotron resonance mass spectrometry (FT-ICR MS) was also used to scan for thousands of organic compounds in the water samples.

Overall, while selected isotopic and geochemical tracers were found to be definitive for labelling water sources in some locations, it is unreliable to attempt any universal labelling of water sources based solely on individual tracers or simple combinations of tracers. Understanding of the regional hydrogeological system, and interpretation of tracer variations in the context of a biogeochemical systems approach on a case by case basis offers the greatest potential for comprehensive understanding and labelling of water source and pathways. While limited in number of samples, the survey demonstrates the complimentary use of various fingerprinting techniques.

Preliminary evaluation of statistical approaches for differentiating various water types using inorganic, organic and combined datasets yielded promising results. These methods potentially offer multiple lines of evidence for fingerprinting and should be further evaluated, refined and applied as part of more comprehensive future investigations.

While organic and inorganic tracers were capable of fingerprinting process-affected water sources from different operators, identification of seep sources along the Athabasca River was

much more challenging due to the presence of complex water mixtures including groundwater and significant river water. The presence or absence of process-affected water in seeps along developed portions of the river remains to be verified and will require further baseline surveys.

FT-ICR MS offers capability to resolve thousands of organic compounds, and may be the simplest, most cost-effective approach to build a baseline dataset for use in identification of process-affected waters in the natural aquatic environment. A wide range of organic compounds are observed in process-affected water and these are not limited to naphthenic acids and hydrocarbons.

Further work to constrain sources, pathways and receptors of process-affected water needs to be undertaken. From a riverine perspective, synoptic surveys offer an integrative method for better understanding of evolution of the Athabasca River and tributaries as it may be affected by addition of both natural and potentially process-affected water.

We find no evidence of robust connections between tailings ponds and the river seeps that were sampled over the 125-km reach traversing the oil sands development area, although many seeps were not sampled. Although the seeps we did sample appear to be directly related to occurrence of natural groundwater seepage, we do not have enough evidence at this point to rule out the possibility that minor or trace amounts of process-affected water may be present in some of these seeps.

ACKNOWLEDGEMENTS

The Oil Sands Research and Information Network (OSRIN), School of Energy and the Environment (SEE), University of Alberta provided funding for this project.

The authors wish to thank Dr. Jun Han and Dr. Christoph Borchers, University of Victoria Proteomics Centre for guidance and expert advice on the application and interpretation of the FT-ICR MS results. Dr. Roger Foxall, Genome BC also played an important role in introducing us to the technique and its possible applications. Dr. Preston McEachern, Alberta Environment played a pivotal role in defining the scope and objectives of this pilot study, and was the catalyst for obtaining the financial support. These contributions are much appreciated. Thanks also to Dr. Andres Marandi, Tallinn University of Technology, Estonia and Carly Delavau, University of Manitoba, for reviewing the report and providing useful comments.

1 INTRODUCTION

This report summarizes the geochemical and isotopic results for a pilot study conducted by Alberta Innovates – Technology Futures (AITF; formerly Alberta Research Council) on behalf of the Oil Sands Research and Information Network (OSRIN), University of Alberta. The objective of this pilot study was to assess the ability of isotopic and geochemical tracers for fingerprinting the sources of process-affected water from a variety of oil sands operators in northeastern Alberta, and to compare these signatures to background concentrations in natural surface waters and groundwaters. By request from Alberta Environment (AENV), the ability to label and detect process-affected waters was also tested in a number of high conductivity groundwater seeps identified from an electromagnetic survey of the Athabasca River extending from Fort McMurray downstream to the Firebag River.

The seep sampling campaign targeted saline groundwater seeps in areas of high electrical conductivity previously mapped by WorleyParsons (2010) along a 125-km reach of the Athabasca River from Fort McMurray downstream to confluence of the Firebag River (Figure 1). This reach traverses the primary area of oil sands mining development. Groundwater seep sampling was carried out by AITF with isotopic and geochemical analysis performed by AITF and a variety of external laboratories. Several groundwater wells from the Alberta Groundwater Observation Well Network (GOWN) were also sampled as part of routine water testing programs by consultants retained by AENV. Selected groundwater samples, and their geochemical results were made available to AITF for the purposes of this study, and samples were subsequently analyzed for a range of organic compounds and isotope tracers by AITF and its external laboratories.

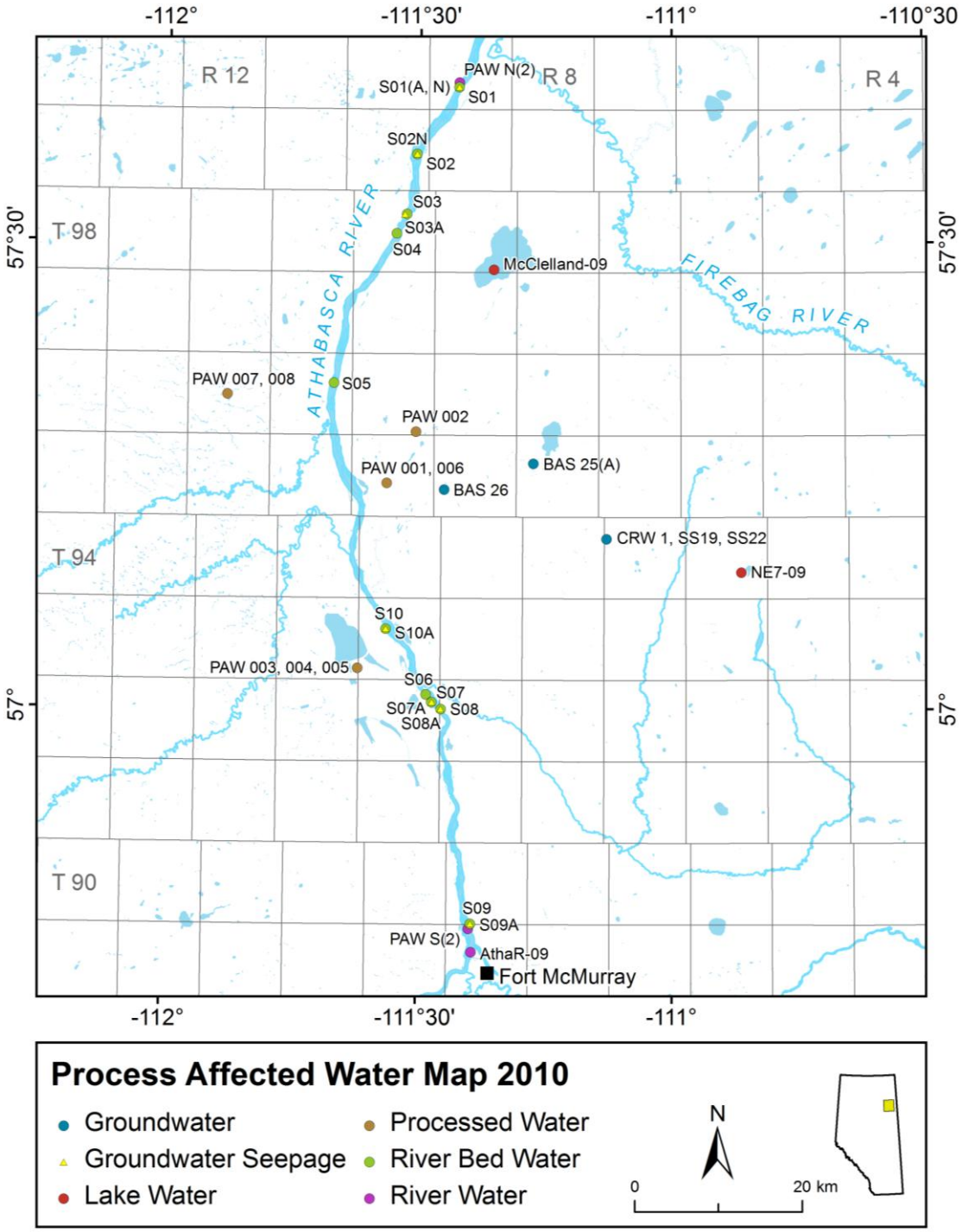

Figure 1. Map showing the locations of groundwater wells, seeps, process-affected water and surface water samples obtained for this study.
River Bed Water refers to water that was collected just above the river bottom sediment/surface water interface.

The sampling program was designed as a pilot study to test labelling properties of a comprehensive suite of isotopic and geochemical tracers for differentiating natural versus

anthropogenic contaminants, and for identifying and quantifying their presence in complex water mixtures. While the number of water samples collected and analyzed for each type of water was limited, this reconnaissance-level survey was designed to provide new insight and broader direction for ongoing research programs in the region that seek to assess potential for hydrologic connections between tailings ponds and rivers as a possible pathway for naphthenic acids and other environmentally sensitive compounds to reach the natural aquatic environment.

2 BACKGROUND

2.1 Geology

The 125-km reach of the Athabasca River from Fort McMurray to the Firebag River incises several geological formations including the Cretaceous Clearwater and McMurray Formations, and various underlying Devonian formations (Figure 2). The Clearwater Formation is uppermost in the sequence and is exposed along the upper banks of the Athabasca River. The Clearwater Formation overlies the McMurray Formation which outcrops along most of the river from Fort McMurray to the Firebag River. Devonian carbonate outcrops along the Athabasca River from Fort McMurray to 62 km north and appears again at 99 km to the end of the study area. All formations are overlain by Quaternary sediments. Geological features of the study region are described in detail by Hein et al. (2001) and Barson et al. (2001). A brief overview of the important geological characteristics is provided below.

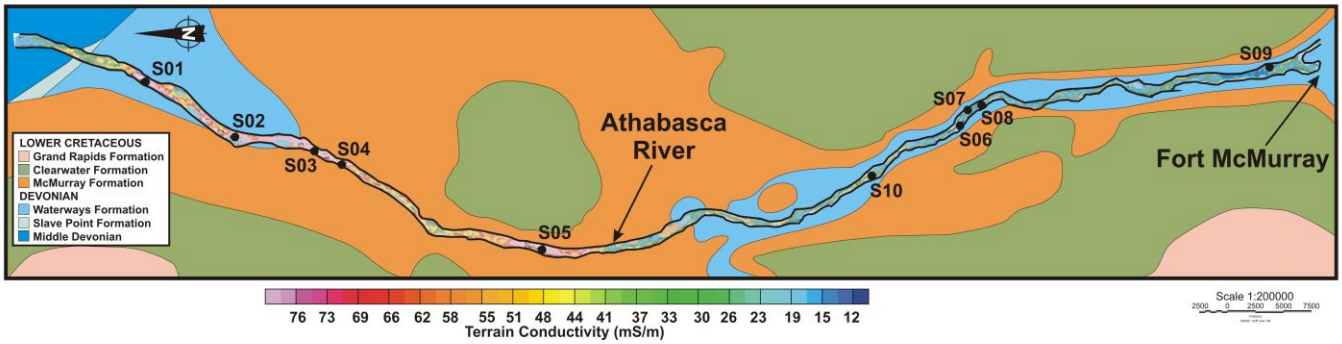

Figure 2. Geological map of bedrock subcrop along the Athabasca River, north of Fort McMurray (Modified from WorleyParsons 2010)

2.1.1 *Quaternary Sediments*

The surface of the bedrock underlying the Quaternary sediments in the region represents one of the major unconformable surfaces of the Western Canadian Sedimentary Basin (WCSB) – the pre-Quaternary unconformity, which spans the period of erosion from the Late Cretaceous – Early Tertiary to the onset of glaciation in the Early Quaternary. The most important features of these overburden sediments are isolated upland remnants and deep, broad relicts of paleo-river channel systems that formed during the Late Tertiary, but which were later modified by glacial and present-day fluvial processes. Remnants of buried fluvial channels provide a historical

record of the erosion that has occurred on the bedrock surface from the Late Cretaceous to the Late Pleistocene. The lowermost unit of drift consists predominantly of coarse sediment deposited by preglacial and glacial fluvial systems. Basal fluvial sediments are present as thick sequences within the floors of the buried bedrock channels and multiple overlying till units attest to multiple glacial and interglacial cycles during the Quaternary (Andriashek 2003).

2.1.2 *Clearwater Formation*

Regionally the Clearwater Formation is an aquitard (Hitchon et al. 1989, 1990) consisting of a ~10 m shale unit in the upper portion of the formation. Although the formation generally consists of shale, the unit grades into silt and fine sands suggesting that the shale unit may not be continuous (Bachu and Underschultz 1993). Along the northern section of the Athabasca River, outcrops of Clearwater Formation unconformably overly the McMurray formation (Figure 3). Exposed outcrop is generally thin (<1m) and composed of fine-grained sediments (Hein et al. 2001). The Clearwater Formation contains natural gas and some accumulation of bitumen.

Figure 3. Photos showing outcropping of Clearwater Formation sediments overlying Upper McMurray Sediments along the Athabasca River, north of Fort McMurray.

2.1.3 *McMurray Formation*

The Upper McMurray Formation is disconformably bounded above and below by the Clearwater Formation and the Sub-Cretaceous unconformity, respectively (Wightman et al. 1995). The formation consists of interbeded sands, shales and silts, and large areas of bitumen-saturated sands that locally act as flow barriers (Bachu and Underschultz 1993). The McMurray Formation dips to the southwest and is overlain by a thick succession of Clearwater Formation deposits (Figure 4).

Figure 4. Photos showing exposed McMurray Formation overlying Devonian age carbonate outcrops along the Athabasca River, north of Fort McMurray.

Photo to the right is located adjacent to sample location S09(A).

2.1.4 *Waterways Formation (Devonian Unit)*

The Waterways Formation, part of the Devonian succession, underlies the McMurray Formation and comprises a series of carbonate aquifers separated by intervening evaporite deposits and shaly aquitards (Figure 5). Devonian units in the area support regional groundwater flow systems that originate from the Rocky Mountains overthrust belt and discharge in northeastern Alberta and Saskatchewan. Groundwater is characterized by extremely high salinity, particularly in the vicinity of evaporitic beds.

Figure 5. Photos showing exposed Devonian-aged carbonate bedrock along the Athabasca River, north of Fort McMurray.

3 METHODS

3.1 WorleyParsons Electromagnetic Survey of the Athabasca River

WorleyParsons was contracted by AITF to conduct a waterborne electromagnetic (EM) terrain conductivity survey (WorleyParsons 2010). This survey was conducted in June of 2009 and encompassed a 125-km reach of the Athabasca River from the city of Fort McMurray downstream to the confluence of the Firebag River (Figure 6). A 15-foot inflatable jet boat was used during this survey and eight passes were made down the reach of river under investigation to ensure the best coverage of riverbed features. Electrical conductivity along with bathymetry

data were used to correct the terrain conductivity for varying water depth. As a result, the corrected EM31 conductivity data represent the terrain conductivity of the river bottom sediments and pore fluids. The results are displayed as a color shaded grid with warm colours (reds and pinks) representing high conductivity values and cool colours (blues) representing low conductivity values. Generally, terrain conductivity values were lower for coarse grained materials (sands/gravels) than for fined grained silts and clays. The background terrain

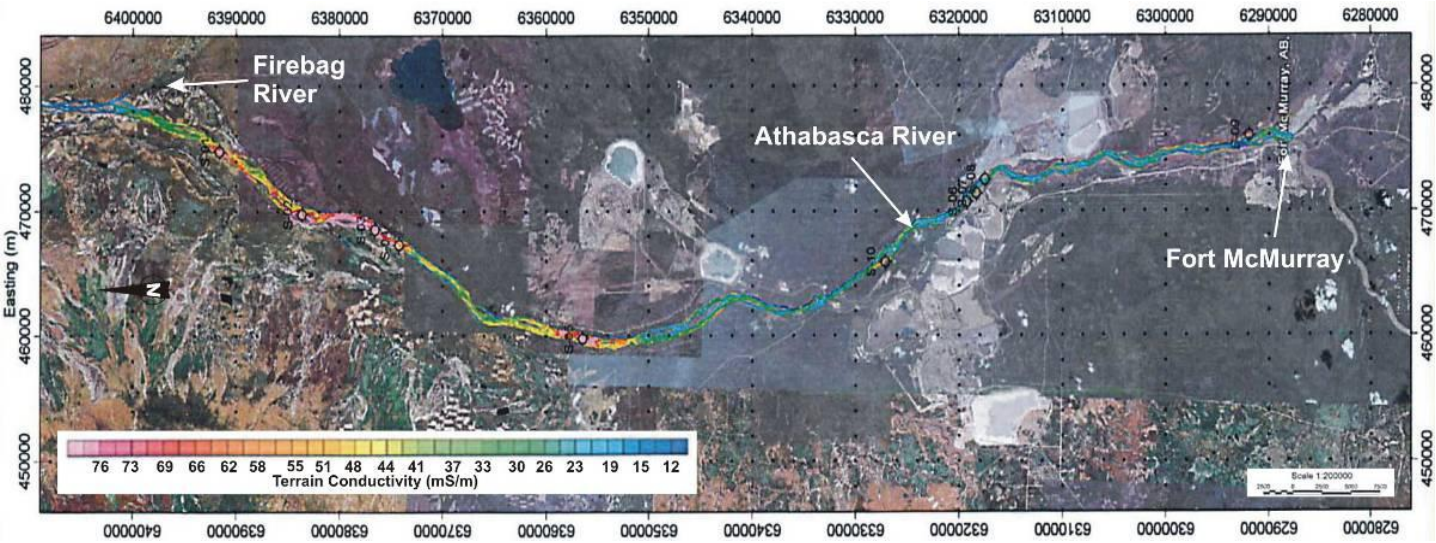

conductivity was <40 mS/m, with zones of relatively high conductivity values >80 mS/m.

Figure 6. EM survey showing terrain conductivity of the river bottom sediments and pore fluids along the Athabasca River from Fort McMurray to the Firebag River, 125 km north (Modified from WorleyParsons, 2010)

River EC and water samples were also measured/collected at ten locations where EM terrain conductivity values were elevated. Samples were collected using a peristaltic pump with the sampling tube located approximately 10 cm above the riverbed. Electrical conductivity of the river water averaged 240 µS/cm (range 196 µS/cm to 281 µS/cm). The survey revealed ten zones of elevated terrain conductivity and suggested that these zones may be related to elevated salinity of pore water contained in the river bed.

3.2 Sample Collection

In total 40 samples were collected for this study (Table 1). These included:

- 10 river water samples (near bed interface)
- 8 river bed seeps (below sediment interface)
- 9 process-affected waters including one blank
- 4 river waters (mid-channel, mid-depth)
- 6 groundwater samples

- 3 other surface waters

Table 1. Summary of samples collected during this study.

Sample ID	Sampling Dates	Lat (N)	Long (W)	Location
River Water (near bed interface)				
S01	Jun-09	57.67	111.42	Overlying Dev (Waterways Fm.)
S02	Jun-09	57.59	111.51	Overlying Dev (Waterways Fm.)
S03	Jun-09	57.53	111.53	Overlying McMurray Fm.
S04	Jun-09	57.51	111.55	Overlying McMurray Fm.
S05	Jun-09	57.35	111.67	Overlying McMurray Fm.
S06	Jun-09	57.02	111.48	Overlying Dev (Waterways Fm.)
S07	Jun-09	57.01	111.47	Overlying Dev (Waterways Fm.)
S08	Jun-09	57.00	111.45	Overlying Dev (Waterways Fm.)
S09	Jun-09	56.77	111.39	Overlying Dev (Waterways Fm.)
S10	Jun-09	57.09	111.56	Overlying Dev (Waterways Fm.)
River Bed Seeps (below sediment interface)				
S01A	13-Aug-09	57.67	111.42	Dev (Waterways Fm.)
S01N	05-Nov-09	57.67	111.42	Dev (Waterways Fm.)
S02N	05-Nov-09	57.59	111.51	Dev (Waterways Fm.)
S03A	13-Aug-09	57.53	111.53	McMurray Formation
S07A	14-Aug-09	57.01	111.47	Dev (Waterways Fm.)
SO8A	14-Aug-09	57.00	111.45	Dev (Waterways Fm.)
S09A	14-Aug-09	56.77	111.39	Dev (Waterways Fm.)
S10A	14-Aug-09	57.09	111.56	Dev (Waterways Fm.)

Sample ID	Sampling Dates	Lat (N)	Long (W)	Location
Process-Affected Water				
PAW 001	18-Aug-09	57.24	111.56	tailings pond – Albian
PAW 002	18-Aug-09	57.30	111.51	coarse tailings – Albian
PAW 003	19-Aug-09	57.04	111.62	tailings pond – Syncrude
PAW 004	19-Aug-09	57.04	111.62	tailings pond – Syncrude
PAW 005	19-Aug-09	57.04	111.62	coarse tailings – Syncrude
PAW 006	20-Aug-09	57.24	111.56	tailings seepage – Albian
PAW 007	04-Nov-09	57.34	111.88	coarse tailings – CNRL
PAW 008	04-Nov-09	57.34	111.78	recycled tailings – CNRL
PAW 009				DI Blank
Athabasca River Water (mid-channel, mid-depth)				
PAW N	21-Sep-09	57.67	111.42	Athabasca River, beginning of survey
PAW N2	05-Nov-09	57.67	111.42	Athabasca River, beginning of survey
PAW S	21-Sep-09	56.77	111.40	Athabasca River, end of survey
PAW S2	05-Nov-09	56.77	111.40	Athabasca River, end of survey
Groundwater Wells				
BAS25	Sep-09	54.26	111.27	McMurray Formation
BAS 25 A	Sep-09	54.26	111.27	McMurray Formation
BAS 26	Sep-09	57.24	111.45	McMurray Formation
CRW 1	Sep-09	57.18	111.13	Clearwater Formation
SS 19	Sep-09	57.18	111.13	Surficial Sands
SS 22	Sep-09	57.18	111.13	Surficial Sands
Other Surface Waters				
NE7-09	Sep-09	57.15	-110.86	lake
McClelland-09	Sep-09	57.47	-111.35	lake water

Sample ID	Sampling Dates	Lat (N)	Long (W)	Location
AthaR-09	Sep-09	56.74	-111.39	Athabasca River Water

The downstream portion of the Athabasca River of interest to Alberta Environment included sections that are only accessible by boat and helicopter. During August 13 and 14, 2009, employees from AITF were transported in a jet boat down the Athabasca River to sample seepage zones (samples labelled ending with "A"). On November 5, 2009, personnel from AITF were transported in a helicopter to sample seepage zones (sample labels ending with "N"). A timeline of river and seep sampling for August and November is presented in Table 2.

Table 2. Timeline for seep and river sampling conducted along the Athabasca River from August 13 to November 5, 2009.
Distance is measured as km north of Fort McMurray along the Athabasca River.

Location	Date	Time
PAW N – 112.5 km	08/13/2009	11:30
S01(A) – 112 km	08/13/2009	12:30
S03(A) – 94.8 km	08/13/2009	16:30
S08(A) – 30.6 km	08/14/2009	9:30
S07(A) – 31.8 km	08/14/2009	13:00
S10(A) – 42.2 km	08/14/2009	14:30
S09(A) – 4.7 km	08/14/2009	17:30
PAW S - 4.0 km	08/14/2009	18:00
PAW N2 – 112.5 km	11/05/2009	13:00
S01(N) – 112 km	11/05/2009	12:30
S02(N) – 102.3 km	11/05/2009	15:30
PAW S2 – 4.0 km	11/05/2009	17:00

Seep sampling locations were selected from elevated terrain conductivity zones along the Athabasca River bed mapped by WorleyParsons (2010). Groundwater from the elevated terrain conductivity areas was sampled by driving a ½-inch PVC drive point 0.5 to 1 m below the riverbed surface. One end of a ¼-inch diameter polyethylene (PE) tubing was connected to the drive point and the other end was connected to a peristaltic pump. Measurements of Eh and pH were made in the field using a sealed flow-through cell. Values were recorded when readings were stable. Eh was calibrated in Zobell's solution (Nordstrom 1977) and Light's solution (Light 1972). pH was calibrated with standard buffer solutions at pH 4, 7, and 10. Calibration of the Eh and pH probes was checked before and after each sampling location. Dissolved H_2S concentrations were determined on 25 mL samples from each seep using a Hach DR2010 spectrometer following the methylene blue procedure (American Public Health Association et al. 1992). Measurements of alkalinity were made in the field on filtered samples using a Hach

digital titrator and bromcresol green / methyl red indicator and with 1.6 N H_2SO_4. Temperature and conductivity were also measured from seepage zones in the field.

Water was collected from each seep for routine analysis, trace metals, total organic carbon (TOC), natural organic compounds (NOC), naphthenic acids, volatile priority pollutants (VPP) and extractable priority pollutants (EPP). Each seep was also sampled for the stable isotopes, $\delta_{18}O$, δ^2H, $\delta^{13}C_{DIC}$, $\delta^{13}C_{DOC}$, $\delta^{34}S_{SO4}$, $\delta^{11}B$, $\delta^{81}Br$, $\delta^{37}C$, and $^{87}Sr/^{86}Sr$ ratios. Radiogenic isotopes ^3H and ^{14}C were also analyzed to determine the age of seep waters. All of the above samples were field filtered using 0.45 µm cellulose nitrate filters except those for naphthenic acids, VPP, EPP, enriched tritium (^3H) and ^{14}C. Samples were refrigerated immediately after sampling and shipped to AITF in Victoria for processing and redistribution to subcontracted labs within a few days. See Table 3 for a summary of laboratories used for the different collected samples, volume and bottle requirements and reporting units and standards.

Table 3. Summary of laboratories used for the different analyses, volume and bottle requirements and reporting units and standards.

Laboratory	Analysis	Volume/Bottle	Standard/Units
ISOTECH	^{14}C	125 mL HDPE	pMC, years
University of Calgary	$\delta^{11}B$ $\delta^{34}S$,$\delta^{18}O$ in SO_4	30 mL HDPE 1L HDPE	SRM-951, per mil (‰) V-CDT, per mil (‰)
University of Waterloo	^3H $\delta^{13}C_{DOC}$ $^{87}Sr/^{86}Sr$ $\delta^{81}Br$ $\delta^{37}Cl$	500 mL HDPE 1L amber HDPE 1L HDPE 1L HDPE 1L HDPE	Enriched, scintillation, TU V-PDB, per mil (‰) NIST987, absolute ratio SMOB, per mil (‰) SMOC, per mil (‰)
AITF Victoria	$\delta^{18}O\delta^2H$ $\delta^{13}C_{DIC}$	30 mL HDPE 30 mL HDPE	V-SMOW, per mil (‰) V-PDB, per mil (‰)
AITF Vegreville	Routine, TOC Trace metals Naphthenic Acids VPP EPP	500 mL HDPE 125 mL HDPE 1 L Amber Glass 60 mL scint. vial 60 mL scint. vial	mg/L ppb mg/L ppb ppb
Proteomics Victoria	Natural Organic Compounds	30 mL HDPE	

Surface water samples from the Athabasca River were collected following the same procedures described above in August (PAW S, PAW N) and November (PAW S2, PAW N2). Water from the Athabasca River was collected at the southern and northern most reaches of the survey at sampling locations S09 and S01, respectively.

Process-affected water was collected from three mine sites: Shell Albian Sands (Shell), Syncrude Canada Ltd. (Syncrude) and Canadian Natural Resources Ltd. (CNRL) (Figure 1). AITF employees, with the assistance of Shell personnel, collected three process-affected water samples from Shell Albian including water from the tailings pond (PAW001), a seepage collection ditch (PAW006) and coarse tailings (PAW002). Syncrude provided AITF with three sealed 5-gal pails containing PAW from their tailings pond (PAW003 and PAW004) and a sample of coarse tailings (PAW005). Personnel from AITF and CNRL collected two process-affected water samples from the site; one sample was collected from a pond containing recycled tailings pond water (PAW008) and the second sample (PAW007) was collected near the tailings slurry discharge pipe just prior to reaching the tailings pond. Therefore, PAW007 is classified as a coarse tailings sample. At the time of sampling, there was no safe access to the CNRL tailings pond to collect a process-affected water sample.

Six groundwater samples (Figure 1) including one duplicate (BAS25A) were collected by WorleyParsons and shipped to AITF. Field measurements, routine and trace metal analysis were also provided with the water samples. The groundwater samples were analyzed for stable and radiogenic isotopes and natural organic compounds.

3.2.1 *Groundwater Seeps*

Groundwater was collected from seven selected seepage areas in high conductivity zones mapped by WorleyParsons (2010) in June 2009 (Figure 1). Several other areas that were mapped as high conductivity zones during the EM survey and visited at that time could not be sampled from the boat in August due to low water levels, and no direct seepage evidence above the water line was observed. In some of these cases silty-clay sediments were observed along the shoreline and riverbed, suggesting that the elevated conductivity values measured by the EM survey could potentially have been due to high reflectance of the underlying sediment instead of discharging saline groundwater. A thorough evaluation of such anomalies was not conducted. Note that many additional high conductivity seeps mapped in the EM survey were not visited, but may be important targets for more comprehensive follow-up investigations.

Table 4 presents a brief description of each of the seven seepage areas sampled in this study and the following sections provide more details about each seep site.

Table 4. Field parameters measured from seeps situated along the Athabasca River. Alkalinity is in mg/L of $CaCO_3$.

Location	Distance km	EC µS/cm	Temp deg C	pH	Eh mV	H_2S µg /L	Alkalinity mg/L	Formation
S09A	4.7	1100	13.8	8.42	173	0.0	248	McMurray
S08A	30.6	980	15.4	7.39	63	5	156	Waterways
S07A	31.8	4600	16.7	7.02	76	29	540	Waterways
S10A	42.2	8180	16.3	7.05	55	7	396	Waterways
S03A	94.8	1010	13.7	7.25	164	10	228	McMurray

S02N	102.2	3710	4.4	7.48	250	19	376	Waterways
S01A	112	2670	14.9	7.06	305	0.0	184	Waterways
S01N	112	3090	2.8	7.26	59	65	920	Waterways

3.2.1.1 Seep S09A

The first high conductivity area sampled is located 4.7 km downstream from Fort McMurray within the Waterways Formation (Figure 7). It was not possible to collect seepage from the river bed due to the low hydraulic conductivity of the sediments. However samples were collected from a spring discharging from the eastern riverbank of the Athabasca River adjacent to the elevated conductivity zone (Figure 8). The shoreline near the spring was composed mainly of cobbles that terminated against a steep cut bank of Devonian carbonate rock overlain by a thick succession of oil-saturated McMurray Formation Sediments (Figure 4, photo to the right). Seep S09A is located upstream from oil sands development.

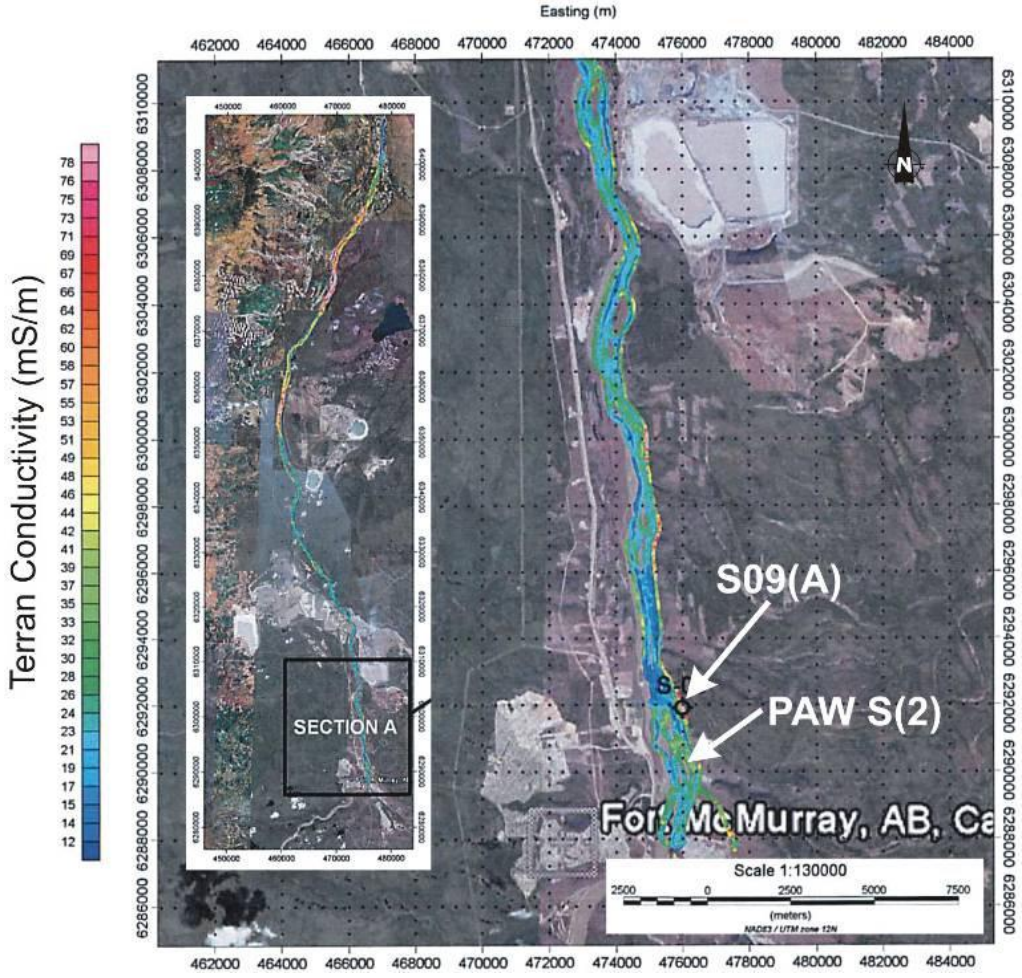

Figure 7. Location of seep S09A
Modified from WorleyParsons 2010.

Figure 8. Photos showing a spring along the Athabasca River at location S09A.

Discharge from the spring possibly originates from the McMurray Formation, although this could not be confirmed due to the steep river bank limiting access to observe the discharge point (Figure 8). Flow from this spring was estimated at 6 to 8 L/min. EC of the spring water was 1,100 µS/cm, 3 times higher than Athabasca River water. The pH of the spring water was 8.42 and conditions were mildly reducing with an Eh of +173 mV. No H_2S odour was observed at the seepage area.

3.2.1.2 Seep S08A

Seepage area S08A was located in the Waterways Formation approximately 30.6 km down-stream from Fort McMurray (Figure 9). A piezometer was driven into the sandy riverbed to collect water from the elevated conductivity zone (Figure 10). Significant oil sands development was observed on both shores of the river.

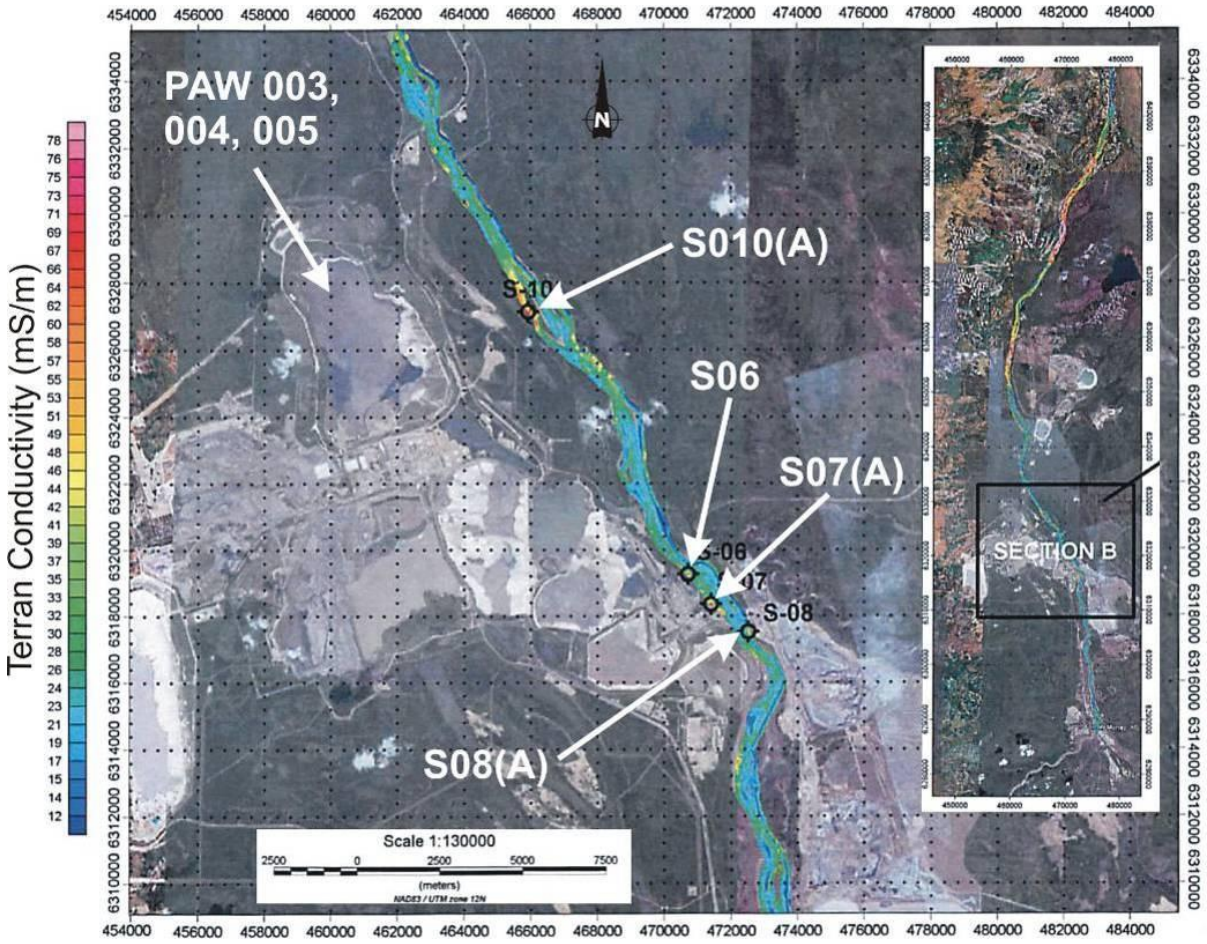

Figure 9. Seep sampling locations S08A, S07A, S010 and PAW-003, -004 and -005.

Water from seep S08A had an EC of 980 µS/cm, 3 times higher than Athabasca River water. The pH of the seepage water was 7.39 and mildly reducing conditions (Eh of +63 mV). Dissolved H_2S concentration in the seep water was elevated at 5 µg/L.

Figure 10. Seep sample collection from location S08A.
Photo to the left shows a piezometer driven into the Athabasca river bed to collect groundwater at location S08A. Photo to the right shows sampling proximity to oil sands development.

3.2.1.3 Seep S07A

Seepage area S07A was located in the Waterways Formation approximately 32 km downstream from Fort McMurray. The high conductivity zone was situated against the western shore of the Athabasca River, adjacent to nearby oil sands development (Figure 11). A drive-point piezometer was driven into the sandy riverbed within the area of elevated electrical conductance.

Figure 11. Seep sample collection at location S07A.
Photo to the right shows proximity of the sampling point a flare stack on an oil sands development.

Water collected from seep S07A had an EC of 4,600 µS/cm, 14 times greater than Athabasca River water. The pH of the seep water was neutral at 7.02 and the Eh was mildly reducing at +76 mV. Dissolved H_2S concentration from the seep water was 29 µg/L.

3.2.1.4 Seep S10A

Seepage area S10A is located in the Waterways Formation near the western shore of the Athabasca River, approximately 42.2 km downstream from Fort McMurray (Figure 9). The shoreline and riverbed has low relief, consisting of unconsolidated silty-sand. Along the western shore of the Athabasca River, groundwater was observed flowing in sheet-like discharge from the river bank (Figure 12). There is significant oil sands development to the west of the sampling location.

Figure 12. Seep sample collection at location S10A.
Photo to the left shows a piezometer driven into the Athabasca river bed to collect groundwater at location S10A. Photo to the right shows highly reflective water on the bank indicating occurrence of groundwater seepage on the western shore of the Athabasca River adjacent to the sampling location.

The highest EC measurement in the entire survey as collected from this seepage zone at 8,180 µS/cm, 25 times greater than Athabasca River water. The pH of the seep water was neutral at 7.05 and the Eh was mildly reducing at +55 mV. The dissolved H_2S concentration from the seep water was 7 µg/L.

3.2.1.5 Seep S03A

Seepage area S03A is located in the McMurray Formation along the Athabasca River, 94.8 km downstream from Fort McMurray (Figure 13). Seep S03A is located at the head of an extensive high conductivity zone. A piezometer was driven into the sandy riverbed above a large point bar island (Figure 14). S03A is not situated in a developed area.

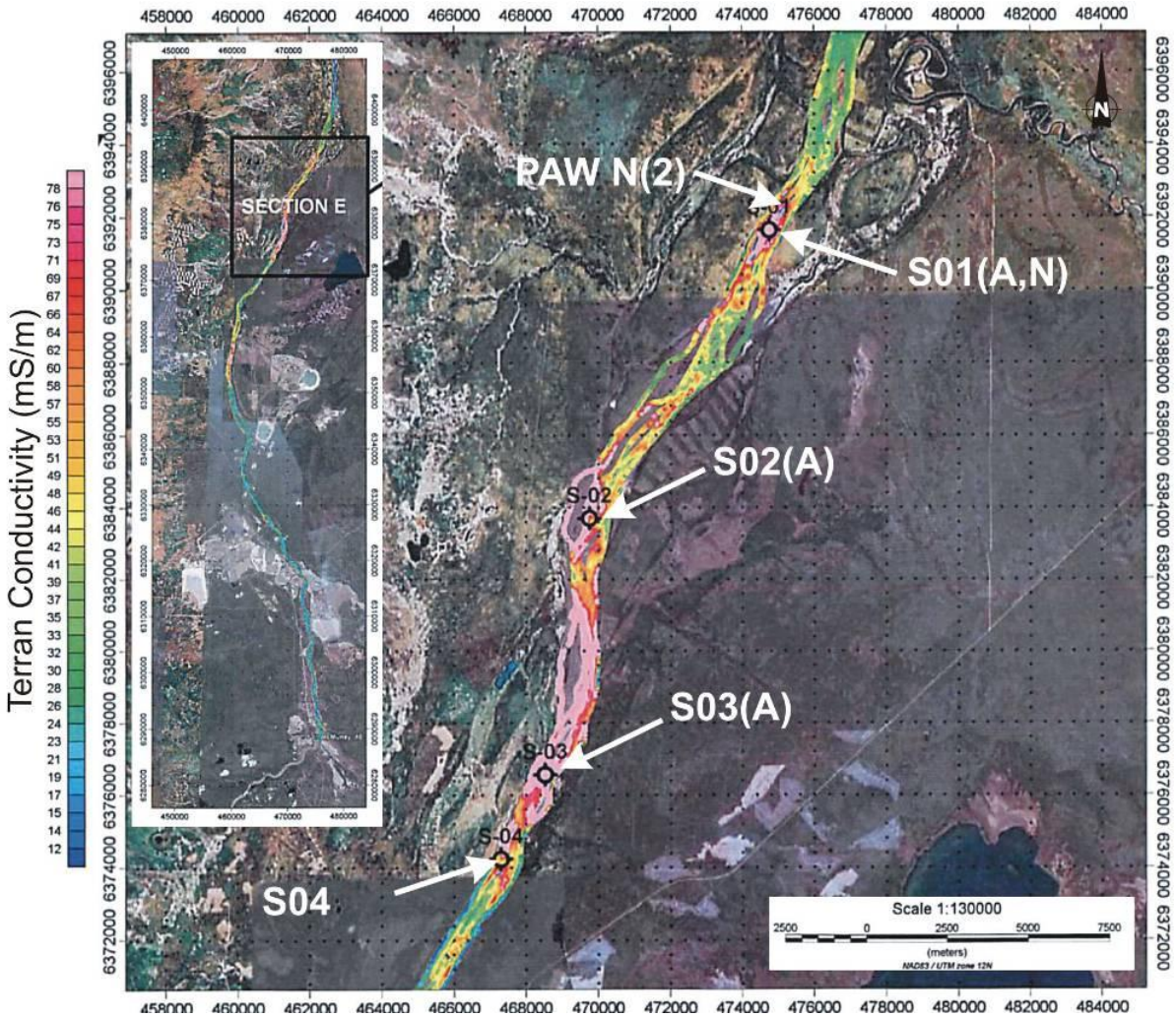

Figure 13. Location of seeps S03A, S02A and S01(A, N).
Modified from WorleyParsons 2010.

Figure 14. Seep sample collection from location S03A.

Water from seep S03A had an EC of 1,010 µS/cm, 3 times greater than Athabasca River water. The pH of the seepage water was 7.25 with mildly reducing conditions (Eh of +164 mV). Dissolved H_2S concentration in the seep water was 10 µg/L.

3.2.1.6 Seep S02N

Seep S02N is located in the Waterways Formation along the Athabasca River, approximately 102.2 km downstream from Fort McMurray (Figure 13). S02N is located near the northern limit of the same expansive EM anomaly as S03A. A piezometer was driven through the surface of a point bar island near the shoreline (Figure 15). S02N is not situated in a developed area.

Figure 15. Seep sample collection at location S02N.

Water collected from seep location S02N had an EC of 3,710 µS/cm, 11 times greater than Athabasca River water. The pH of the seepage water was 7.42 with oxidizing conditions (Eh of +250 mV). Dissolved H_2S concentration measured from the seepage water was 19 µg/L.

3.2.1.7 Seep S01A, N

Seep S01 is located in the Waterways Formation along the Athabasca River, approximately 112 km downstream from Fort McMurray (Figure 16). Seep S01A was sampled in August 2009 by driving a piezometer into the sandy river sediments, a few hundred metres south of a point bar island (Figure 17). This location was resampled in November 2009 on the point bar island by driving a piezometer through the sandy sediments adjacent to the shoreline. S01 is not situated in a developed area.

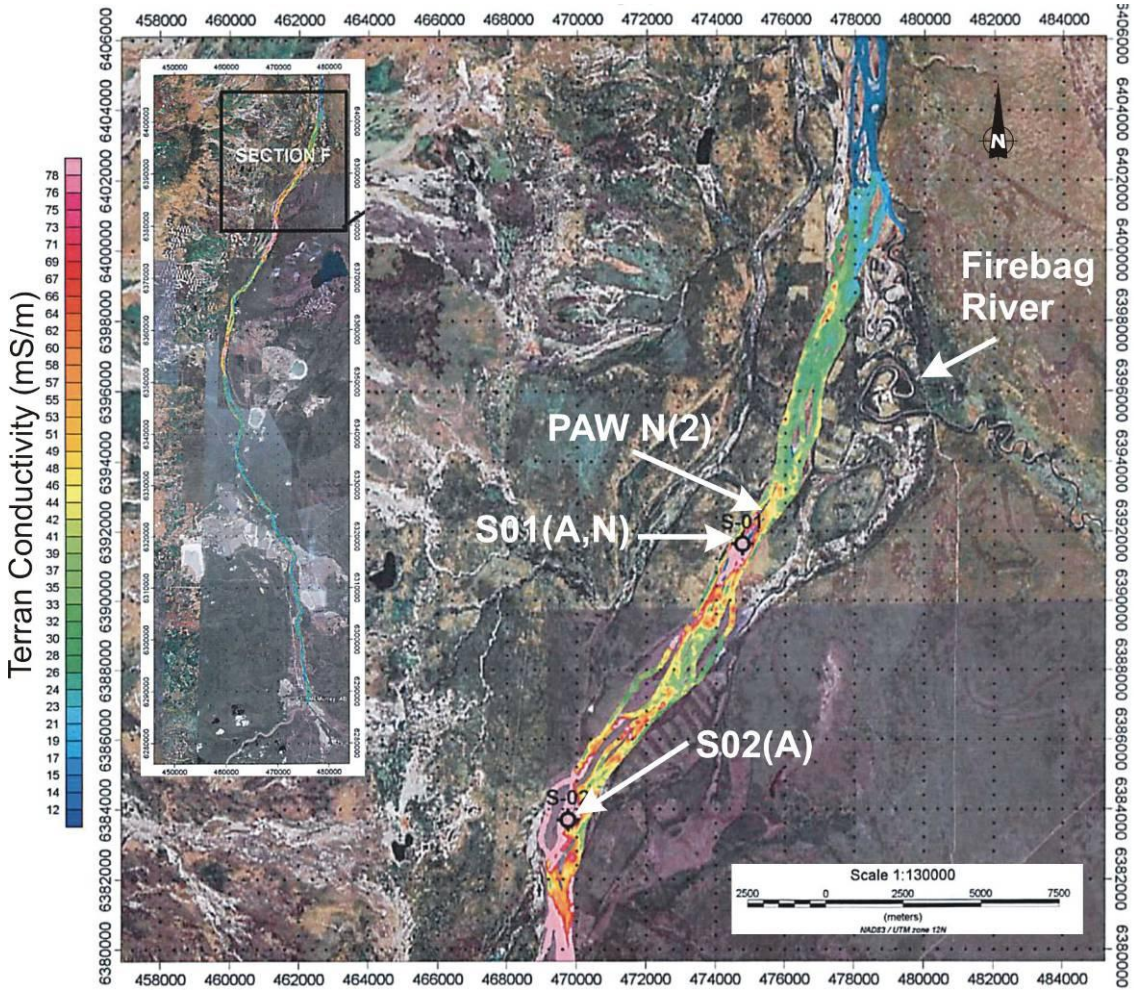

Figure 16. Location of seeps S02A and S01(A, N). Modified from WorleyParsons 2010.

Figure 17. Seep sample collection at location S01.
Photo to the right shows seep sampling during August 2009 looking south towards a point bar island. Photo to the right shows seep sampling on the point bar island in November 2009.

Water collected from seep location S01 had an EC of 2,670 µS/cm in August and 3,090 µS/cm in November, 8 and 9 times greater than Athabasca River water, respectively. Measurements of pH, Eh, alkalinity and H_2S also show differences between sampling dates (Table 5). The variation in measurements may be due to combination of seasonality, location differences and piezometer depth.

Table 5. Field parameters measured along the Athabasca River during the study period.

Location	**Date** 2009	**Distance** km	**EC** µS/cm	**Temp** degC	**pH**	**Eh** mV	**Alkalinity** mg/L	**Formation**
PAWS	Aug	4.0	-	-	-	-	-	Waterways
PAWS2	Nov	4.0	655	0.2	8.51	510	160	Waterways
S09	Jun	4.7	200	14.0	7.62	400	88	Waterways
S08	Jun	30.6	210	13.9	7.57	518	68	Waterways
S07	Jun	31.8	230	13.3	7.80	530	88	Waterways
S06	Jun	33.3	265	13.4	7.69	513	112	Waterways
S10	Jun	42.2	255	15.7	7.9	416	96	Waterways
S05	Jun	83.2	280	13.9	7.85	553	92	McMurray
S04	Jun	92.3	245	13.3	7.67	404	88	McMurray
S03	Jun	94.8	235	13.8	7.71	402	84	McMurray
S02	Jun	102.2	240	13.5	7.58	402	100	Waterways
S01	Jun	112	245	14.6	7.76	405	92	Waterways
PAWN	Aug	112.5	330	13.0	7.48	434	96	Waterways
PAWN2	Nov	112.5	650	1.1	8.11	347	128	Waterways

3.2.2 *Athabasca River*

Athabasca River water samples were initially collected in June 2009 by WorleyParsons at the time of the EM survey. Samples were taken about 10 cm above the seep sampling location, and

evidently are close enough to the seep to be somewhat influenced by its discharge (locations S01 to S10). Nonetheless, they still give some indication of variations in river water along the reach of the river included in the survey. Two additional river samples, PAWS and PAWS2, were collected by AITF at the beginning of the seep survey and two more samples, PAWN and PAWN2, were collected from mid-depth at the end of the survey (Figure 18). Differences between the pairs are useful for examining net changes in river geochemistry over the reach of the survey (Table 5).

Figure 18. Southern sampling location along the Athabasca River, PAW S(2).

3.2.3 *Groundwater*

Six groundwater samples collected by WorleyParsons on behalf of Alberta Environment were submitted for isotopic and organic analyses by AITF. The samples included two from the basal McMurray Formation, one from the Clearwater Formation and two from surface sediments (Quaternary) (Table 6).

Table 6. Stable isotope values measured from groundwater collected from water wells. Note that BAS25 and BAS25A are duplicates.

Well ID	$\delta^{18}O$ (‰)	$\delta^{2}H$ (‰)	$\delta^{13}C_{DIC}$ (‰)	$\delta^{13}C_{DOC}$ (‰)	$\delta^{34}S_{SO4}$ (‰)	$^{87}Sr/^{86}Sr$	$\delta^{37}Cl$ (‰)	Formation
BAS25	-22.2	-171.56	-2.61	-28.3	n/a	0.70943	0.19	McMurray
BAS25A	-22.2	-170.89	-2.56	-28.7	n/a	0.70946	0.13	McMurray
BAS26	-19.2	-147.91	-7.36	-27.7	9.78	0.71002	n/a	McMurray
CRW 1	-19.9	-154.13	4.05	n/a	n/a	n/a	n/a	Clearwater
SS 19	-18.3	-141.41	-12.78	-28.0	n/a	0.71121	-0.98	Quaternary
SS 22	-19.2	-148.89	-11.93	-28.0	29.49	0.71040	0.28	Quaternary

3.2.4 *Process-Affected Water*

The locations of various process-affected water sampling stations are shown in Figure 9 and Figure 19. A list of samples and field parameters measured during the survey are given in Tables 7 and 8.

Table 7. Field parameters measured from process-affected water.
Note that PAW003 and PAW004 are duplicates.

Location	EC µS/cm	Temp degC	pH	Eh mV	Alkalinity mg/L	Type
PAW 001	2530	19.3	7.78	463	324	tailings pond
PAW 002	1535	10.6	7.4	465	300	coarse tailings
PAW 003	3880	10.6	8.23	442	580	tailings pond
PAW 004	3780	11.3	8.24	438	544	tailings pond
PAW 005	n/a	n/a	n/a	--	n/a	coarse tailings
PAW 006	1670	9.0	7.87	428	432	tailings seepage
PAW 007	2325	10.0	7.65	400	932	coarse tailings
PAW 008	1000	10.6	7.15	419	352	recycled tailings

Table 8. Stable isotope values measured from process-affected water.
Note that PAW003 and PAW004 are duplicates.

Well ID	$\delta^{18}O$ (‰)	$\delta^{2}H$ (‰)	$\delta^{13}C_{DIC}$ (‰)	$\delta^{13}C_{DOC}$ (‰)	$\delta^{34}S_{SO4}$ (‰)	$^{87}Sr/^{86}Sr$	$\delta^{37}Cl$ (‰)	$\delta^{11}B$ (‰)
PAW 001	-14.5	-130.07	-4.60	-29.47	14.16	0.71217	0.39	22
PAW 002	-14.7	-130.48	-2.23	n/a	n/a	n/a	n/a	23
PAW 003	-12.4	-113.71	-1.41	-29.49	8.06	0.70823	0.32	25
PAW 004	-12.4	-113.87	-1.38	-29.89	7.84	0.70824	0.75	22
PAW 005	-12.8	-115.44	n/a	DNS	DNS	DNS	DNS	n/a
PAW 006	-15.7	-133.59	-6.49	-28.88	17.04	0.70909	0.21	25
PAW 007	-15.63	-130.06	-21.1	n/a	n/a	n/a	n/a	n/a
PAW 008	-15.44	-131.44	-12.0	n/a	n/a	n/a	n/a	n/a

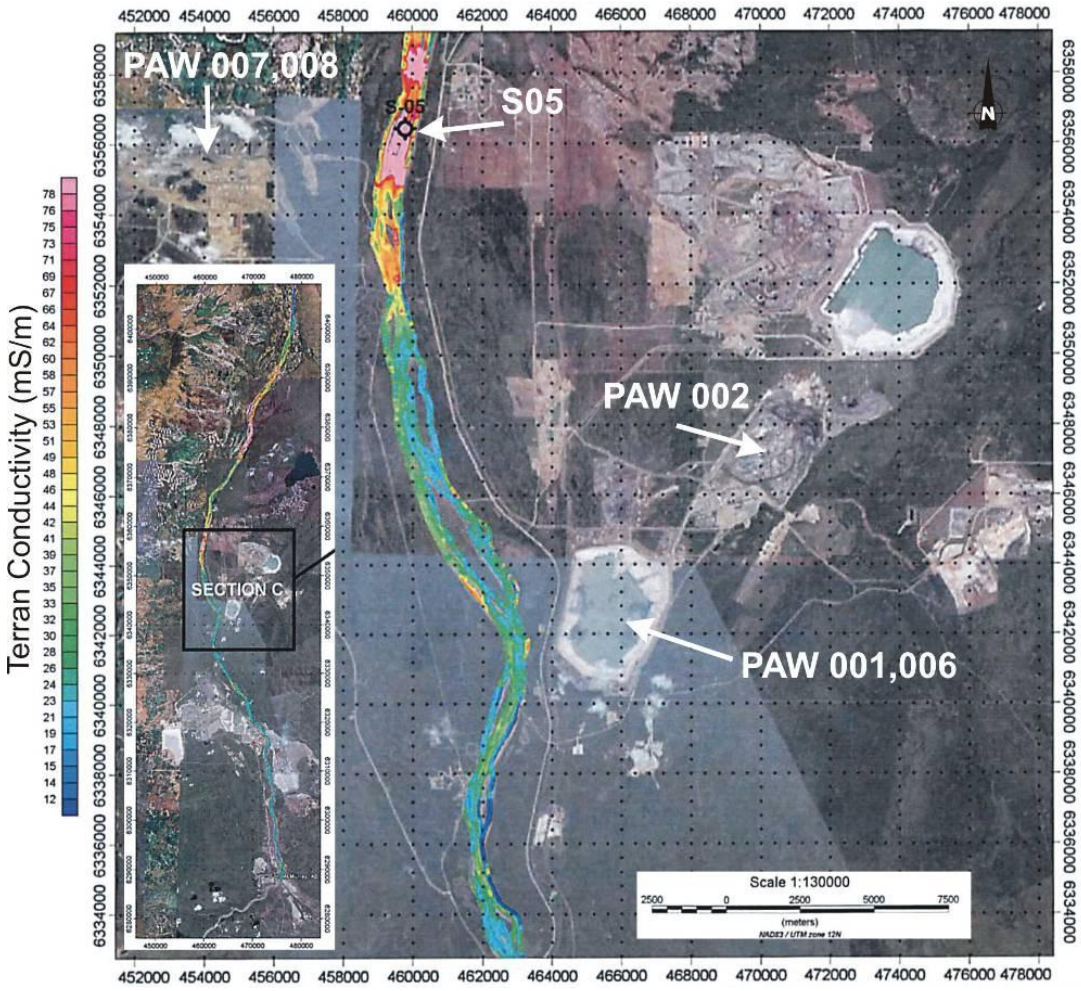

Figure 19. Various process-affected water sampling locations.
See Figure 10 for additional locations.

3.3 Laboratory Analyses

Table 3 provides a summary of the analytical laboratories contracted to undertake the various analyses including information on bottle types and volumes used for each tracer, as well as laboratory isotope standards and units used for reporting. In all cases, stable isotope analyses were undertaken by standard isotope ratio mass spectrometry (IRMS) and ^{14}C was analyzed by accelerator mass spectrometry (AMS). The organics included in the Volatile Priority Pollutants (VPP) and Extractable Priority Pollutants (EPP) were analyzed by gas chromatograph mass spectrometry (GCMS). The natural organic compound analyses were performed by electrospray ionization Fourier transform ion cyclotron resonance mass spectrometry (FT-ICR MS).

3.4 Isotope Tracers

A variety of isotopic tracers were used in this study including oxygen and hydrogen contained within the water molecule, isotopes of selected solutes dissolved within the water, and tracers of water age and evolution.

3.4.1 *Water Isotope Tracers (^{18}O, ^{2}H and ^{3}H)*

The stable isotopes of water, ^{18}O and ^{2}H, are naturally occurring and incorporated within the water molecule ($H_2{}^{18}O$, $^{1}H^{2}H^{16}O$). They are particularly useful tracers of water cycling as they undergo measureable and systematic fractionation as water is transported, evaporates and exchanges among phases in the water cycle. These fractionations result in differing isotopic labelling of precipitation, groundwater and surface waters that can be used to identify water sources, mixing, flow pathways, and have great potential for quantitative evaluation of water balance. Values are reported in per mil relative to Vienna Standard Mean Ocean Water (V-SMOW).

Tritium (^{3}H) is a radioactive isotope of hydrogen present in the water molecule with a half-life of 12.43 years. While produced naturally in the atmosphere, ^{3}H was introduced in high concentrations by thermonuclear weapon testing in the 1950s and 60s, and is a valuable diagnostic tracer of modern recharge. The presence of significant tritium is an indicator of water that has been in contact with the atmosphere during the last 60 years. Values are reported in tritium units where 1 TU = 1 ^{3}H per 1,018 atoms or 0.118 Bq kg^{-1}.

3.4.2 *Solute Tracers (^{13}C, ^{34}S, ^{37}Cl, ^{81}Br, $^{87}Sr/^{86}Sr$ and ^{11}B)*

Carbon-13 (^{13}C) is the rare stable isotope of carbon with a relative abundance of 1.1%. Values are reported in per mil relative to Pee Dee Belemnite (V-PDB). Due to kinetic and equilibrium fractionation processes, the isotopic signature of δ13C can show a natural variation of almost 100‰. The $\delta^{13}C$ signatures in dissolved inorganic carbon (DIC) can be used to understand the role of carbonate dissolution as a regulator of natural water composition. In surface water systems, atmospheric $CO_2(g)$ has a $\delta^{13}C \approx -7‰$. When the $CO_2(g)$ dissolves in water, ^{13}C is slightly depleted, resulting in a $\delta^{13}C \approx -8‰$ for $CO_2(aq)$. However, subsequent hydration of $CO_2(aq)$ favours the heavier isotope and produce a $\delta^{13}C \approx 2‰$ in HCO_3^-.

The overall $\delta^{13}C$ of the dissolved carbonate depends therefore on the relative proportions of $CO_2(aq)$, HCO_3^- and CO_3^{2-}. If carbonate species in groundwater are equilibrated with calcite in a closed system with respect to gas exchange, groundwaters are expected to maintain a stable chemical and isotopic composition during flow through the aquifer. In general, there is a trend of increasing $\delta^{13}C_{DIC}$ with increasing age along the flowpath (Aravena et al. 1995; Bath et al. 1979; Kloppmann et al. 1998). This increase may be the result of renewed dissolution of carbonate due to dedolomitization or loss of Ca^{2+} from solution into the cation exchanger. Methanogenesis, whereby CO_2 is converted into CH_4 by bacteria, will also increase $\delta^{13}C$ of the remaining CO_2 (Aravena et al. 1995). Overall, the presence of dissolved inorganic carbon in the hydrosphere and associated isotopic fractionation presents the opportunity to study gas-water exchange processes and to measure water transport rates in the subsurface system. Also, $\delta^{13}C$ in dissolved organic carbon (DOC) has the potential to label origin of organics, and specifically, may be useful for identifying contact between water and hydrocarbons or bitumen.

Sulfur has 25 naturally occurring isotopes, only four of which are stable. Of those four, two (^{32}S, light and ^{34}S, heavy) make up the majority (99.22%) of sulfur on Earth. The vast majority

(95.02%) of sulfur is found as ^{32}S with only 4.21% in ^{34}S. The bulk Earth sulfur isotopic ratio is thought to be the same as the ratios from the Vienna Canyon Diablo Troilite (V-CDT), a meteorite found in Arizona. As such, the isotopic composition of CDT is accepted as the international standard and is therefore set as 0‰. Deviation from the CDT composition is expresses as $\delta^{34}S$. Positive values correlate to a greater amount of ^{34}S and more negative values correlate with greater ^{32}S in samples. Formation of sulfur minerals through non-biogenic processes does not strongly differentiate the light and heavy isotopes, although $\delta^{34}S$ values in minerals such as gypsum and barite are associated with a small (~1.65 ‰) fractionation from the brine solution at the time of precipitation (Thode and Monster 1965). Due to the conservative nature of $\delta^{34}S$ in non-biological processes, sulfur isotopes can serve as a tracing element to identify their source. On the other hand, biological processes, such as metabolism by the bacteria *Desulfovibrio* and *Desulfatomaculum*, can lead to significant isotope fractionation of sulfur (Nakai and Jensen 1964). These bacteria flourish in anoxic environments by oxidizing organic matter using oxygen derived from sulfate ions. In this process, the sulfur is reduced from +6 to -2 and is subsequently expelled as H_2S, which is depleted in ^{34}S compared to the sulfate. Sulfate metabolism can result in an isotopic depletion of -18‰, and repeated cycles of oxidation and reduction can result in values up to -50‰. Because of large apparent fractionations, ^{34}S is an important tracer of biogeochemical processes such as methanogenesis in oil-bearing reservoirs. More recently, there is an emerging tread of combining $\delta^{34}S_{SO4}$ with $\delta^{18}O_{SO4}$ to identify and characterize these processes (Cendon et al. 2004, 2008).

Halogens (primarily Cl and Br) and their isotopes ($\delta^{37}Cl$ and $\delta^{81}Br$) are increasingly being applied to understand the aqueous system in various geological settings. Chlorine has isotopes with mass numbers ranging from 32 to 40. Among them, two stable species (^{35}Cl and ^{37}Cl) are the most common, with relative abundances of 75.8% and 24.3%, respectively. Bromine has two stable species, ^{79}Br and ^{81}Br with relative abundance of ~50.7% and ~49.3% respectively, and at least another 23 radioactive species. Interest in the halogens as tracers in aqueous environments is mainly due to the fact that Cl is often the major dissolved anion and both Cl and Br are fairly conservative in marine and groundwater systems. As such, Farber et al. (2007) use $\delta^{37}Cl$, in combination with Br/Cl to determine the origin of groundwater sources and the contribution of deep subsurface brines to regional groundwater resources in the Jordan Valley, Israel. On the other hand, the application of $\delta^{81}Br$ is hampered by the complexity and poor precision of analyzing Br stable isotopes. Eggenkamp and Coleman (2000) were the first to report $\delta^{81}Br$ signatures of natural samples. In their study, they reported the $\delta^{81}Br$ of 11 oil field brines and established the first natural range of variation for $\delta^{81}Br$. Shouakar-Stash et al. (2005) developed new methodology for analyzing Br stable isotopes and examined 26 sedimentary and crystalline shield formation waters. The range of $\delta^{81}Br$ variability was updated (0.00‰ to +1.8‰ relative to Standard Mean Ocean Bromide). These studies revealed potential for using Br stable isotope ratios to determine the solute sources of natural waters and evaluating geochemical and hydrogeological processes. In this study, we apply Cl and Br isotopes together to characterize and evaluate the origin and evolution of groundwater in the study domain.

Strontium is an alkaline earth element with a valence of +2. Strontium has four naturally occurring isotopes. Three of them are non-radiogenic, including ^{84}Sr (~0.56%), ^{86}Sr (~9.87%), and ^{88}Sr (~82.53%). The fourth isotope, ^{87}Sr (7.04%), is radiogenic, as it is formed over time by the δ-decay of ^{87}Rb, with a half-life of about 4.88×10^{10} years. The Rb-Sr decay system has been widely used in geochronology and remains one of the most useful geochemical tracers, while $^{87}Sr/^{86}Sr$ is a function of the relative abundance of Rb-Sr decay and the age of the material since it crystallized. The ratio of $^{87}Sr/^{86}Sr$ is commonly used as an indicator of weathering source and groundwater movement as this ratio is fixed in minerals at the time of crystallization, is retained during incorporation of minerals into sedimentary rocks, and this signature is also transferred to solution during the weathering process.

Systematic variations in $^{87}Sr/^{86}Sr$ have been established for the Phanerozoic Oceans and these values are not changed by exchange reactions or by kinetic effects. Likewise, dissolved strontium in groundwater also carries the isotopic signature of the parent weathering source. $^{87}Sr/^{86}Sr$ ratios can therefore be used to provide information on the types of materials that groundwater has interacted with, and these can in turn be applied to deduce flow paths (Collerson et al. 1988, Peterman and Stuckless 1992). Important reference values for this study include Devonian carbonates, typically ranging from 0.7078 to 0.7083 (± 0.00004), Cretaceous carbonates ranging from 0.7070 to 0.7077, and Quaternary carbonates ranging mainly from 0.7080 to 0.7090 (Faure 1986, p. 188). Strontium is an alkaline earth element with a valence of +2. Since its ionic radius (1.32Å) is only slightly larger than that of calcium (1.18 Å), it is common that Sr^{2+} substitutes for Ca^{2+} in minerals including plagioclase feldspar, calcite, dolomite, aragonite, gypsum and apatite. As such, strontium is an important trace element in calcium bearing hydrological cycles. Moreover, kinetic and equilibrium fractionation of $^{87}Sr/^{86}Sr$ are negligible at the low temperature of biology and hydrology systems because the large atomic mass of Sr, which means that Sr isotopes pass from bedrock to soil into biologically-available solutions without measurable fractionation (i.e., retaining the same ratio of ^{87}Sr to ^{86}Sr). As a result, strontium isotopic signature can be a sensitive fingerprinting tracer for hydrological cycles especially for calcium rich groundwater system.

Boron has two naturally occurring stable isotopes, ^{10}B with an abundance of 19.8%, and ^{11}B with an abundance of 80.2%. The wide range of $\delta^{11}B$ (-16‰ to +59‰) values observed in the natural environment make it an ideal tracer for fingerprinting purposes. Of particular interest, evaporites, especially non-moraine evaporites, typically contain very high concentrations of borate minerals. A survey of $\delta^{11}B$ values was carried out by Swihart et al. (1986), focusing on borate minerals from marine and nonmarine evaporates of various ages. The mean $\delta^{11}B$ values for marine evaporites was determined to be +25‰, compared to -7‰ for non-marine evaporates. The large difference between the boron isotope composition of marine and non-marine evaporites offer great promise for distinguishing the origin of metasedimentary rocks and associated fluid. The distinctive boron isotope composition of marine evaporites has also led to the use of $\delta^{11}B$ values in studying the origin of saline basin brines. Boron isotopes measured in formation waters from the Gulf Coast Basin show an inverse correlation between boron concentrations and $\delta^{11}B$ values (Moldovanyi et al. 1993). This relationship suggests mixing

between evaporite brines and boron released from clay minerals during burial diagenesis deep within the basin. Moreover, the study also suggests that boron may be a valuable tool for tracing the evolution of oil-bearing reservoirs and metalliferous basinal brines.

Overall, a range of solute tracers, including $\delta^{13}C$ in dissolved inorganic carbon, $\delta^{37}Cl$, $\delta^{81}Br$, $^{87}Sr/^{86}Sr$, $\delta^{34}S$ in sulfate, and ^{11}B may provide an enhanced perspective on chemical evolution during surface/groundwater exchange and are applied collectively to provide a sharper focus on chemical interaction and mixing of water sources.

3.4.3 *Water Age and Evolution (^{14}C)*

Dating of groundwater and solutes is essential to understanding the dynamics of the flow system. In addition, dating results can also be used quantitatively to evaluate numerical modeling simulations, and to detect and investigate perturbations arising from pumping and waste disposal. The ^{14}C content in dissolved inorganic carbon is a well-established technique for constraining the age of waters for groundwaters younger than 50,000 years old (see Fontes and Garnier 1979).

3.4.4 *Tracers for Hydrocarbon Source and History*

A combination of high-resolution characterization of natural organic compounds, naphthenic acid profiles, extractable priority pollutants (EPP), and volatile priority pollutants (VPP) were analyzed on the different water samples to see if these tracers can be used to shed light on the source and history of hydrocarbons. Fourier transform ion cyclotron resonance mass spectrometry (FT-ICR MS) is being employed to analyze natural organic compounds dissolved in water samples. This technique offers the highest available broadband mass resolution power and mass accuracy, therefore makes it possible to identify individual compounds in a complex mixture of organics.

3.5 Geochemical Modeling

Geochemical models were used to calculate saturation indices for discrete mineral phases (MINTEQ2A) and to refine ^{14}C ages using geochemical mass-balance reactions (NETPATH). The models used are summarized below.

3.5.1 *MINTEQ2A*

MINTEQA2[1] is an equilibrium/mass-transfer model that calculates saturation indices for discrete mineral phases (Allison et al. 1990). The database of MINTEQA2 was modified to make it consistent with that of WATEQ4F (Ball and Nordstrom 1991). Additional solubility data for Co (Papelis et al. 1988), PO_4 (Baker et al. 1998), and siderite (Ptacek 1992) was also incorporated into the database. MINTEQA2 allows oxidation–reduction potentials (ORP) either to be entered as measured Eh or H_2S or to be calculated from a measured oxidation–reduction couple.

[1] See http://www.epa.gov/ceampubl/mmedia/minteq/

3.5.2 *NETPATH Modeling*

The computer program NETPATH[2] was used to correct the ^{14}C ages using inverse geochemical modeling to simulate geochemical reaction models by using chemical and isotopic data (Parkhurst and Charlton 2008, Plummer et al. 1991, 1994). NETPATH can be used to model the processes of dissolution, precipitation, ion exchange, oxidation / reduction, degradation of organic compounds, incongruent reaction, gas exchange, mixing, evaporation, and dilution. The inverse model NETPATH can be used to adjust radiocarbon data for geochemical reaction effects and to refine estimates of radiocarbon age (e.g., Aravena et al. 1995, Bayari et al. 2009, McMahon et al. 2008, Plummer and Sprinkle 2001, van der Kemp et al. 2000).

4 RESULTS

A comprehensive summary of the data currently available are included as Appendix 1 and Appendix 2. We are still waiting for results for a few routine, trace metals, and stable isotopes, analyses. Unfortunately, due to analytical difficulties, a large number of halogen stable isotope analyses are still outstanding, especially for $\delta^{81}Br$. The coarse tailings samples contained large amounts of sediment and organic residue and were consequently very difficult to filter. The small volumes of water obtained from these samples did not allow for the full suite of analyses to be performed.

4.1 Water Isotopes ($\delta^{18}O$, $\delta^{2}H$, ^{3}H)

Various types of waters sampled in this survey are plotted in $\delta^{2}H$ -$\delta^{18}O$ space in Figure 20.

[2] See http://wwwbrr.cr.usgs.gov/projects/GWC_coupled/netpath/

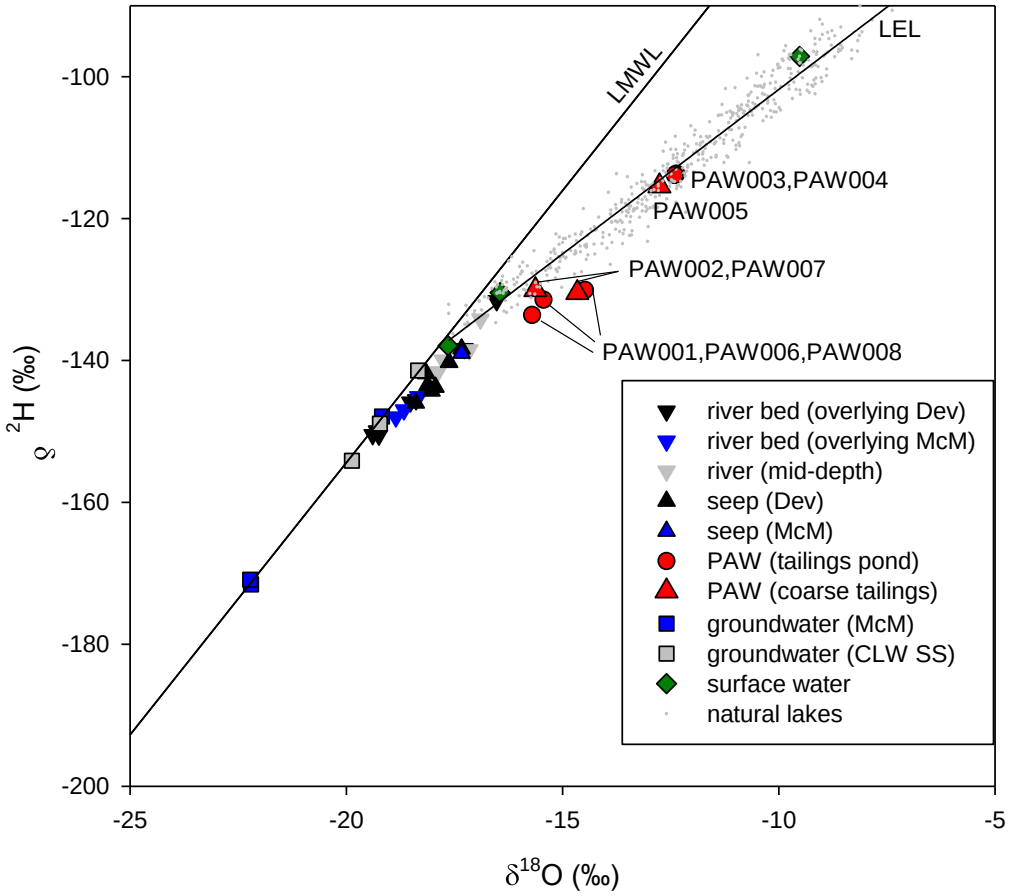

Figure 20. Stable water isotope compositions of various waters collected during this study relative to the local meteoric water line (LMWL) and local evaporation line (LEL).

Note that the fine dots indicate isotopic composition of lakes sampled in the Fort McMurray area, 2002-2010.

4.1.1 *Oxygen-18 and Deuterium*

Oxygen-18 and deuterium measured in groundwater samples ranged from -18.34‰ to -22.22‰ for $\delta^{18}O$ and -141.4‰ to -171.6‰ for $\delta^{2}H$ and plot close to the Local Meteoric Water Line (LMWL, Edmonton). The most depleted groundwater sample (BAS25 and duplicate BAS25A) has an isotopic signature consistent with deep groundwater containing a significant component of heavy-isotope depleted sub-glacial paleorecharge, similar to some Cretaceous groundwaters and many saline springs sampled in the Fort McMurray area (e.g., Grasby and Chen 2005). Other groundwater samples plot intermediate between these deeper groundwaters and the mean annual precipitation, suggesting stronger but variable connections between deep groundwater and modern recharge sources. The isotopic composition of mean precipitation lies close to the

intersection of the LMWL and the Local Evaporation Line (LEL), defined by regression of lake water values in the area.

Tailings ponds and other process-affected waters have isotopic signatures reflecting evaporative enrichment during residency in surface storage, and are offset significantly to the right of the LMWL. The composition of the process-affected water samples ranged from -12.40‰ to -14.48‰ in $\delta^{18}O$ and -113.7‰ to -130.5‰ in $\delta^{2}H$. Several process-affected water samples plot roughly along the defined Local Evaporation Line (LEL). Process-affected water samples from Shell Albian and CNRL tailings ponds plot just below the LEL. This likely indicates that the initial $\delta^{18}O$ and $\delta^{2}H$ composition of water used in the bitumen refining process was more negative than the weighted mean annual composition of precipitation, as would be expected for water sources from the Athabasca River, which drains higher altitude regions upstream. More depleted signatures may also indicate an influence from trapped water within the bitumen zone or from groundwater use or dewatering. Process-affected water samples obtained from the tailings ponds have almost the same isotopic signature as the coarse tailings samples, indicating that water in the processing circuit at all of the sites is evaporatively enriched before being discharged to the pond. This may be due to evaporative enrichment during the processing, or use of recycled water.

The $\delta^{18}O$ and $\delta^{2}H$ signatures of the different tailings ponds may therefore not be solely related to pond water balance as in the case of natural lakes. The most enriched process-affected water samples were from Syncrude tailings pond (PAW003, PAW004) and the least enriched were seepage collection and recycled water ponds from CNRL and Shell Albian (PAW006, PAW008). The degree of evaporative enrichment observed in the process-affected water samples was not as great as observed in some natural closed-basin lakes, despite recycling, although this is likely to be reflective of higher inflow and hence lower evaporation/inflow ratios which determines offset from the LMWL. Differences in enrichment could also be influenced by differences in the residence times of water in the different ponds (longer residence time and more evaporation in the Syncrude pond). Other factors might include the age of the tailings ponds, or recycling/processing methods.

There are a number of samples for the Athabasca River. Ten grab samples were taken along the course of the geophysical survey near the river bed interface (S01 to S10) in June, 2009, and samples were also taken from the main river channel at the upstream and downstream ends of the reach in September 2009 (PAWS and PAWN) and November 2009 (PAWS2 and PAWN2). It should be noted that the river samples were taken as grab samples at mid-depth in the centre of the channel but without depth/width integration. The $\delta^{18}O$ and $\delta^{2}H$ compositions of the Athabasca River at the start of the survey (just north of Fort McMurray) are only slightly more negative ($\delta^{18}O$ = -17.9 ‰, $\delta^{2}H$ = -141.6‰) than the compositions measured at the end of the survey ($\delta^{18}O$ = -16.9 ‰ and $\delta^{2}H$ = -134.17 ‰) near the confluence with the Firebag River) indicating a small degree of net evaporative enrichment along this stretch of the river. The $\delta^{18}O$ and $\delta^{2}H$ composition of the Athabasca River samples was intermediate between groundwater and

the process-affected waters, with values ranging from -17.15‰ to -17.88‰ in $\delta^{18}O$ and -138.5‰ to -141.6‰ in $\delta^{2}H$.

In general the $\delta^{18}O$ and $\delta^{2}H$ composition of river bed seeps were intermediate between the Athabasca River water and groundwater with an isotopic range from -16.52‰ to -18.4‰ in $\delta^{18}O$ (from -131.6‰ to -150.5‰ in $\delta^{2}H$). S03A was the only seep sampled along the stretch of the river where the McMurray Formation outcrops, all of the other seeps were located where Devonian carbonates outcrop. The range of $\delta^{18}O$ and $\delta^{2}H$ composition of the seeps and the presence of ^{3}H are consistent with the seeps containing a mixture of groundwater discharge and river water.

While the groundwater and tailings pond waters are distinct from one another, direct identification of process-affected water in seeps using stable isotopes of water alone is complicated by the intermediate isotopic composition of the Athabasca River. In general, seep signatures appear to reflect mixtures of groundwater and Athabasca River water and/or other surface water.

4.1.2 *Tritium*

Tritium was found to range from below detection limit (<0.8 TU) to 7.4 TU in groundwater samples. The absence of tritium in samples from the groundwater well with the most depleted stable isotope signatures (BAS25), is consistent with groundwater at this location containing a significant component of sub-glacial paleorecharge with no mixing with modern recharge. Tailings ponds and other process-affected waters were found to have tritium levels ranging from 7.8 TU to 12.8 TU, with a range spanning that of local precipitation, shallow groundwater, and local lakes. Athabasca River waters were also found to contain tritium, ranging from 7.9 TU to 13.1 TU. Groundwater seeps were found to contain between 9.2 TU and 12.8 TU. This is consistent with the seep samples containing a mixture of groundwater and Athabasca River water. While presence of tritium in seeps suggests a component of modern recharge and/or river water, no definitive labelling of process-affected waters in seeps is possible with tritium alone.

A plot of enriched tritium versus electrical conductivity (Figure 21) illustrates the tendency for river water to be more dilute and to contain higher levels of tritium than groundwater. Process-affected waters and seeps tend to have higher EC and higher tritium but the signatures are not distinct enough to partition source components.

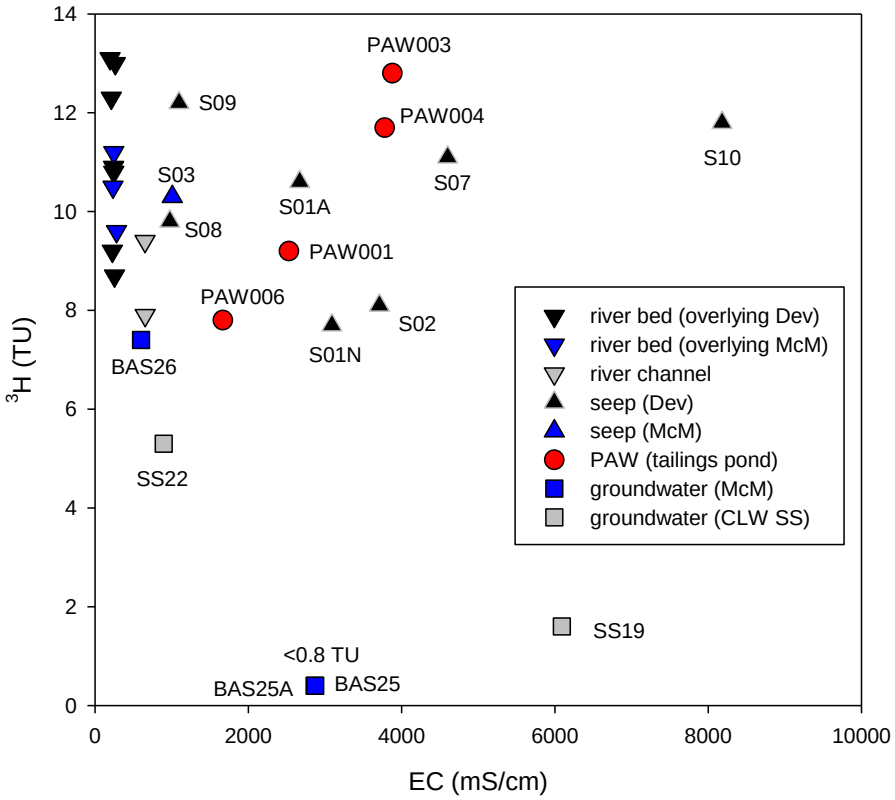

Figure 21. Relationship between enriched tritium and electrical conductivity in various waters collected during this study.

4.2 Solute Isotopes

4.2.1 $\delta^{13}C_{DOC}$

The $\delta^{13}C_{DOC}$ signature of dissolved organic carbon varies with total organic carbon content and by water type (Figure 22). Variations in $\delta^{13}C_{DOC}$ with electrical conductivity are also shown (Figure 23). Process-affected waters have a $\delta^{13}C_{DOC}$ range of -28.88‰ to -29.89‰; ground-waters range from -27.73‰ to -28.67‰ and the Athabasca River waters range between about -27.60‰ and -26.70‰. The process-affected waters, groundwaters and river water all seem to have fairly discrete ranges of $\delta^{13}C_{DOC}$. In contrast, the river bed seepage samples have a much wider range, between -26.71‰ and -29.31‰. The seeps with the most negative $\delta^{13}C_{DOC}$ were S03, the only seep located along the stretch of the Athabasca River where the McMurray Formation outcrops, and S10A, the seep with the highest electrical conductivity. The similarity between the $\delta^{13}C_{DOC}$ of the process-affected waters and S03 may indicate that dissolved organics in the McMurray Formation, with more negative $\delta^{13}C_{DOC}$, are a significant influence on both samples. Additional samples from the McMurray Formation are recommended to better characterize this end member.

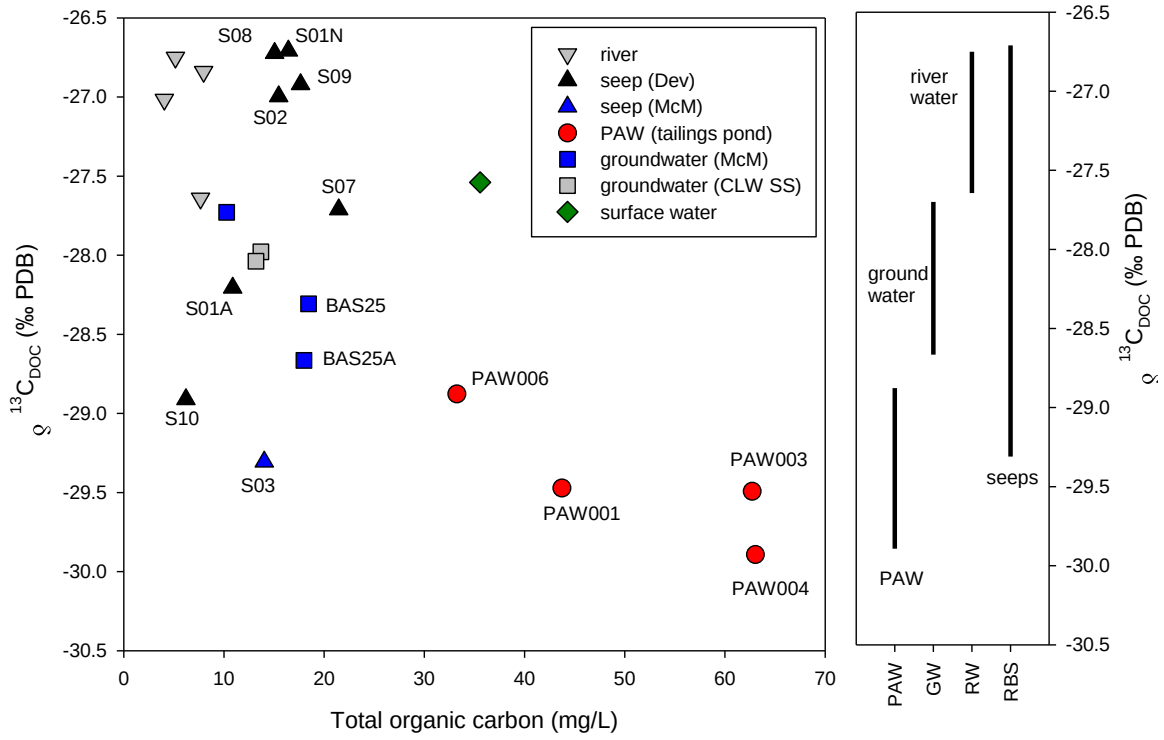

Figure 22. Variation in $\delta^{13}C_{DOC}$ with total organic carbon content in different types of water.

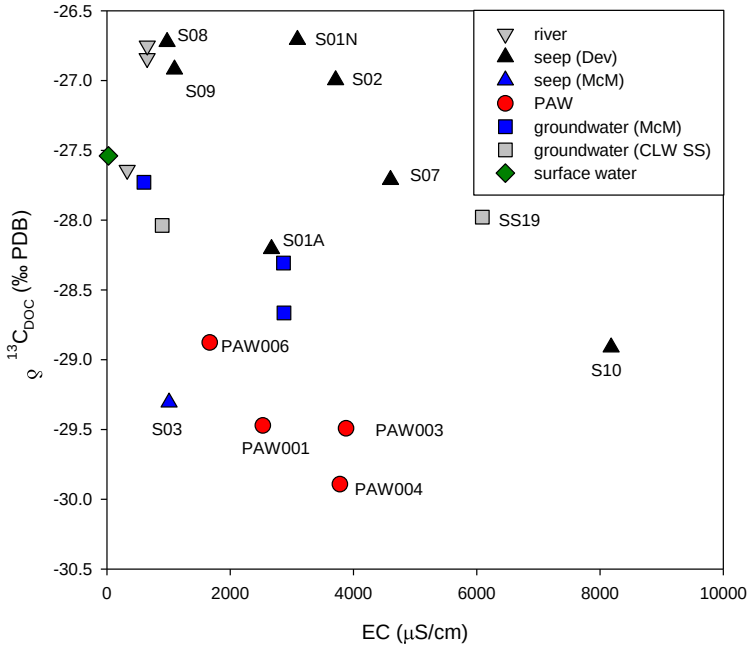

Figure 23. Relationship between carbon-13 in dissolved organic carbon and electrical conductivity of various waters.

The effectiveness of $\delta^{13}C_{DOC}$ labelling of the various types of water still needs further assessment with a larger sampling pool. Characterizing the $\delta^{13}C_{DOC}$ of organic-rich formation waters should be done. The samples available for this study from groundwater wells situated in the McMurray Formation are fairly dilute and possibly not representative of the more saline, organic-rich portions of the unit.

4.2.2 $\delta^{13}C_{DIC}$

The $\delta^{13}C$ signatures in dissolved inorganic carbon ($\delta^{13}C_{DIC}$) show a large range, varying from -21.08‰ to 4.05‰. River water samples plot in a fairly tight cluster characterized by $\delta^{13}C$ in the range of -9.6‰ to -5.6‰ and low alkalinity (Figure 24).

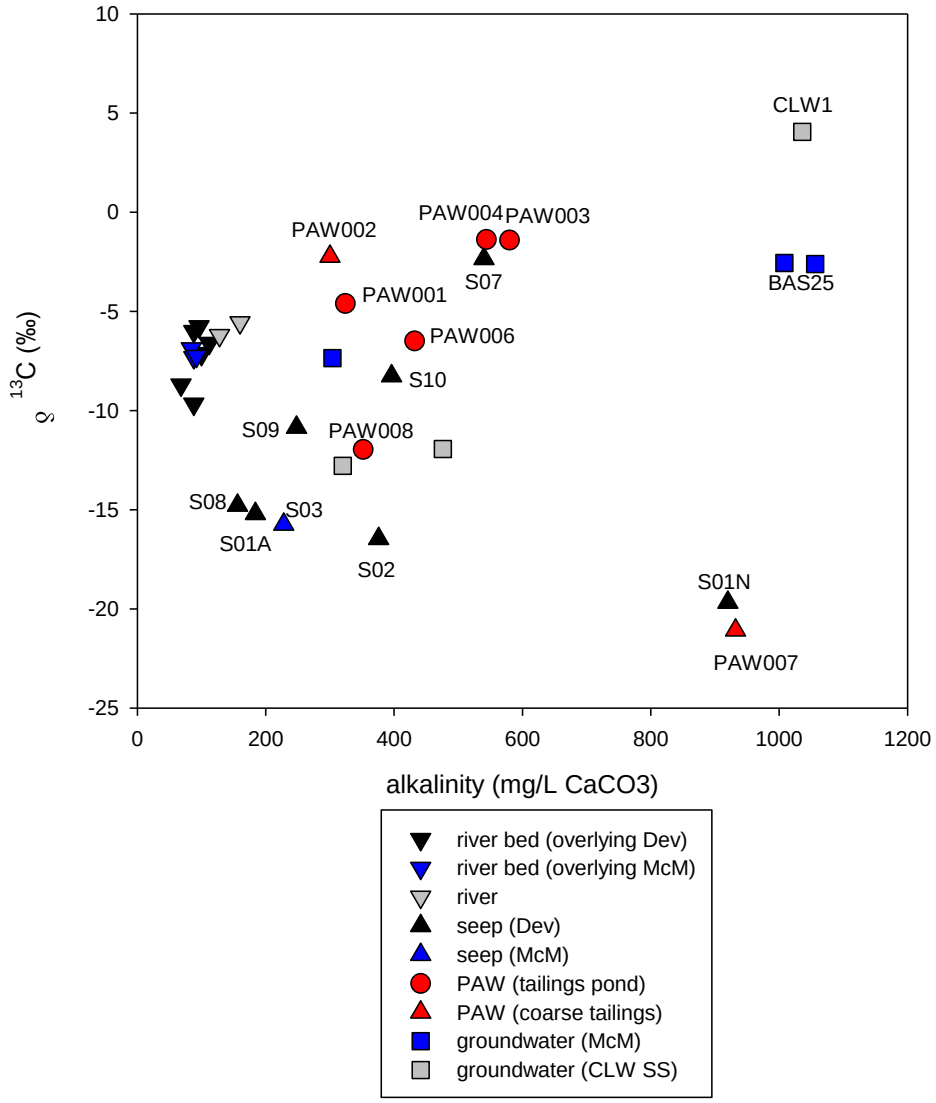

Figure 24. Relationship between carbon-13 in dissolved inorganic carbon and alkalinity in various waters.

The process-affected waters also display a relatively wide range in both $\delta^{13}C_{DIC}$ and alkalinity. Comparison between signatures of coarse tailings and the tailings pond show that changes occur over the processing circuit. The coarse tailings sample from Shell Albian (PAW002) had a slightly more positive $\delta^{13}C$ signature than the tailings pond (PAW001) which was slightly more positive than tailings seepage sampled at Shell Albian (PAW006). The coarse tailings sampled from CNRL (PAW007) plots as an anomaly among process-affected waters, with a negative $\delta^{13}C$ signature and very high alkalinity. There is a large shift between the signature of this water and a recycled tailings pond at CNRL (PAW008). This may be due to fact that CNRL injects waste carbon dioxide (CO_2) into the tailings slurry lines before they discharge to the pond. However, a natural seep (S01N) bears a similar signature.

A wide range of overlap among process-affected waters, groundwaters and river bed seepage makes it difficult to use the $\delta^{13}C_{DIC}$ alone to label the various waters.

4.2.3 *$^{87}Sr/^{86}Sr$*

The isotopic composition of strontium can be a sensitive tracer for hydrological cycles in calcium rich systems, and can provide information on the origin of the dissolved solids. Substitution of Sr^{2+} for Ca^{2+} in plagioclase feldspar, calcite, dolomite, aragonite, gypsum and apatite can result in unique signatures for different units that can give a history of the rock type that water has been in contact with. The range of $^{87}Sr/^{86}Sr$ signatures observed in the river water in this study is tightly constrained (Figure 25), with ratios ranging from 0.7102 to 0.7107, indicating a stable weathering source.

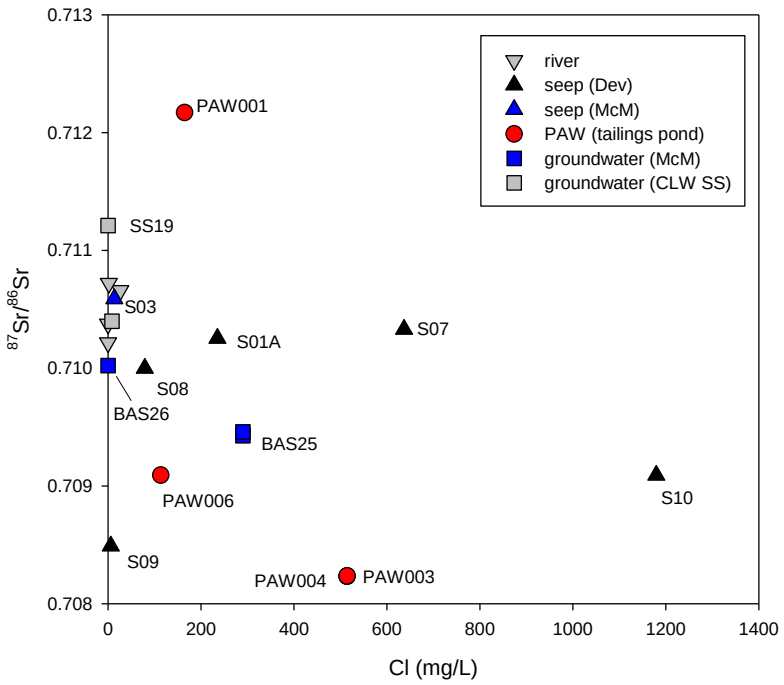

Figure 25. Relationship between strontium isotope signatures and chloride in various waters.

The different tailings pond waters have distinct $^{87}Sr/^{86}Sr$ signatures with a range somewhat larger than the range of groundwater or surface waters sampled in this survey, but less variable than previously observed in the area (ranging from 0.7074 to 0.7125, unpublished data). Note that a result for PAW007 is not yet available. $^{87}Sr/^{86}Sr$ signatures in the seeps vary from 0.7085 to 0.7106. It is significant to note that the seep with the highest chloride occurs in an area of Devonian subcrop (S10) and has a strontium signature typical of Devonian evaporates. Variations of $^{87}Sr/^{86}Sr$ in the other seeps likely reflect mixing of dissolved solids with multiple younger sources. In groundwater, the $^{87}Sr/^{86}Sr$ signatures range between 0.7094 and 0.7112. As process-affected water is a complex mixture of dissolved solids from river water and formation water, further work is required to assess full potential for labelling using $^{87}Sr/^{86}Sr$.

4.2.4 $\delta^{37}Cl$

We are still waiting for a few $\delta^{37}Cl$ results, but the data currently available (Figure 26) show a fairly large range in chlorine stable isotope signatures, with $\delta^{37}Cl$ values ranging from -1.62‰ to 1.02‰ in the different water types. In groundwaters, $\delta^{37}Cl$ values range from -0.98‰ to 0.28‰, which is similar to the $\delta^{37}Cl$ distribution in the Athabasca River (from -0.85‰ to 0.49‰). The process-affected waters have $\delta^{37}Cl$ signatures that vary between 0.21‰ and 0.75‰. The largest range in $\delta^{37}Cl$ signatures was found in the river seeps which had values ranging from -1.62‰ to 1.02‰. The seep S07 had the most positive $\delta^{37}Cl$ signature, and this was in an area of Devonian subcrop.

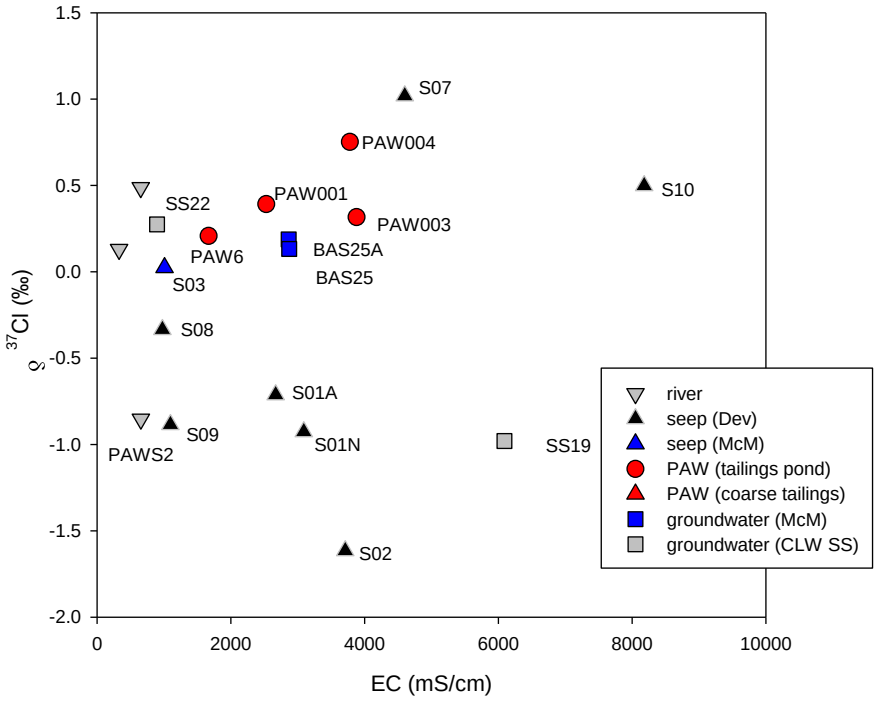

Figure 26. Relationship between chlorine-37 and electrical conductivity in various waters.

4.2.5 $\delta^{11}B$

$\delta^{11}B$ signatures demonstrate a wide range of variability (Figure 27). The seep samples had the largest range in $\delta^{11}B$ signatures with values ranging from 17‰ to 49‰. The very positive 49‰ $\delta^{11}B$ composition measured at S07 is of particular interest since this sample also had a very positive $\delta^{37}Cl$ signature. Process-affected waters had $\delta^{11}B$ signatures between 22‰ to 25‰. The coarse tailings from Shell Albian (PAW2 $\delta^{11}B$ = 23‰) is similar to the $\delta^{11}B$ signature for the tailings pond at Shell Albian (PAW1 $\delta^{11}B$ = 22‰). The two Athabasca River samples had $\delta^{11}B$ signatures of 16‰ and 20‰. More samples are necessary to further evaluate the possibility of using $\delta^{11}B$ values identify process-affected waters.

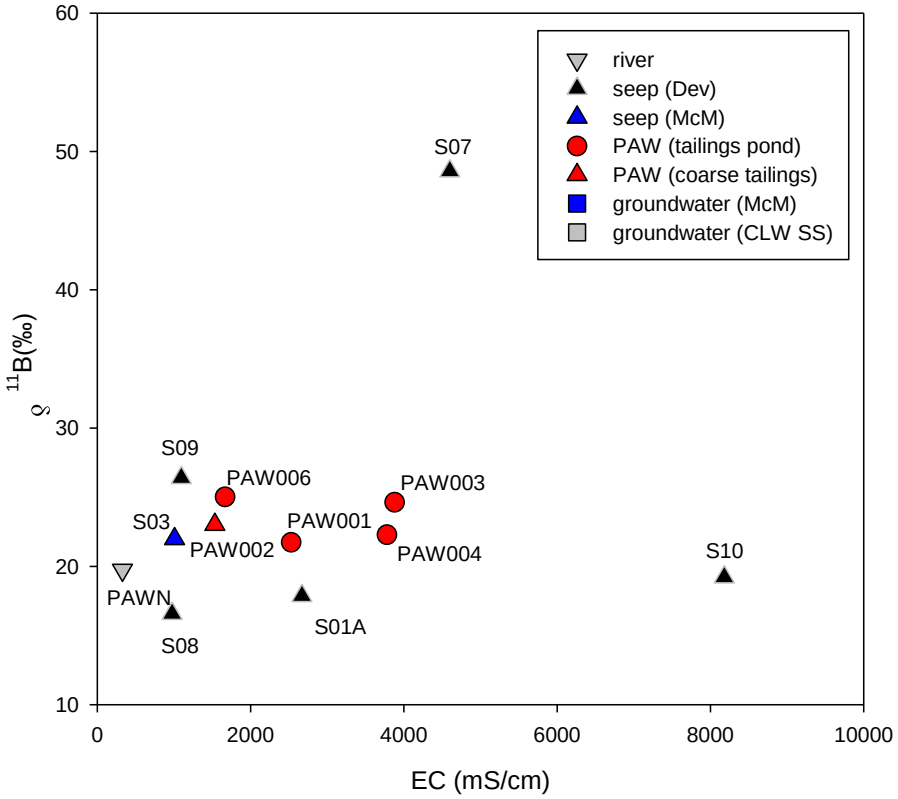

Figure 27. Relationship between boron-11 and electrical conductivity in various waters.

4.2.6 $\delta^{34}S$

Since sulfur is an important heteroatom in oil sands production, isotope signatures of dissolved sulfate ($\delta^{34}S_{SO4}$) were also investigated to understand sulfur-related geochemical processes (Figure 28). A wide range of $\delta^{34}S_{SO4}$ values were observed, ranging from -22.50‰ to 29.49‰. Samples from river bed seeps demonstrate the widest variability from -22.50‰ to 11.34‰ in $\delta^{34}S_{SO4}$.

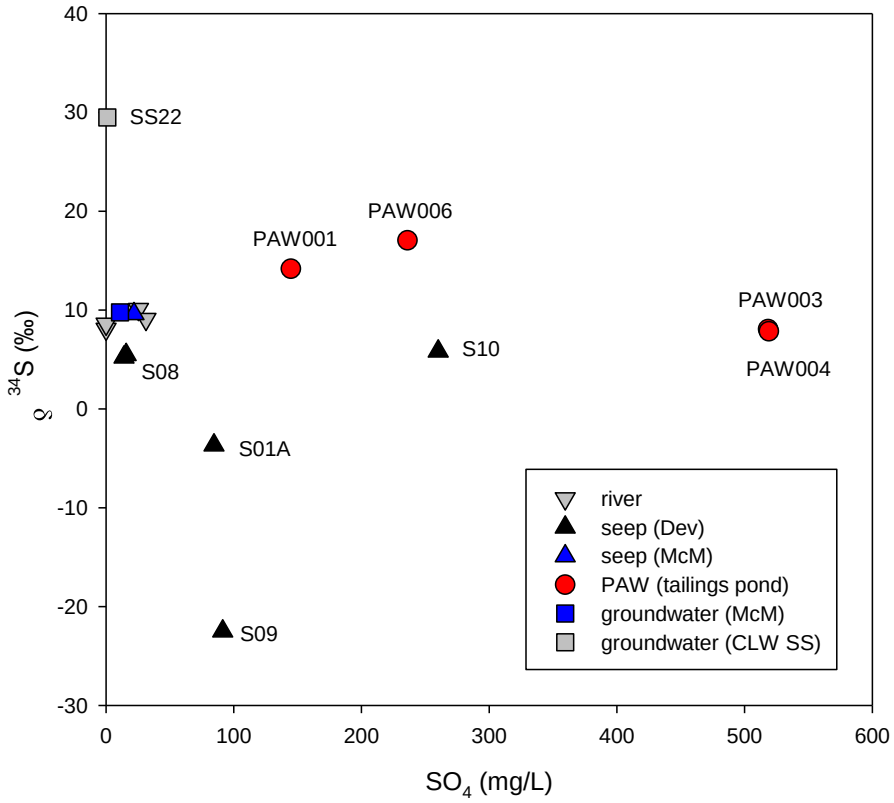

Figure 28. Relationship between sulfur-34 and sulfate concentrations in selected waters.

Process-affected waters and river waters showed similar distribution patterns in $\delta^{34}S_{SO4}$, varying between 7.84‰ and 17.04‰ for the former, and 8.09‰ to 10.09‰ in the latter. Groundwater samples reveal over 20‰ variability in $\delta^{34}S_{SO4}$ (from 9.78‰ to 29.49‰). The distinct $\delta^{34}S_{SO4}$ distribution in river bed seepage and groundwater suggests that different sulfate sources and modification processes in the different types of water. $\delta^{34}S_{SO4}$ values between 7‰ and 15‰ are generally considered to have atmospheric input as their main sources. Sulfate sources in the area also include oxidation of sulfides particularly in shales, commonly producing SO_4 with $\delta^{34}S$ ranging from +5‰ to-20‰, and Devonian evaporates commonly more enriched than about 20‰. Very high $\delta^{34}S_{SO4}$ values (>30.0‰) are usually an indicator of bacterial sulfate reduction. Based on this understanding, it appears that oxidation or atmospheric interaction may be dominant process in seeps and river water whereas bacterial sulfate reduction may be important for the sulfur cycle in some groundwater formations (e.g., SS22). Process-affected water may be fairly constant and intermediate in composition because it is regulated by sulfur composition of bitumen and secondarily by mixing between sulfate derived from evaporate dissolution, atmospheric sources, and with river water strongly influenced by atmospheric and weathering inputs. Additional distinction is provided when both sulfur-34 and carbon-13 are compared

(Figure 29). In this case, with the exception of S07, river seeps are shown to be more similar to river water or groundwater than process-affected water.

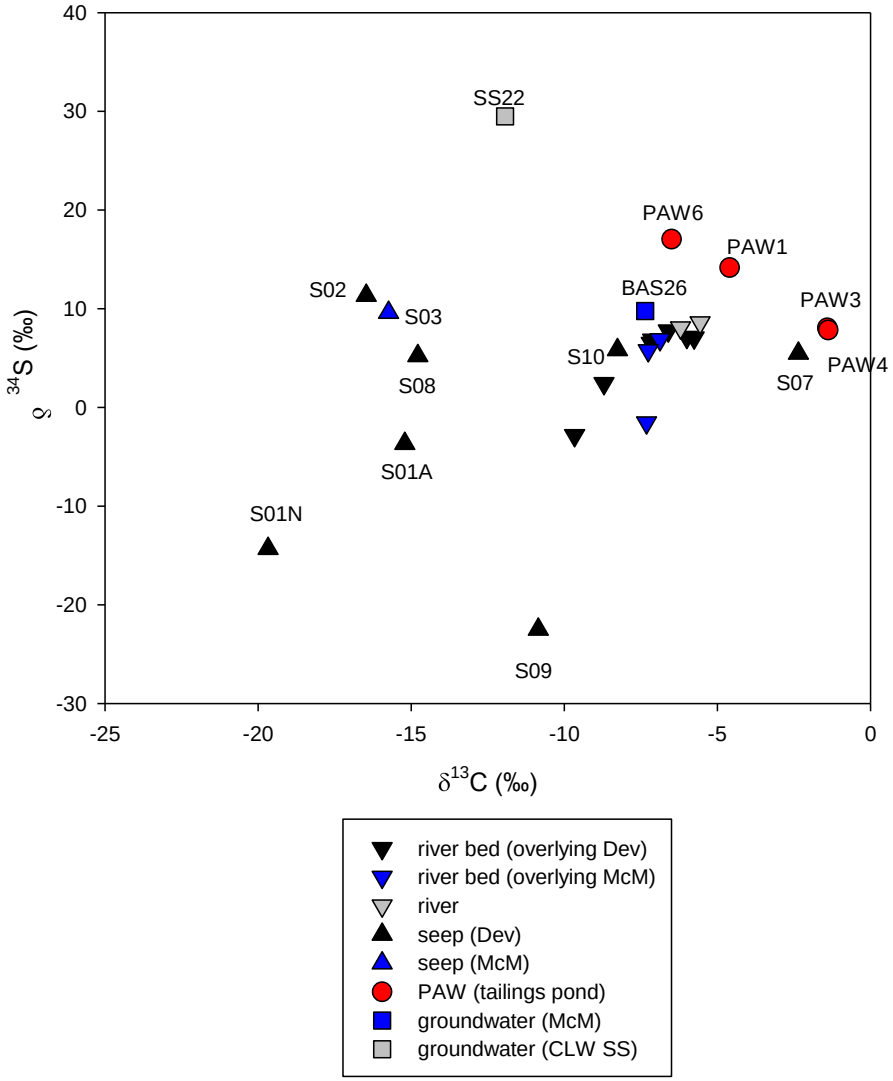

Figure 29. Relationship between sulfur-34 and carbon-13 in dissolved inorganic carbon in various waters.

4.2.7 *Radiocarbon*

^{14}C in dissolved inorganic carbon was measured in 30 samples to assess the age of solutes and water (Figure 30). While absolute age dating can be complicated by chemical reactions and mixing, especially in shallow aquifer systems, the percentage modern carbon (pMC) is a useful qualitative indicator of the water age. The lowest ^{14}C concentrations, 2.4 pMC to 2.6 pMC, were measured in BAS25 the McMurray Formation groundwater samples previously noted as having the stable isotope signature of sub-glacial paleorecharge and tritium levels of <0.8 TU. These

water samples are apparently representative of very old groundwaters, likely recharged during the last glaciation possibly as long ago as 30,000 years. Other groundwater samples ranged from 55 pMC to 75.6 pMC suggesting somewhat younger ages of 2,000 years to 5,000 years. In comparison, Athabasca river water was found to have pMC ranging from 87.3 to 89.5, which indicates a mean age of about 1,000 years, consistent with the river being fed by a small but significant portion of old groundwater. Seeps were found to range between 62.7 pMC and 88.7 pMC indicating mean water ages in the range of about 1,000 years to 4,000 years. The fairly low ^{14}C concentrations of process-affected waters are surprising since they are all known to be produced recently and in contact with modern atmospheric carbon. This artificially old age may be due to inputs of "dead carbon" by carbonate dissolution or methanogenesis. The samples from Shell Albian (PAW002, PAW001, PAW006) all had similar ^{14}C concentrations (36 pMC to 39 pMC) and the samples from Syncrude (PAW003, PAW004) also had the same ^{14}C concentrations (17 pMC). The high content of modern carbon in seeps, even those sampled in the Devonian and McMurray Formation substrates is significant, as it indicates an environment of significant mixing with modern waters, even where deep old groundwaters are apparently discharging.

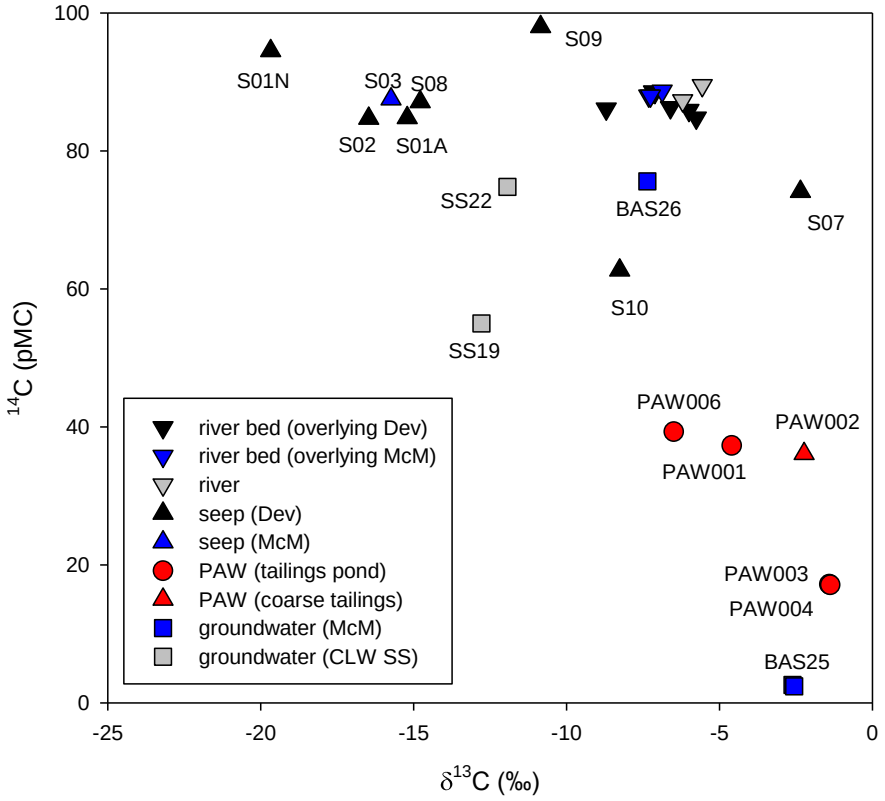

Figure 30. Relationship between carbon-14 and carbon-13 in dissolved inorganic carbon.

4.2.8 *Major Ions and Trace Elements*

The major ion geochemistry of waters sampled in this survey (Figure 31) was within the range previously measured for the major hydrostratigraphic units in the region (unpublished data). River waters are typically Ca-Na-Mg-HCO_3 type waters. The six groundwater samples were from the McMurray Formation (BAS25, BAS25A, and BAS26), Clearwater Formation (CRW1) and from two surficial aquifers (SS19, SS22). While these samples provide general information about the isotopic and geochemical signatures of formation waters and surficial aquifers for comparison with process-affected waters, their selection was based on opportunistic sampling facilitated by Alberta Environment. As such, the results do not capture the full range of variation observed in groundwater chemistry. The McMurray samples available for this survey were all fairly dilute Na-HCO_3 type waters. High salinity Na-Cl type waters also occur commonly in the McMurray and Devonian formations but are not represented. The river seeps show a large range in compositional types, ranging from Ca-Na-Mg-HCO_3 type waters (S03 and S09) similar to river water compositions, to Na-Ca-Cl type waters (S10). The process-affected waters tended to have Na as their dominant cation and a mixed anion composition, and plot in a fairly tight cluster on the Piper plot, with the exception of PAW006. This sample was collected from a seepage collection system so it likely represents a mixture of tailings pond water with surficial groundwater.

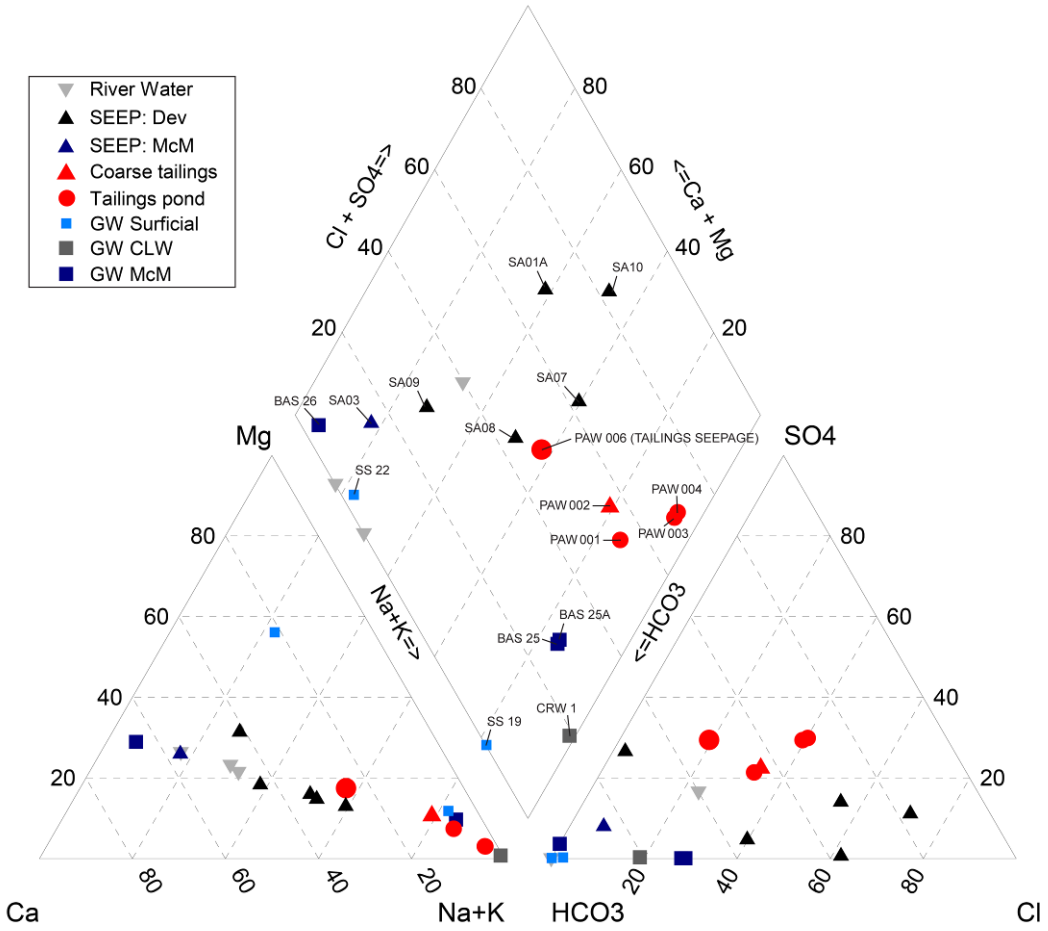

Figure 31. Piper plot showing variation in major ion signatures.

The ratio of major ion compositions for the process-affected water overlaps with groundwater from the Lower Grand Rapids and Clearwater Formations and alone would not be useful for fingerprinting.

There were some significant differences in trace ion concentrations between the different water types that suggest they may be of use for identifying process-affected waters. Trace ion concentrations are available for four tailings ponds and one coarse tailings sample. We are still waiting on results for one additional tailings pond sample and one additional coarse tailings sample. Coarse tailings (PAW002) was found to have significantly higher concentrations of many trace elements than the tailings pond at the same facility (PAW001) even though the EC measured in the pond was higher than the EC of the coarse tailings and the samples have similar major ion ratios (Figure 31). Coarse tailings had higher concentrations of some trace ions including Al, Si, Fe, and Mn (Table 9) as well as high concentrations of total organic carbon. The concentrations of Li and Mo were generally higher in the tailings pond waters than in any of the groundwater sampled in this survey. Other elements like Si, Fe and Mn tended to have

higher concentrations in groundwater than in process-affected water. This is attributed to lower mobility under oxic conditions. Selected variations in trace metals in relation to electrical conductivity are shown in Figure 32.

Table 9. Summary of trace element signatures in various process-affected water samples.

Operator	Sample ID	Li (µg/L)	Al (µg/L)	Si (µg/L)	Ti (µg/L)	Cr (µg/L)	Mn (µg/L)	Fe (µg/L)	Co (µg/L)	Zn (µg/L)	Mo (µg/L)	As (µg/L)
Albian	**PAW001 (tailings pond)**	169.6	46.48	6220.55	1	0.66	65.27	47.63	6.47	1.39	63.18	4.59
	PAW002 (coarse tailings)	194.26	9731.31	22103.79	79.82	59.4	2678.5	72528.08	42.41	111.47	35.5	17.55
	PAW006 (tailings seepage)	171.73	27.32	10855.36	2.2	0.62	1242.54	123.49	35.8	1.42	6.75	5.46
Syncrude	**PAW003 (tailings pond)**	227.76	53.8	4927.61	1.04	0.66	54.47	71.17	2.93	2.17	142.83	7.25
	PAW004 (tailings pond)	230.05	41.97	4994.23	1.01	0.91	53.64	60.88	2.96	1.82	143.87	6.98

When plotted with our fairly limited groundwater dataset the potential for using trace elements like Mo and Li appears quite promising, however, Devonian brines in the region are known to have overlapping concentrations. We suggest that a priority for future work should be to develop a more comprehensive groundwater dataset representative of regional variability.

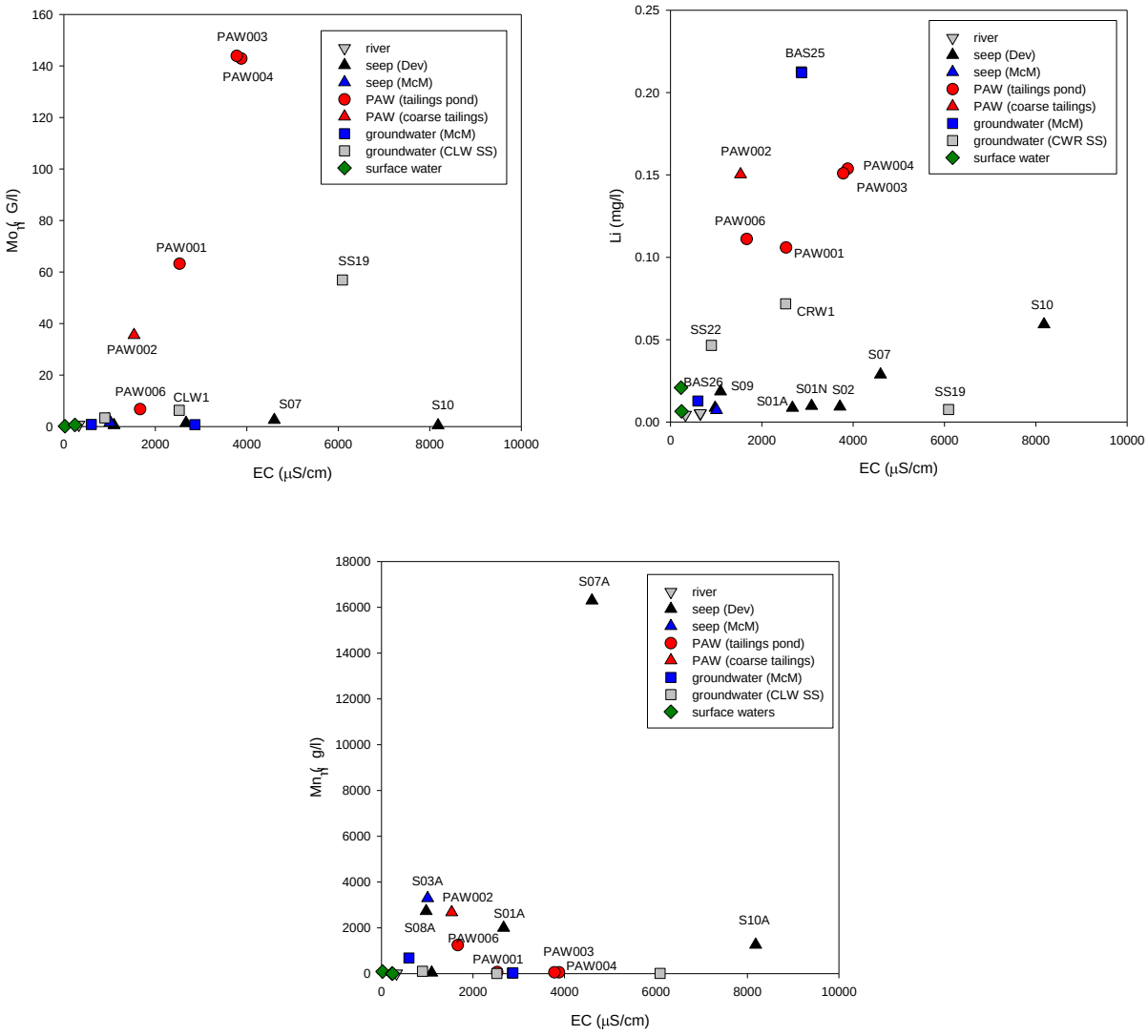

Figure 32. Relationship between trace metals (molybdenum, lithium, manganese) and electrical conductivity of various waters.

4.3 Geochemical Modelling

4.3.1 *MINTEQA2*

We are still waiting for the results of routine and trace geochemical analyses on the seep and river samples, but speciation modelling using MINTEQA2 has been performed using all of the available geochemical data (selected results presented in Tables 10 to 12).

Saturation indices near zero indicate equilibrium conditions and could indicate a mineral phase controlling water chemistry. The saturation indices calculated for the process-affected waters

did not indicate any unusual mineral phases controlling water chemistry. The saturation indices for many of the samples are near zero for carbonate minerals indicating carbonate dissolution is an important control on water chemistry.

Table 10. Carbonate mineral saturation indices calculated using MINTEQA2.

Well	**Calcite** $CaCO_3$	**Dolomite** $CaMg(CO_3)_2$	**Siderite** $FeCO_3$	**Magnesite** $MgCO_3$	**Rhodochrosite** $MnCO_3$	**Strontianite** $SrCO_3$
S09A	0.965	1.809	-3.621	0.295	-0.855	-0.703
S08A	-0.324	-0.949	-0.679	-1.181	0.202	-1.934
S07A	0.292	0.308	0.402	-0.546	0.910	-1.238
S10A	0.358	0.415	1.055	-0.504	-0.347	-1.257
S03A	-0.101	-0.552	-2.943	-1.000	0.251	-1.715
S01A	-0.254	-0.863	-6.042	-1.164	-0.263	-1.779
PAW 001	0.038	0.142	-9.001	-0.468	n/a	-0.972
PAW 002	-0.352	-0.728	-1.646	-0.908	-0.927	-1.331
PAW 003	0.419	0.787	-8.394	-0.163	0.261	-0.354
PAW 004	0.404	0.775	-8.409	-0.165	-0.806	-0.357
PAW 006	0.67	1.066	-8.318	-0.125	-0.805	-0.586
BAS 25	0.061	0.162	-7.778	-0.399	-2.501	-0.757
BAS 25A	0.397	0.833	-7.791	-0.064	-1.523	-0.413
BS 26	-0.113	-0.759	-8.27	-1.146	-1.283	-2.076
CRW 1	-0.584	-1.278	-7.144	-1.195	-0.538	-1.182
SS 19	0.23	0.561	-8.711	-0.17	-1.977	-1.198
SS22	0.542	1.318	-6.567	0.276	-1.534	-0.837
NE-09	-3.308	-6.948	-6.473	-4.183	-0.664	-5.353
McClell-09	0.233	0.499	-8.558	-0.273	-3.25	-1.495
AthaR-09	-0.279	-0.955	-7.349	-1.216	-2.502	-1.939

The saturation indices for typical evaporite minerals indicated all of the waters are undersaturated with respect to halite, gypsum and mirabilite. The highest salinity seep sample, S10A, was the least undersaturated for evaporite minerals.

Table 11 Halite and sulfate mineral saturation indices calculated using MINTEQA2.

Well	**Halite** NaCl	**Gypsum** $CaSO_4 \cdot 2H_2O$	**Mirabilite** $Na_2SO_4 \cdot 10H_2O$
S09A	-8.156	-1.753	-7.178
S08A	-6.827	-2.636	-7.623
S07A	-5.228	-2.327	-6.386
S10A	-4.861	-1.006	-5.014
S03A	-8.068	-2.25	-8.338
S01A	-6.184	-1.606	-6.557
PAW 001	-5.954	-2.055	-5.692
PAW 002	-5.959	-1.897	-5.293

Well	Halite NaCl	Gypsum $CaSO_4 \cdot 2H_2O$	Mirabilite $Na_2SO_4 \cdot 10H_2O$
PAW 003	-5.061	-1.766	-3.997
PAW 004	-5.062	-1.771	-4.03
PAW 006	-6.208	-1.323	-5.247
BAS 25	-5.401	-5.135	-7.672
BAS 25A	-5.405	-5.135	-7.68
BS 26	-10.288	-2.491	-9.059
CRW 1	-5.594	-4.743	-6.151
SS 19	-9.036	-5.455	-8.75
SS22	-7.945	-3.884	-8.681
NE-09	-12.226	-5.430	-13.681
McClell-09	-10.399	-4.962	-11.808
AthaR-09	-9.229	-2.372	-8.747

Near-equilibrium conditions with respect to Fe-hydroxide exist for some samples, indicating this mineral phase may be controlling the concentration of Fe and other trace metals. Silicate minerals are near equilibrium in process-affected water samples with the exception of PAW002.

Table 12. Oxide mineral saturation indices calculated using MINTEQA2.

Well	Fe-Hydroxide $Fe(OH)_3$	Goethite α-FeO(OH)	Gibbsite $Al(OH)_3$	Chalcedony SiO_2	Christobalite SiO_2
S09A	0.044	5.52	0.886	0.039	0.128
S08A	-0.821	4.717	1.603	0.114	0.199
S07A	-0.74	4.847	1.988	-0.099	-0.016
S10A	-0.24	5.332	1.781	-0.478	-0.394
S03A	-1.761	3.712	2.418	0.345	0.434
S01A	-2.67	2.849	1.969	0.179	0.265
PAW 001	-1.76	3.924	1.262	0.009	0.009
PAW 002	5.073	10.426	4.394	-4.508	-4.508
PAW 003	-0.683	4.670	1.309	0.035	0.035
PAW 004	-0.734	4.647	1.153	0.029	0.029
PAW 006	-1.434	3.855	1.467	0.401	0.401
BAS 25	-2.48	2.689	2.087	0.077	0.185
BAS 25A	-1.788	3.381	1.752	0.095	0.203
BS 26	-0.778	4.391	2.241	-0.011	0.097
CRW 1	-0.876	4.293	2.215	0.023	0.131
SS 19	0.32	5.489	0.206	-0.745	-0.637
SS22	0.362	5.531	1.441	0.198	0.306
NE-09	-5.481	-0.047	0.335	-0.634	-0.542
McClell-09	-1.434	3.973	0.261	0.134	0.227
AthaR-09	0.062	5.47	1.121	-0.875	-0.782

4.3.2 *NETPATH*

The computer program NETPATH was used to estimate mean ^{14}C ages using a variety of different ^{14}C age correction models (Table 13).

Table 13. ^{3}H and ^{14}C results for water samples, with ages interpreted with the aid of NETPATH.
A dash (-) indicates that the water age is interpreted to be modern.

	$\delta^{13}C_{DIC}$ (‰)	**pMC** (%)	**Tritium** (TU)	Mass Balance (yrs)	Vogel (yrs)	Tamers (yrs)
S01	-14.2	88.5	10.8	1000	-	-
S02	-14.3	88.6	10.9	1000	-	-
S03	-6.9	88.7	10.5	990	-	-
S04	-7.3	88.0	11.2	1060	-	-
S05	-7.3	88.0	9.6	1060	-	-
S06	-6.6	86.3	13.0	1220	-	-
S07	-6.0	85.9	9.2	1260	-	-
S08	-8.7	86.1	12.3	1240	-	-
S10	-5.8	84.8	8.7	1360	20	-
S01A	-15.2	84.8	10.6	-	20	-
S01N	-19.7	94.5	7.7	-	-	-
S02N	-16.5	84.7	8.1	-	30	-
S03A	-15.7	87.5	10.3	-	-	-
S07A	-2.4	74.1	11.1	-	1150	-
SO8A	-14.8	87.1	9.8	-	-	-
SO9A	-10.8	98.0	12.2	-	-	-
S10A	-8.3	62.7	11.8	-	2500	-
PAW001	37.3	14.2	9.2	8850	6800	2700
PAW002	-2.2	36.1	n/a	8500	7080	3370
PAW003	-1.4	17.2	12.8	17700	13200	8900
PAW004	-1.4	17.1	11.7	17900	13260	9000
PAW006	-6.5	39.3	7.8	6400	6380	2260
PAWN2	-6.2	87.3	9.4	-	-	-
PAWS2	-5.6	89.5	7.9	-	-	-
BAS25	-2.6	2.6	<0.8	29200	28800	25300
BAS25A	-2.6	2.4	<0.8	29770	29500	25500
BAS26	-7.4	75.6	7.4	-	970	-
SS19	-12.8	55.0	1.6	4000	3600	-

The simulations used inverse geochemical modeling to simulate geochemical reaction models using chemical and isotopic data. The presence of ^{3}H and higher percentages of ^{14}C indicate that many of the samples contain a component of modern water which is not unexpected given the hydrogeological setting. The ^{14}C ages should consequently be viewed as estimates that reflect

mean ages consisting of a mixture of younger and older waters. The absence of ^{3}H (<0.8 TU) in BAS25 and BAS25A indicates that these do not contain recent (post-1950s) recharge. The corrected ^{14}C ages for these samples are in the range of 25,000 yBP to 30,000 yBP. There was measureable ^{3}H in the other groundwater samples (BAS26, SS19, SS22) indicating a component of post-1950's recharge in the groundwater sampled in those wells and the calculated ^{14}C ages are much younger. All of the seep samples contained ^{3}H indicating the discharge of young groundwater, or mixing between modern river water and any discharging groundwater. The fairly low concentration of carbon-14 in process-affected water samples (Figure 30) has already been discussed. These waters are known to be young and are in contact with the atmosphere, yet they contain very low percentages of modern carbon, indicating large inputs of dead carbon. The calculated mean ^{14}C ages for process-affected waters appear to be unrealistically old. Further work will be required to understand details of the geochemical reactions affecting carbon-14 during oil sands processing.

4.4 Synoptic Variations along the Athabasca River

A synoptic view of changes in field parameters and isotopes along the survey reach of the Athabasca River is shown in Figures 33 and 34. While downstream changes in some field parameters and isotopes appear to be related to occurrence of a few dominant seeps, notably S08A and S07A, located at 30.6 km and 32 km, respectively, it is important to note that the density of river and seep survey points is not sufficient to adequately capture all variations expected along the reach. Nevertheless, it is possible to see the impact of river bed seepage on water near the river bed interface (black line, Figures 33 and 34). Notably, the field parameters (pH, EC, alkalinity), as well as $\delta^{18}O$, $\delta^{2}H$ and $\delta^{13}C_{DOC}$ are evidently affected by seep inputs.

Note that the samples taken in June 2009 generally have more negative $\delta^{18}O$ compositions than the samples taken later in the season, reflecting increased snowmelt contributions to river flow in June, and also higher levels of evaporative enrichment in rivers and tributaries occurring over the course of the open water season. Samples taken at the upstream end of the river reach (S09) were taken near the river bed just downstream from the confluence of the Clearwater River and appear to be enriched in $\delta^{18}O$ and $\delta^{2}H$ as a result. The grab samples taken at S06 and S07 are likely more representative of the Athabasca River. More negative $\delta^{18}O$ and $\delta^{2}H$ compositions at these locations are thought to reflect inputs from tributaries entering the river after Fort McMurray. Moving downstream from S07 to S01, there is a gradual increase noted in the $\delta^{18}O$ and $\delta^{2}H$ composition of the river possibly indicating contributions of evaporated surface water or formation water occurring along its course.

The seeps with the most negative $\delta^{13}C_{DOC}$ were S03 and S10. SO3 was the only seep sampled along the stretch of the Athabasca River where the McMurray Formation outcrops. S10A, located in a reach with Devonian outcrop, had the highest electrical conductivity. Other interesting variations are observed for $\delta^{34}S$, $^{87}Sr/^{86}Sr$, and ^{3}H. More subtle variations are observed for $\delta^{13}C$ and ^{14}C (Figure 34).

While limited in terms of number of sampling locations for river and seeps, the synoptic survey approach offers great potential for understanding the evolution of river water as it transits the oil sands development area. A comprehensive higher resolution survey targeting mapped seepage points and various control sections of the river should be conducted and repeated at regular intervals to establish current and future conditions. Priority pollutants and organic compound scans should also be included, as discussed in the following section.

4.5 NA, VPP and EPP Organics Analyses

Selected samples were analysed for naphthenic acid (NA) concentrations, volatile priority pollutants (VPP) and extractable priority pollutants. Results for detected compounds are summarized in Appendix 2, and a complete list of scanned compounds, detection limits and analytical uncertainties are provided in Appendix 4. The groundwater samples provided by Alberta Environment consultants were not submitted for these analyses as they were to be analyzed separately as part of the GOWN network.

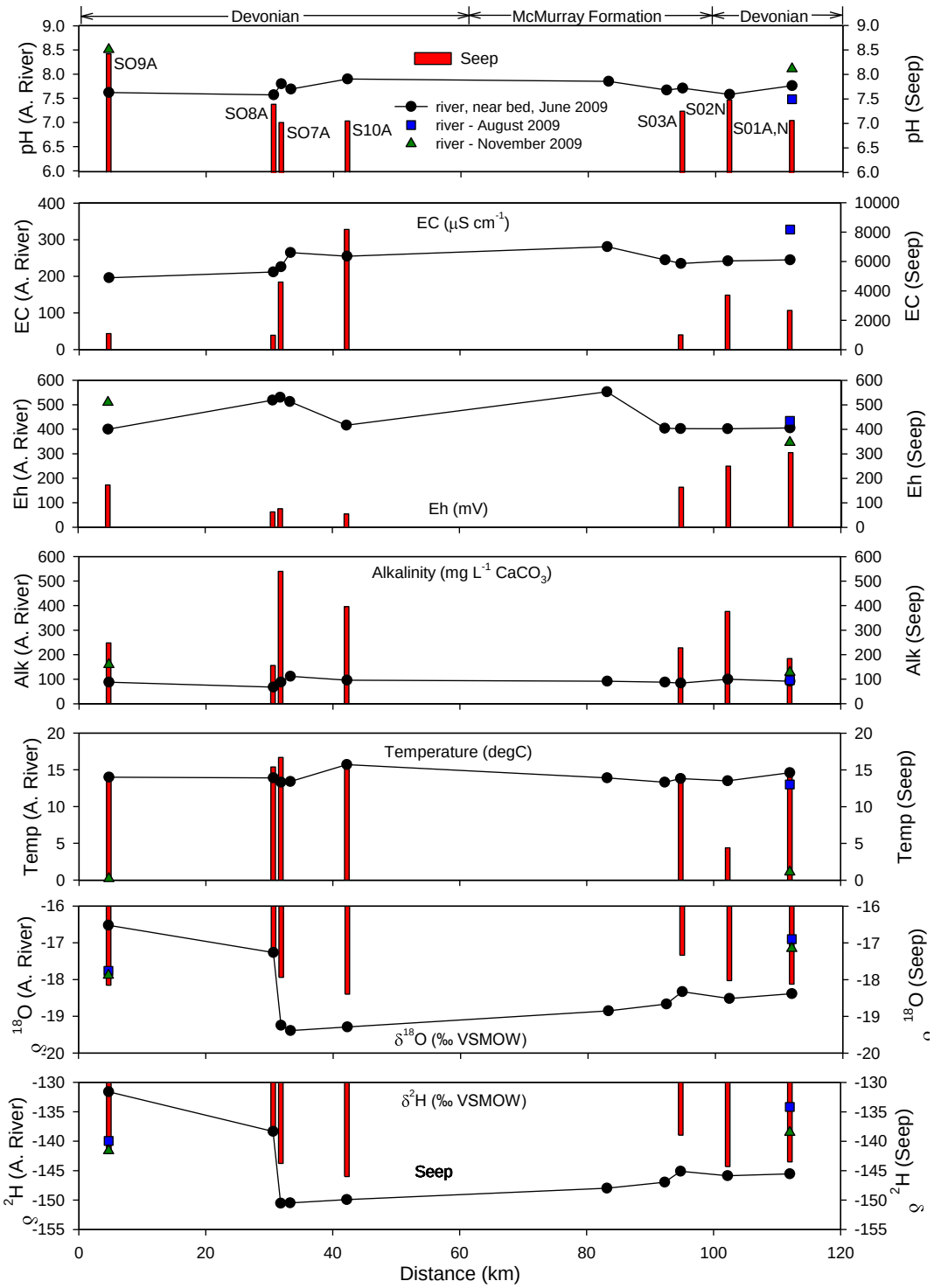

Figure 33. Variations in selected field parameters and $\delta^{18}O$ and $\delta^{2}H$ in Athabasca river water and seeps along the 125-km survey reach.
Note that river, near bed samples were taken from ~10cm above the river bed; River samples are taken at mid-depth from mid-channel.

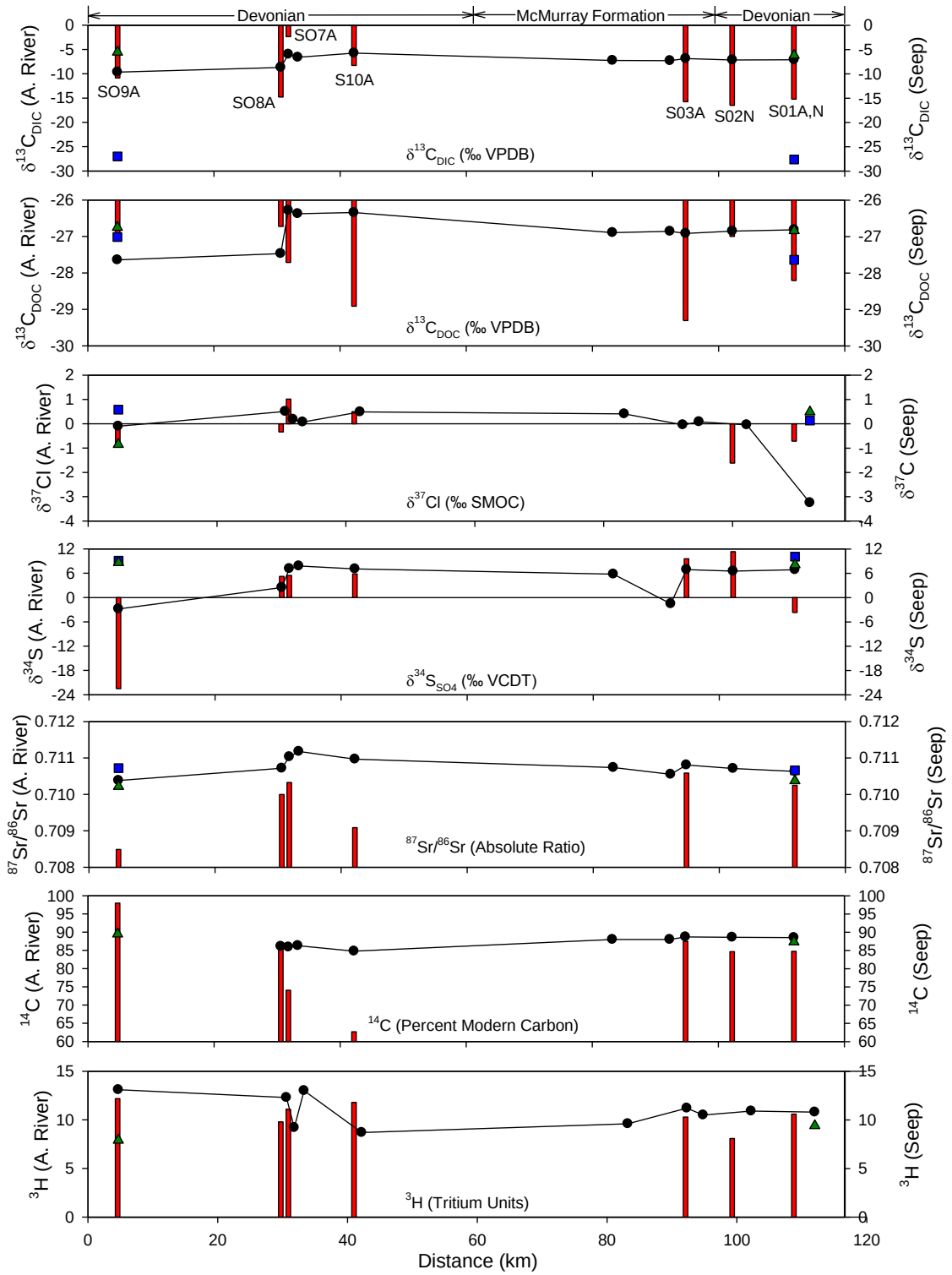

Figure 34. Variations in isotope signatures of river water and seeps along the 125-km survey reach.
See Fig. 33 for definition of symbols.

Overall, process-affected waters were found to have the highest concentrations of NA (Figure 35). Coarse tailings from CNRL (PAW007) had the highest NA concentrations measured, although a sample from the recycled tailings pond sampled at CNRL had much lower concentrations (PAW008). Note that coarse tailings sampled at Syncrude (PAW005, NA = 1.84 mg/L) is not plotted in Figure 35 as it is missing EC data. Coarse tailings at Syncrude and Shell Albian had lower concentrations of NA in the coarse tailings than in the tailings ponds.

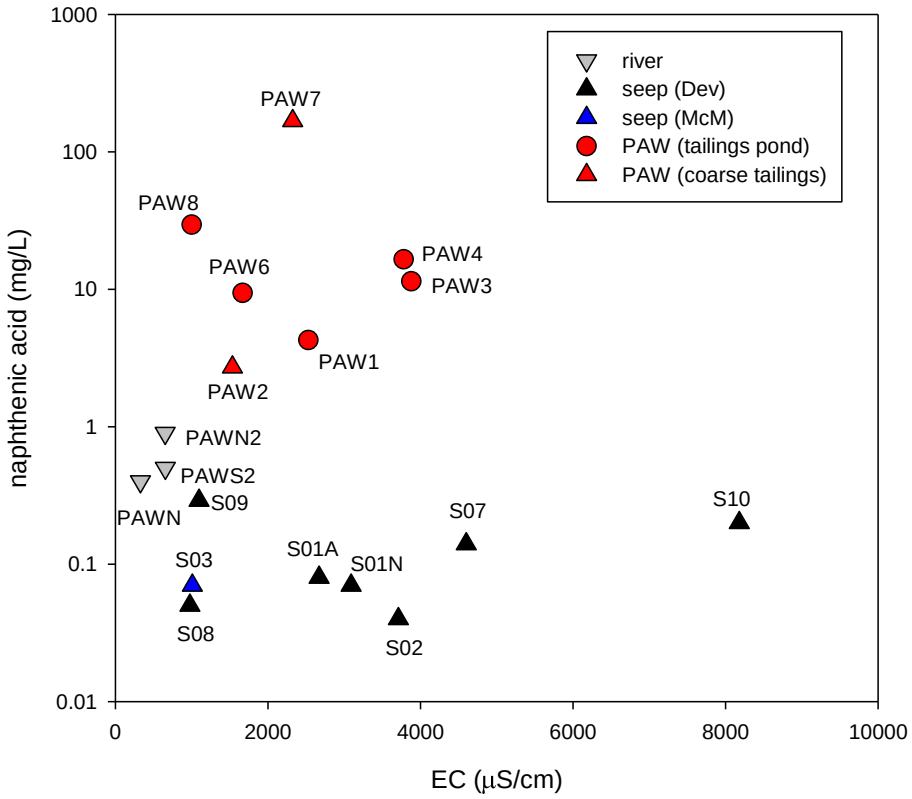

Figure 35. Relationship between naphthenic acid concentration and electrical conductivity of various waters.

NA concentrations are available for the river samples collected at the beginning (PAWS, and PAWS2) and end (PAWN, PAWN2) of the surveys. Note that EC data are missing for PAWS, so this point it is not included on Figure 35. The September 2009 samples had the same NA concentrations at the beginning and end of the surveys (NA = 0.4 mg/L). In the November 2009 survey the river water sample collected at the end of the survey had slightly higher concentrations (PAWN2, NA = 0.9 mg/l) than the beginning (PAWS2, NA = 0.5 mg/L). It is important to note that the river water NA concentrations were higher than any of the seeps sampled. Without any NA concentrations from any high salinity groundwater wells it is difficult to know what the inputs from bedrock sources might be. The highest NA concentration measured for a seep was for S09 which is located upstream of most of the surface oil sands

activities. The seep is located along the stretch of the river where Devonian units outcrop, however, the seep itself appeared to contain water similar to the overlying McMurray Formation.

The presence of polycyclic aromatic hydrocarbons (PAH) was also of interest and 17 PAH's were screened for as part of the EPP analyses (see Appendix 4). The only PAHs detected were in the process-affected waters (Table 14). No river or seep samples had detectable concentrations of PAHs. A complete list of detected compounds is given in Appendix 2.

Table 14. Samples with detectable concentrations of PAHs.

		Phenanthrene (µg/l)	Acenaphthene (µg/l)	Chrysene (µg/l)
Detection limit +/- uncertainty		0.1 +/- 1.5	0.1+/-0.4	0.1 +/- 0.1
Shell Albian	PAW2 (coarse tailings)	35.3	8.5	15.2
Syncrude	PAW5 (coarse tailings)	6.3	nd	nd
CNRL	PAW8 (recycled tailings pond)	41	5.5	nd

* nd = not detected

4.6 Natural Organic Compounds (NOC)

Electrospray ionization Fourier transform ion cyclotron resonance mass spectrometry (FT-ICR MS) was employed to analyze dissolved organic compounds in the different water samples. This technique has the highest broadband mass resolution power and mass accuracy currently available, making it possible to identify individual compounds in a complex mixture of organics. See Appendix 5 for details on methodology used. A total of 25 samples were submitted for FT-ICR MS analysis and as expected, thousands of peaks were detected in each sample (Figure 36). In general, the process-affected waters (tailings ponds and coarse tailings) have a large number of peaks (between 4,431 and 5,588 per sample), indicating the presence of a variety of organic compounds. Groundwater samples had the next highest number of peaks (between 2,661 and 4,440 peaks per sample) followed by lake waters (from 1,841 to 1,852 peaks per sample). As with many of the other geochemical and isotopic parameters measured in this survey, the river bed seeps had a large range in the number of peaks present in the FT-ICR MS. In some locations, such as S02 and S10, ~6,000 peaks are identified in the mass spectrum, while in other locations (e.g., S01A and S09), ~3,000 peaks are identified. The large variability in the organic composition in river bed seeps is consistent with the broad range presented in groundwater.

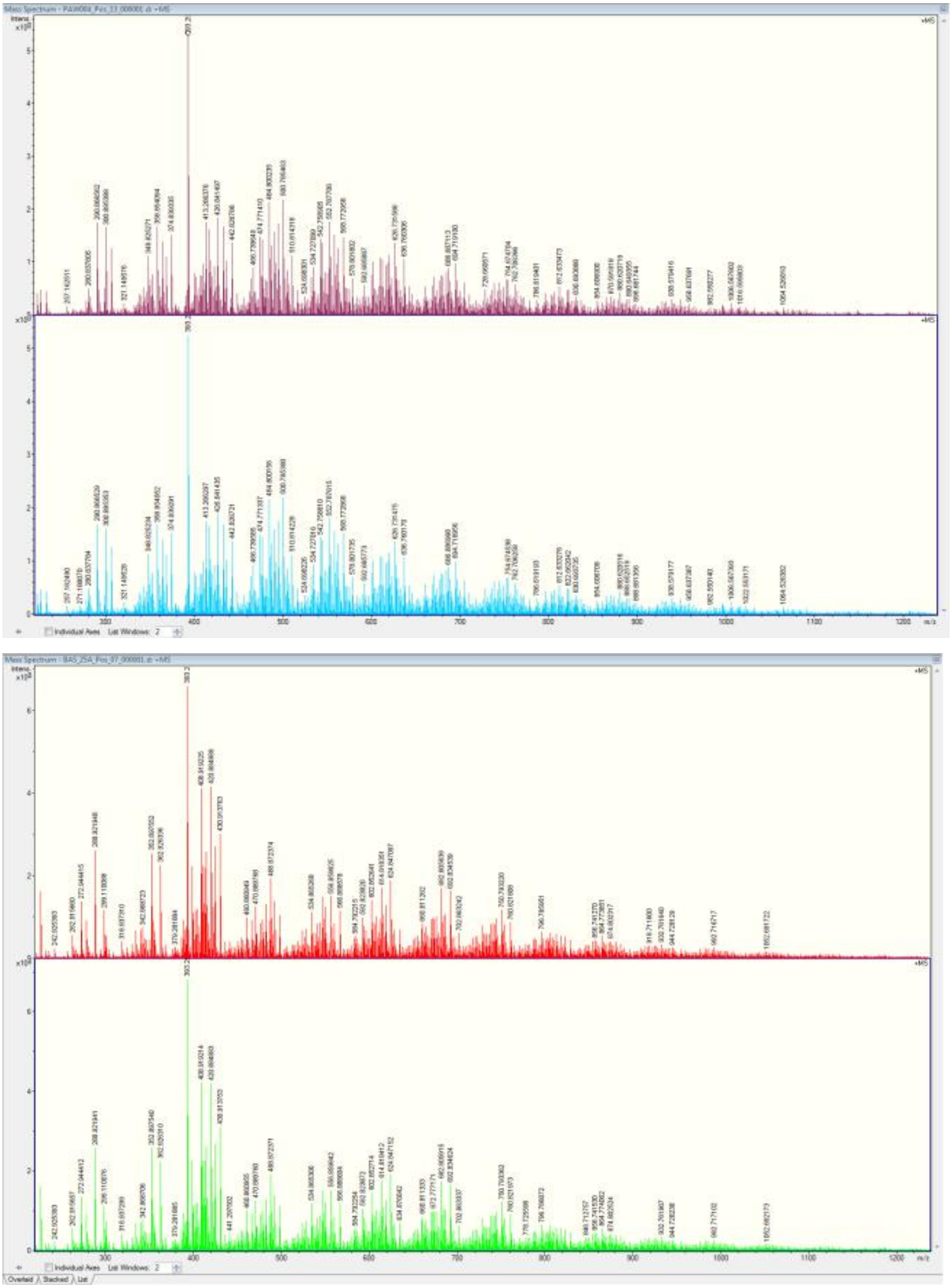

Figure 36. FT-ICR MS mass spectrum of water samples in this pilot study.

Top: PAW003 and PAW004 are repeat samples from a tailings pond from Syncrude. Bottom: BAS25 and BAS25A are duplicate samples from a groundwater well located in the McMurray Formation.

The x-axis is the mass-to-charge ratio (m/z), which is directly related to the molecular weight of target compounds. Because of the ultrahigh mass accuracy of the FT-ICR MS, the reliable m/z range can be expanded up to 1,200. The y-axis indicates the signal intensity, which can be affected by a few factors, namely the concentration of the compounds and the ionizing efficiency during the electrospray processes. In addition to the 25 water samples, 4 blank/control samples were also analyzed to identify possible contamination from materials used in sample collection and storage. The intensity range and number of peaks from the FT-ICR MS analyses for blank/control samples using an amber HDPE bottle, a clear HDPE bottle, a seep sampling apparatus rinse and a field blank, are listed in Table 15. The numbers of peaks identified in the blank samples are in general about an order of magnitude lower than the number found in most of the water samples analyzed in this survey.

Table 15. Overview of QA/QC results for FT-ICR MS.

Intensity Range	5% to 95% ranking intervals		
	Amber	Clear	Apparatus Rinse
Min	3.9×10^5	3.9×10^5	4.0×10^5
Max	6.6×10^6	5.3×10^6	8.0×10^6
# of Peaks	751	709	776

Moreover, the intensities of the blank analyses are two orders of magnitude lower than was observed in the water samples. As such, we are fully confident that the noise from sample handling and apparatus contamination are very limited.

The results of each FT-ICR MS analysis include thousands of peaks each with different intensities and we've included only a few of the mass spectrum results as examples (Figure 36). Differences in the NOC present in the various samples can be identified by simple visual comparison of the different spectra. For example, there are significant differences in the intensity pattern in the m/z range of 320 to 360 between groundwater from the McMurray Formation (BAS25 and BAS25A) and the tailings pond waters (duplicates PAW003 and PAW004). Intensity signals in this range are apparently stronger in process-affected water samples than in the groundwater samples from the well at BAS25.

Visually comparing and describing the patterns in this complex dataset is not straightforward, so here we employ Kendrick Mass Defect (KMD) plots to illustrate and visualize all of the resolved peaks in the broadband FT-ICR MS mass spectrum (Hughey et al. 2001). Basically, a KMD plot sorts identified peaks (i.e., compounds) into homologous series according to alkylation, class (number of heteroatoms) and types (rings plus double bonds). The neutral mass of CH_2, 14.0157 Da, is converted to a Kendrick mass of 14.0000 Da. As such, compounds with the same nitrogen, oxygen and sulfur composition, and the same number of rings (plus double bonds), but

different number of CH_2 units will differ in Kendrick mass by integer multiples of 14.0000 Da. These compounds are thus easily identified as members of a homologous series. In other words, members of a homologous series will have the same KMD (y-axis), which is unique to that series. For example, the alkylation series of simple alcohols (methanol, ethanol, propanol, butanol etc.) share the same heteroatom composition (O1) but simply differ in the number of CH_2 units (from C1 to C4). Therefore, Kendrick normalization yields series of homologues which appears as a horizontal row in a KMD plot. Each individual series can be distinguished from species of other classes and types with in-depth elemental composition assignment. In this way, a KMD plot presents a compact visual analysis for ultrahigh-resolution broadband mass spectra.

The mass spectra presented in Figure 36 are also presented as 3-dimensional KMD plots in Figure 37. Instead of clustered peaks with obvious periodicities in the mass spectra, the organic compounds present in a water sample demonstrate detectable patterns. Of particular interests are the different types of linear patterns detectable in the KMD plots. Foremost, a large number of homologues are detected in the nominal Kendrick mass range of 200 Da to 600 Da (x-axis).

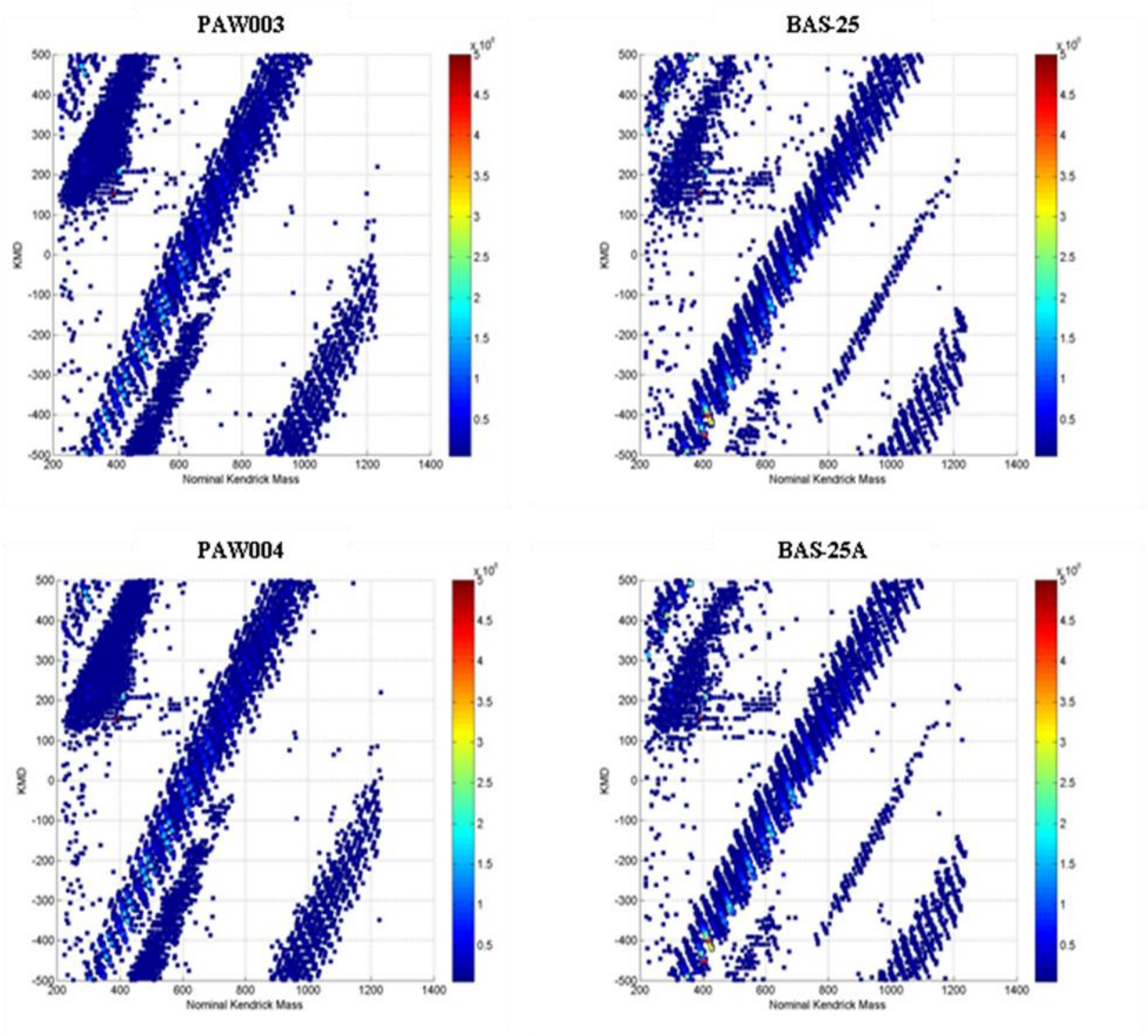

Figure 37. 3D KMD plots for selected process-affected waters and groundwater samples. PAW003, PAW004, BAS25 and BAS25A are the same samples presented in Fig. 36. Colors indicate the signal intensity of the peak, which is related to the concentration and other factors.

The clouded area in the upper-left corner of each KMD plot is characterized by Kendrick mass defects (KMD) >100 and relatively low intensities (indicated by the blueish color). The higher density of points in the top left portions of the KMD plots for PAW003 and PAW004 (Figure 37, left hand plots) indicate that there are more homologues present in these samples than in the BAS25 groundwater samples (Figure 37, right hand plots). The most prominent pattern in the KMD plots above are the bands of shading trending towards the upper right hand corner, but within these bands a finer-scale pattern emerges. The angled stripes present within the bands are the result of a negative correlation between nominal Kendrick mass and the Kendrick mass

defect. In the high nominal Kendrick mass range (between 600 Da and 900 Da), a different pattern emerges, characterized by a negative correlation between nominal Kendrick mass and Kendrick mass defect. As the molecular mass increases, the Kendrick mass defect proportionally decreases, which lead to apparent angled stripes in Kendrick plots. Intriguingly, the stripes usually span ~100 Da in the nominal Kendrick mass. The pattern is most prominent in the high nominal Kendrick mass range (between 600 Da and 900Da) but also develops into the low Kendrick mass range with unusually low mass defect (<0), indicating uncommon heteroatoms such as phosphorus (P). In the extreme high mass range (>900 Da), compounds are characterized by low Kendrick mass defect, and there are apparent differences in the mass distribution pattern between process-affected waters and groundwaters.

Because linear patterns appear to be such important features in the Kendrick plot, we have developed an algorithm to summarize the percentage counts of organic compounds that fit linear patterns with a given slope. A slope of 0° indicates homologues that differ only in their CH_2. Positive slopes indicate increasing Kendrick mass defect as nominal Kendrick mass increases; whereas negative slopes suggest decreasing Kendrick mass defect as nominal Kendrick mass increases. Figure 38 presents the statistical summary for PAW003 in the right hand panel. The y-axis value that corresponds to 0° on the x-axis is 43.04%, which means ~43% of organic compounds detected in PAW003 are homologues. More importantly, the statistical summary indicates that the most significant pattern in the KMD plot for PAW003 has a slope of 55.1° with 49.96% of the organic compounds having this slope. There is a progressive increase of percentage in the negative slope domain.

Comparing the statistical summary of the linear patterns present in the Kendrick plot for BAS25 (Figure 39, right panel) with the statistical summary for PAW003 (Figure 38, right panel) clearly shows the differences in the distribution of organic compounds in the two samples. In the sample from BAS25 only 29.26% of the compounds present are homologues. The most significant pattern is 53.8° which accounts for 51.73% of the organic compounds present. In this sample, there is also an important slope in the negative slope domain, at -60.4° accounting for 30% of the peaks. Statistical analyses of the patterns present in the KMD plots of other samples are included in Appendix 6.

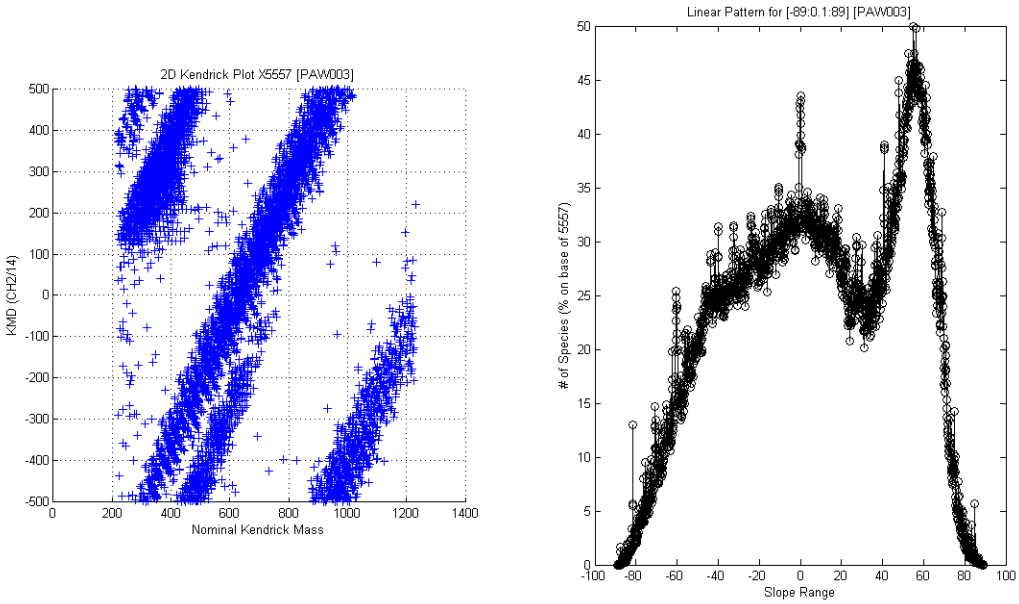

Figure 38. 2D KMD plot (the left panel) and the statistical summary of the linear pattern (the right panel) for PAW003

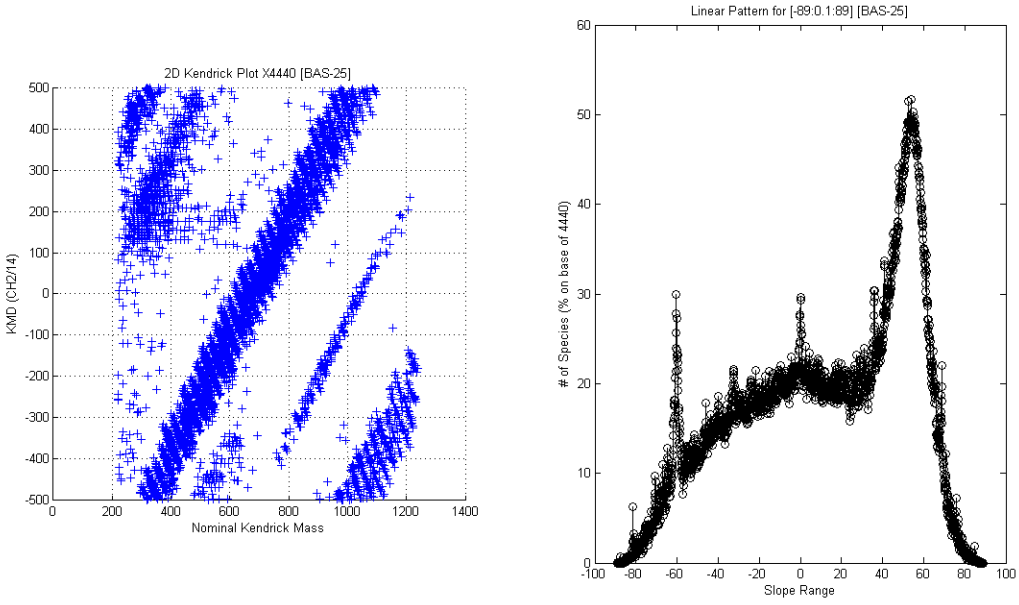

Figure 19. 2D KMD plot (the left panel) and the statistical summary of the linear pattern (the right panel) for BAS25.

5 DISCUSSION

The results of this study provide selected examples to illustrate the potential for labelling of various water sources in the oil sands region using isotopic and geochemical (inorganic and organic) tracers. While significant differences in some analytes can be used to tag water types in some circumstances, the results clearly illustrate that it is often unreliable to attempt labelling of water sources based on individual tracers or simple combinations of tracers. Understanding of the regional hydrogeological system and interpretation of isotopic and geochemical variations in the context of a biogeochemical systems approach offers the greatest potential for comprehensive understanding and labelling of water source and pathways. The multi-tracer suite, particularly isotopes and NOC, provide great potential for understanding the geochemical setting of river seepage, to understand its origin, and to understand the potential for it to contain process-affected water. Likewise, the tracing of process-affected water from its point of origin through the groundwater environment is necessary to identify evolution of geochemical signatures and to predict how and where it is likely to occur in the receiving aquatic environment. From a riverine perspective, synoptic surveys also offer an integrative method for better understanding of evolution of the Athabasca River and tributaries as it may be affected by addition of both natural and potentially process-affected water. Preliminary evaluation of statistical approaches for differentiating various water types using inorganic, organic and combined datasets is discussed below. These methods should be evaluated, refined and applied as part of more comprehensive future investigations.

5.1 PCA of Inorganic Parameters

Principal Component Analysis (PCA) is widely used in ecological and geochemical studies to describe and understand major controlling factors in multi-variable datasets with a large numbers of observations. Here we use PCA to better understand the potential fingerprinting of process-affected waters first using the inorganic tracers (Figure 40), then the NOC characterization (Figure 41), then a comprehensive PCA using the entire dataset (Figure 42).

PCA was performed using the 39 inorganic parameters, including major anions (F^-, Cl^- and SO_4^{2-}), major cations (Na^+, K^+, Mg^{2+}, Ca^{2+} and NH_4^+) and trace elements (Cr, Ni, Cu, Zn etc.). Based upon PCA scores on the first and the second axes, the inorganic geochemical compositions suggest apparent distinction among different types of water (Figure 40, left panel). Process-affected waters (labelled with PAW) are generally distinct from the majority of other water samples, mainly due to their second axis scores. Following PAWs on the second axis, groundwaters (including BAS25, BAS25A and CWR1) and some seep samples (which appear to be located close to industrial development, S07A and S10A) also demonstrate relatively high scores in the second PCA component, while their first axis score remains near zero. Waters from the Athabasca River and the rest of seep samples clustered together, with characteristically low scores (negative) in both the first and second axes. More importantly, PCA analysis appears to distinguish operators. PAW003 and PAW004 from Syncrude apparently obtained similar PCA scores in both the first axis and the second axis (Figure 40, left panel). This is expected considering these are duplicate samples. Although PAW002 is abnormally high in trace

elements, PAW001 and PAW006 are similar in first axis score, but slightly different in the second axis. Both PAW001 and PAW006 were sampled from Shell Albian tailing ponds.

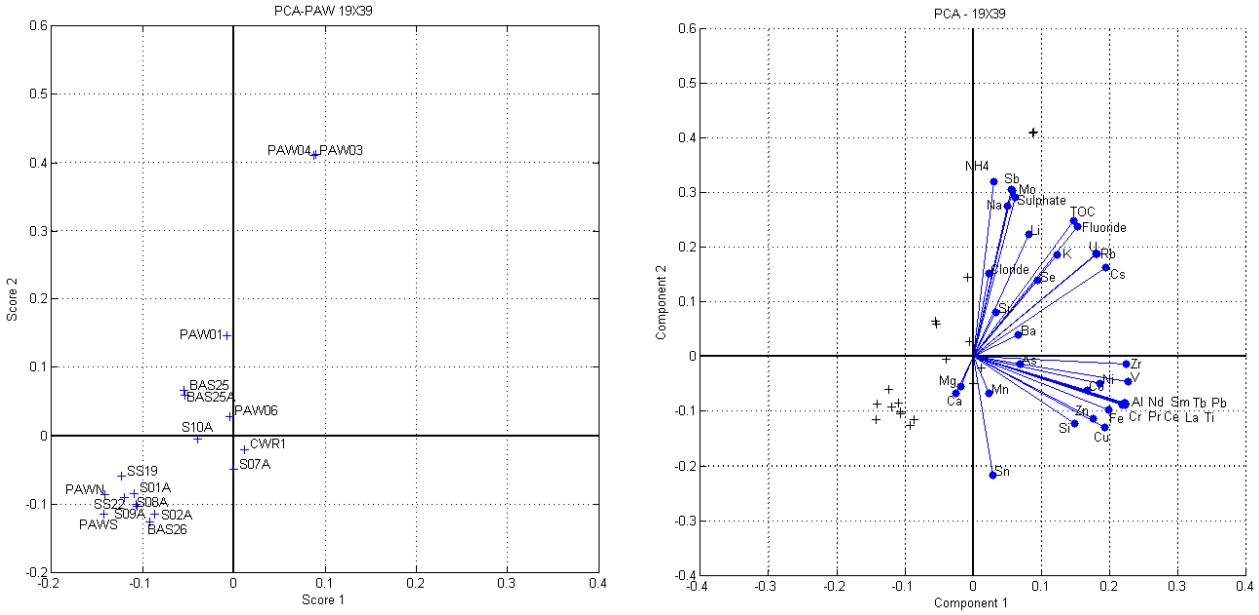

Figure 40. Principle Component Analysis of major ions and trace elements in water samples. The left panel illustrates the PCA scores (the first axis and the second axis) of individual samples. The right panel is a biplot, which imposes the indices of variables over the PCA scores of samples. In this way, the linkage between variables and resultant samples can be visualized.

Since all of the variables are readily identifiable, an effort was made to identify the contribution of individual parameters to the variability of major PCA components (right panel in Figure 40). Clearly, the first axis is dominated by trace elements, while the second axis is dominated by NH_4, Na, SO_4, Sb, Sn, and Mo with minor influence from Mg, Ca, Cl and other trace elements.

The variability distribution of the dataset suggest that trace elements (those contributing to the first axis) are the major factors separating process water (tailings ponds) from natural background, while the major ions further differentiate tailings ponds from various operators. The slightly separation between PAW001 and PAW006 is consistent with NOC compositions. This finding is generally consistent with PCA results based on NOC.

5.2 PCA of NOC

The PCA based on the results of the FT-ICR MS analyses of NOC from 23 observations (water samples) and thousands of parameters (different NOC compounds represented by a different peak) is presented in Figure 41.

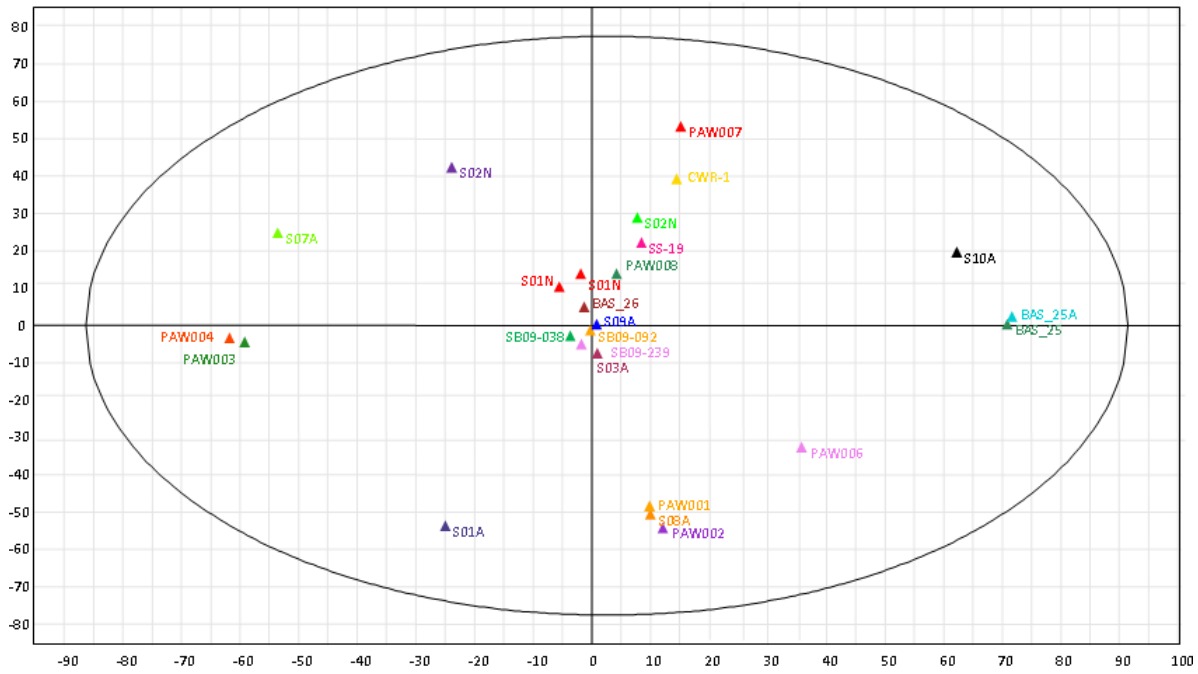

Figure 41. Principle Component Analysis of natural organic compounds dissolved in water samples.
Note that PAW005 (coarse tailing) was not analyzed by FT-ICR MS as insufficient water remained. S01N and S02N were analyzed twice for instrumental conditioning. Considerable differences were observed for duplicated runs, especially for S02N, mainly due to different instrumental conditions.

The PCA results suggest a strong clustering of organic characteristics among various operators. As illustrated in Figure 41, tailings pond samples from Shell Albian (i.e., PAW001 and PAW002) are close to each other, indicating strong similarity in organic compositions. Process-affected waters from Shell Albian (tailings pond water PAW001, and coarse tailings PAW002) are distinct from Syncrude samples mainly based upon the first axis but score similarly to each other in the PCA analysis. PAW006 is also from Shell Albian, but is not simply tailings pond water but rather tailings seepage from a recycled water system. The slight differences in water processes may contribute to the difference between PAW006 and the other two samples from Shell Albian. Nonetheless, PAW006 is still more similar to PAW001/002 than to the rest of the dataset. Both PAW007 and PAW008 are from CNRL. Although the internal similarity between CNRL samples is not as strong as duplicate samples from Syncrude, or multiple samples from Shell Albian, compositional differences among operators still overwhelmingly explain the distributions. Tailings ponds from Syncrude can be distinguished from those from Shell Albian based upon the first axis, while Shell Albian and CNRL can be differentiated by the second axis in PCA.

It is important to note that water samples from subsurface formations and river bed seeps also show intriguing characteristics. Groundwaters generally plot far away from the origin of the PCA axes (see Fig. 41), inferred to reflect complexity and variability in organic compositions.

These include BAS25, BAS25A, CWR1 and SS19. The three samples collected from river reaches close to the industrial development (S07, S08 and S10) are also more distant from the PCA origin. Also, it has not been resolved yet what attributes of the water samples contribute to the high scores in the second axis for the S02 and S01A, since samples collected from the same location but in a different season (i.e., S02 and S01N) are very close to the origin suggesting similarity to the natural background. Seasonality effects on river bed seepages are still not fully understood.

It is also important to note that seep S08A does not match with any groundwater sources characterized to date. In addition, the seep shows similarity in organic composition to the process-affected water source from one operator (Shell Albian) (Figure 41). Because seep sample S08A was collected 50 km upstream of all Shell operations it is considered highly improbable for Shell Albian water to be present in this geographic location. Furthermore, the inorganic signatures we presented in Figure 40 do not match with Shell Albian process-affected water, and a comprehensive PCA based on both stable isotopes and inorganic characteristics does not suggest a match (Figure 42). However, the seep is situated along a developed reach of the river, in an area where all operators have not yet been characterized. As discussed in the following section, seeps are also comprised of complex mixtures of surface water and groundwater, and subject to considerable modification during transport and mixing in the subsurface environment. Further assessment of a more complete suite of natural and process-affected waters will be required to fully understand the origin of this and other seeps.

5.3 Comprehensive PCA

One of the objectives of this pilot study was to apply a multiple tracer approach to fingerprinting process-affected waters. The FT-ICR MS results have shown the potential for high resolution characterization of the dissolved component of the organic components in water to provide distinct labelling of the different water types. Here we attempt to integrate the results of the NOC analyses, with the other isotopic and geochemical tracers using a comprehensive PCA based on 19 observations and 52 parameters to evaluate systematic similarities and differences among their geochemical characteristics (Figure 42). The number of observations for this PCA was decreased to 19 because some samples are still pending analysis or reanalysis (S01N, S02N, PAW007, PAW008).

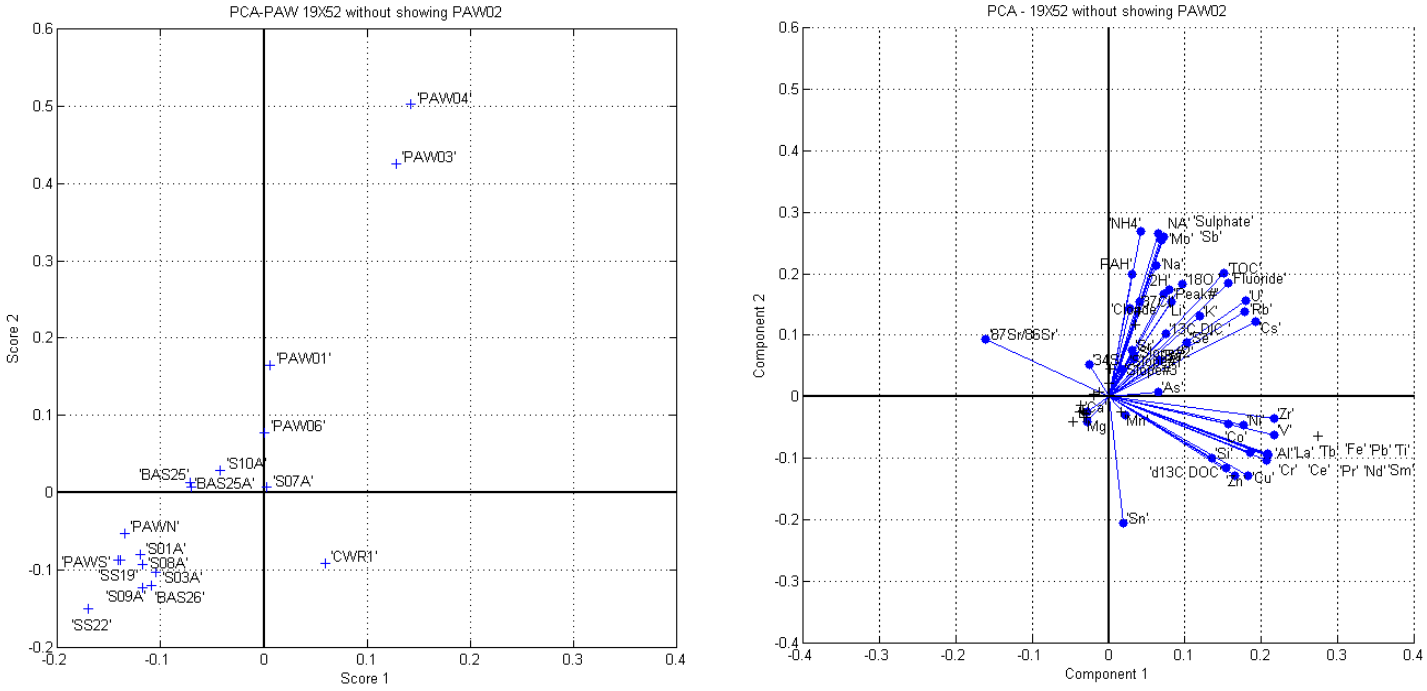

Figure 42. Principle Component Analysis of major ions, trace elements and stable isotopes in water samples.
The left panel illustrates the PCA scores (the first axis and the second axis) of individual samples. The right panel is a biplot, which imposes the indices of variables over the PCA scores of samples. In this way, the linkage between variables and resultant samples can be visualized.

The 52 parameters include:

- 39 inorganic parameters are reported, including major anions (F, Cl and SO_4), major cations (Na, K, Mg, Ca and NH_4) and trace elements (Cr, Ni, Cu, Zn, etc.),
- 7 stable isotope signatures (δ^2H, $\delta^{18}O$, $\delta^{37}Cl$, $\delta^{13}C_{DIC}$, $\delta^{13}C_{DOC}$, $^{87}Sr/^{86}Sr$, $\delta^{34}S_{SO4}$),
- 2 organic parameters from the NA, VPP scans (NA, and sum of PAHs)
- 4 NOC indices (# of peaks, top three slopes in the linear pattern analysis).

The results for the coarse tailings sample PAW002 were left off of these plots because of the anomalously high trace element concentrations. The comprehensive PCA shows that the $\delta^{13}C_{DOC}$, $^{87}Sr/^{86}Sr$ and $\delta^{34}S_{SO4}$ variations appear to be related to trace element variations. $^{87}Sr/^{86}Sr$ and $\delta^{34}S_{SO4}$ are negatively correlated with trace element variations and $\delta^{13}C_{DOC}$ is positively correlated. Variations in δ^2H, $\delta^{18}O$, $\delta^{37}Cl$, $\delta^{13}C_{DIC}$, NA, the sum of the PAHs and the

NOC indices are generally related to major ions. The addition of isotopic and organic tracers to the PCA analyses revealed that $\delta^{13}C_{DOC}$ and $^{87}Sr/^{86}Sr$ contribute significantly to the first axis variation, and $\delta^{18}O$, $\delta^{2}H$ and # of peaks contribute significantly to the second axis of variation. These parameters should have good potential for identifying the different water types. In contrast, the $\delta^{34}S_{SO4}$ and NOC slope indices (top three slopes in linear pattern analysis) had only minor contribution to either the first or second axes, and as such may not be important parameters for distinguishing the different water types.

The addition of NOC indices and stable isotopes to the PCA improved the separation of seep samples such as S07 and S10. This improved separation is mainly based on the second axis and the influence of $\delta^{2}H$, $\delta^{18}O$, and # of peaks. This suggests that stable isotopes and NOC results may be applied in a complimentary way to differentiate water types.

In general the signatures of $\delta^{18}O$, $\delta^{2}H$, $\delta^{34}S_{SO4}$ and $\delta^{13}C_{DOC}$ show that process-affected waters are isotopically distinct from local groundwaters, river water and river bed seepage. Isotopic signatures in groundwater and seepage are variable and complicated (especially the latter), indicating multiple sources and multiple phasing mixing during the transport and migration of water from subsurface to surface system. These types of water should be assessed and evaluated on a case by case basis rather than by regional characterization alone.

5.4 NOC Pattern Analysis

Further characterization of the different water types and operator-specific features was also carried out by comparing the results of the pattern analysis of mass distribution in Kendrick plots. Comparing the pattern analysis from process-affected waters from Shell Albian (Figure 43), reveals remarkably similar NOC characteristics with both samples being dominated by the 55.1° pattern accounting for ~50% of total peaks. PAW001 is a sample from the tailings pond whereas PAW002 is from the coarse tailings. Despite minor differences in geochemistry (e.g., EC: PAW001 = 2,530 µS/cm; PAW002 = 1,535 µS/cm) and major differences in trace element concentration (e.g., Si: PAW001 = 6,621 µg/L; PAW002 = 22,104 µg/L) the organic composition of these two waters was almost identical. Homologues (0° pattern) are also important in both samples. In the negative slope domain, the % of total peaks that can be accounted for with a given slope, increases as the slope gradually approaches zero. A strong correlation between samples can be observed in a crossplot from both samples (right panel Figure 43).

However, distribution patterns are apparently different among operators if we compare selected samples from the three operators (i.e., Shell Albian, Syncrude and CNRL) (Figure 44). Both PAW001(Shell Albian) and PAW003 (Syncrude) show the dominant pattern at 55.1°, while PAW007 (CNRL) reveals a prevailing pattern at 0^{o} in addition to the important pattern at 52.4^{o}, highlighting the importance of homologues. The observation is consistent with the heavily clouded area in the mass range of 200 Da to 600 Da (Appendix 6).

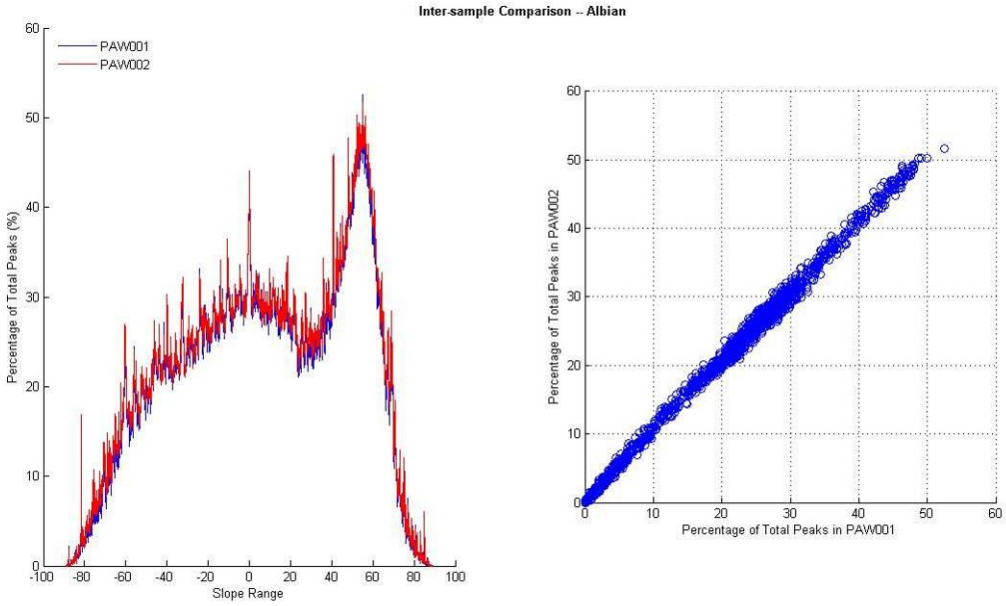

Figure 43. Operator-specific comparison of mass distribution pattern of organic composition in processes affected water (PAW001 and PAW002 from Shell Albian).

In the positive slope range, PAW007 (CNRL) shows a prevailing slope at 52.4°, which identifies a subtle alignment and organizational difference in NOC compared to PAW001 (Shell Albian) and PAW003 (Syncrude). Meanwhile, PAW003 (Syncrude) appears to have a higher percentage of positive slope peaks than PAW001 (Shell Albian), although PAW001 (Shell Albian) and PAW003 (Syncrude) showed exactly the same peak pattern at 55.1°.

Preliminary comparisons of mass distribution patterns between operators and within operators suggest that there are significant pattern differences among operators, as also revealed by the PCA analysis. This feature could be utilized to develop operator-specific fingerprints to identify process-affected waters from individual operators, although a large sampling pool would be necessary to make the fingerprinting pattern reliable and robust.

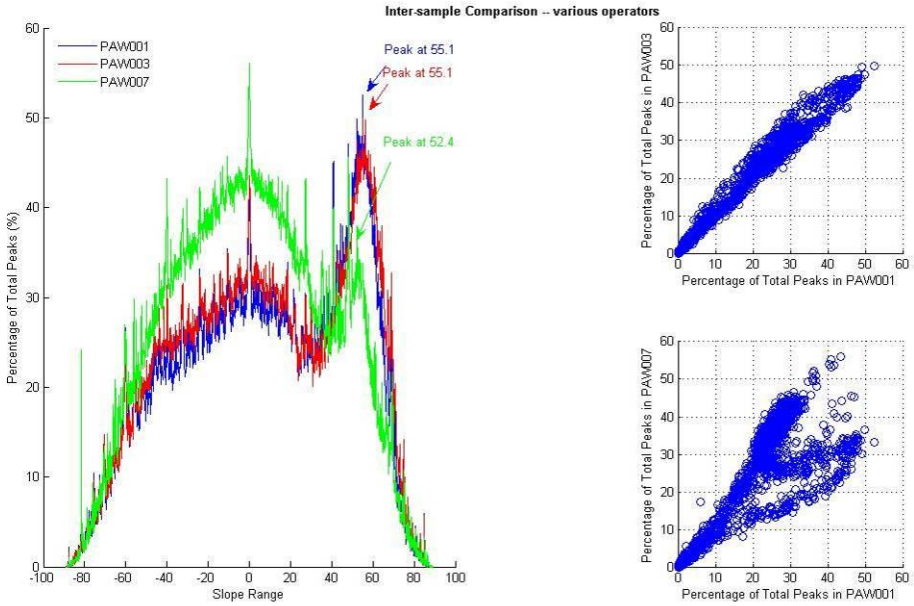

Figure 44. Comparison of mass distribution pattern of organic composition from various operators (PAW001from Shell Albian, PAW003 from Syncrude and PAW007 from CNRL).

Similarities also emerge in comparisons between the river bed seep sample taken from the stretch of the river where the McMurray Formation outcrops (S03) and the nearest McMurray Formation groundwater well (BAS26) (Figure 45). Both of these samples are dominated by peaks that occur at 55.1° and also have similarly high percentages of homologues. The 55.1° peak is not present in the groundwater samples from the Clearwater Formation or the surficial aquifers, but is the dominant peak in all of the process-affected water samples. The only other seep where the 55.1° slope was significant was S09A (peak # 3 in NOC indices), a seep located upstream of development where the bitumen-saturated McMurray Formation is exposed above the Devonian Waterways Formation. This peak may be representative of the NOCs associated with McMurray Formation bitumen, a common component of all of these samples (processed and natural waters).

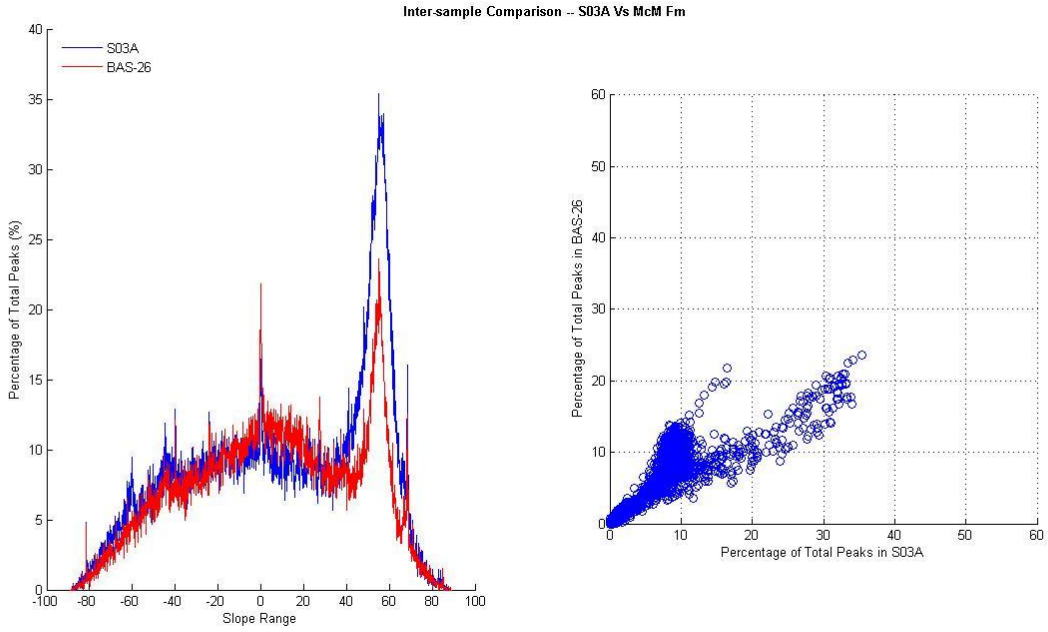

Figure 45. Comparison of mass distribution pattern of organic composition from a river bed seep sample from S03 (McMurray Formation) and a groundwater sample from a well in the McMurray Formation (BAS26).

Comparison of the NOC mass distribution patterns between the Athabasca River sample taken at the beginning of the survey (PAWS) with the patterns in the sample taken at the end of the survey (PAWN) suggest some slight changes in the overall characteristics of the dissolved organic component of the river along this stretch (Figure 46). The most prominent change is the appearance of a peak at -60.4° that is present downstream but absent upstream. This peak is also prominent in the mass distribution profiles from S01 and S10 (high salinity Devonian seep). Seep S01 is located downstream of development but not near any oil sands development whereas seep S10 is located fairly near development, but has a geochemical composition suggesting it is a natural high salinity seep. Further investigation of the compounds that result in the -60.4° peak should be conducted to see if this dissolved organic component is from organics from the underlying Devonian units. FT-ICR MS analyses of background (upstream) Devonian seeps and comprehensive application in synoptic river surveys could improve ability to use the technique for fingerprinting and is strongly recommended.

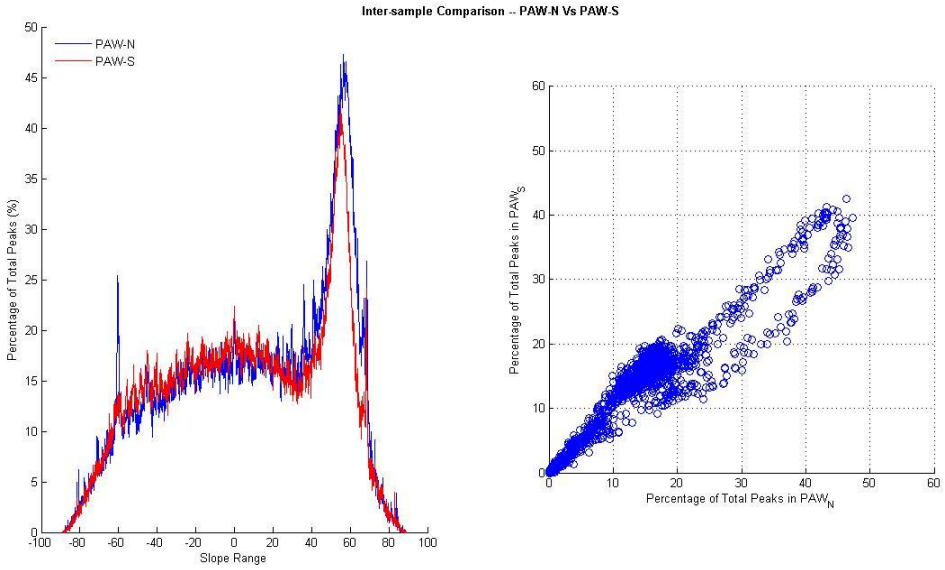

Figure 46. Comparison of mass distribution pattern of organic composition from the Athabasca River study reach at the upstream (PAWS) and downstream (PAWN) cross-sections.

6 SUMMARY

While individual tracers help to label water types in some locations, the results clearly illustrate that it is unreliable to attempt labelling of water sources based solely on individual tracers or simple combinations of tracers. Understanding of the regional hydrogeological system and interpretation of isotopic and geochemical variations in the context of a biogeochemical systems approach on a case by case basis offers the greatest potential for comprehensive understanding and labelling of water source and pathways. While limited in number of samples, the survey demonstrates the value in using a comprehensive suite of analyses for fingerprinting water sources and mixtures in the oil sands region.

The following are also noted as important findings:

- Stable isotopic signatures, in particular $\delta^{18}O$, $\delta^{2}H$, $\delta^{34}S_{SO4}$, $\delta^{13}C_{DOC}$ and $\delta^{13}C_{DIC}$ can be used to indicate the origin of the water, salinity and major input sources.
- Enriched tritium is useful for establishing if groundwaters have a component of modern post-1950s recharge. Process-affected waters contain abundant tritium. Lack of tritium is therefore strong evidence that water is not anthropogenically impacted.
- Carbon-14 may be useful for estimating the mean (or relative) ages of water mixtures in groundwater, river water, and natural seeps when interpreted in the context of a comprehensive reactive transport geochemical model. Process-affected waters have anomalously old radiocarbon signatures. River bed seeps were found to have

relatively young ages which is attributed to a significant content of river water and/or other surface waters.

- Process-affected waters are evaporatively enriched in $\delta^{18}O$ and $\delta^{2}H$ which distinguishes them from groundwater, river water and river bed seepage. However, evaporative signatures are similar to those observed in natural surface waters.
- Process-affected waters are distinguished from natural surface waters based on solute isotopes, major-, minor- and trace element geochemistry, and organic composition.
- Groundwater and river bed seepage are very complicated. Most of these likely contain complex mixtures of multiple sources of water, which varies from site to site.
- Using statistical approaches, (i.e., principle component analysis, PCA) we can identify and distinguish between process-affected water from individual operators using organic and/or inorganic tracers.
- We can identify and distinguish between process-affected water from individual operators based upon the mass distribution patterns of organic compounds alone. These patterns also appear to be distinct from groundwater signatures although more baseline groundwater information is needed to confirm this.
- FT-ICR MS offers capability to resolve thousands of organic compounds, and may be the simplest, most cost-effective approach to identify process-affected waters in the natural aquatic environment. A wide range of organic compounds is observed in process-affected water and these are not limited to naphthenic acids and hydrocarbons.
- We find no evidence of robust connections between tailings ponds and the river seeps that were sampled over the 125-km reach traversing the oil sands development area, although many seeps were not sampled. Although the seeps we did sample appear to be directly related to occurrence of natural groundwater seepage, we do not have enough evidence at this point to rule out the possibility that minor or trace amounts of process-affected water may be present in some of these seeps.

7 RECOMMENDATIONS

The major recommendation is to expand and improve upon comprehensive baseline datasets for water and contaminant sources, pathways, and receptors in the oil sands region. These activities should include:

- **To constrain sources:** More sampling of process-affected waters, natural groundwater and surface water sources is required for isotopes and geochemistry. In particular, establishment of a natural organic compound library to include broad regional information on all water types is required to assist with fingerprinting of process-affected water. Better characterization of natural high organic groundwater endmembers via sampling of groundwater seeps along the Athabasca upstream of

development, and better selected groundwater wells, especially natural high organic groundwater endmembers is important. Expanding the range of process-affected waters to include injected brines and end-pit lake seepage is recommended. Fine-tuning and optimization of FT-ICR MS to increase the signal-to-noise ratio, will improve the separation of the different waters. Automation of data-acquisition and processing will make the approach more efficient. Closer scrutiny of operator-specific oil sands processing methods may also help to understand how different isotopic and geochemical fingerprints develop and how they may evolve over time.

- **To constrain pathways:** More work is required to understand the evolution of water and organic compounds as they are transported via subsurface or surface pathway from tailings ponds or reclamation areas towards natural receptors. This work requires close collaboration with oil sands operators.
- **To constrain sources:** Recall that the electromagnetic survey was successful in identifying hundreds of potential points of high conductivity seepage, and that the drive-point approach was successful in sampling water from seeps, there is a need to expand the sampling program to include and catalogue all major seeps along the Athabasca River and key tributaries slated for oil sand development. For completeness, thermal imaging may be warranted to assist in identifying relatively warm, but lower conductivity seeps. A comprehensive suite of isotopic and geo-chemical tracers is recommended to label the origin of the water, with emphasis on natural organic compounds as well as priority pollutants and any other compounds of interest.

From a riverine perspective, synoptic survey of the river channel, seeps and tributary input may offer an appropriate integrative method for better understanding of evolution of the Athabasca River (its tributaries as well) as it traverses the city of Fort McMurray and the oil sands development region. Addition and influence of both natural and process-affected water, if it occurs, could then be located and characterized, and would provide a logical framework and focus for monitoring and any required mitigation efforts.

8 REFERENCES

Allison, J.D., D.S. Brown and K.L. Novo-Gradac, 1990. *MINTEQA2/PRODEFA2, a Geochemical Assessment Model for Environmental Systems, Version 3.0. User's Manual*. Environmental Research Laboratory, Office of Research and Development, U.S. EPA, Athens, GA.

American Public Health Association, American Water Works Association and Water Environment Federation, 1992. *Standard Methods for the Examination of Water and Wastewater*. http://www.standardmethods.org/ [Last accessed January 13, 2011].

Andriashek, L.D., 2003. *Quaternary geological setting of the Athabasca Oil Sands (in situ) Area*. Alberta Energy and Utilities Board, EUB/AGS Earth Sciences Report 2002-03. 295 pp.

Aravena, R., L.I. Wassenaaar and L.N. Plummer, 1995. *Estimating ^{14}C groundwater ages in a methanogenic aquifer*. Water Resources Research 31: 2307-2317.

Bachu, S. and J.R. Underschultz, 1993. *Hydrogeology of formation waters, Northeastern Alberta Basin*. American Association Of Petroleum Geologists Bulletin 77: 1745-1768.

Baker, M.J., D.W. Blowes and C.J. Ptacek, 1998. *Laboratory development of permeable reactive mixtures for the removal of phosphorus from onsite wastewater disposal systems*. Environmental Science Technology 32: 2308–2316.

Ball, J.W. and D.K. Nordstrom, 1991. *User's manual for WATEQ4F with revised thermodynamic data base and test cases for calculating speciation of major, trace and redox elements in natural waters*. U.S. Geological Survey Open-File Report 91–183.

Barson, D., S. Bachu and P. Esslinger, 2001. *Flow systems in the Mannville group in the east-central Athabasca area and implications for steam-assisted gravity drainage (SAGD) operations for in situ bitumen production*. Bulletin of Canadian Petroleum Geology 49: 376-392.

Bath, A.H., W.M. Edmunds and J.N. Andrews, 1979. *Palaeoclimatic trends deduced from the hydrochemistry of Triassic Sandstone aquifer, United Kingdom*. IN: Isotope Hydrology 1978. International Atomic Energy Agency (I.A.E.A.), Vienna. pp. 545–568.

Bayari, C.S., N.N. Ozyurt and S. Kilani, 2009. *Radiocarbon age distribution of groundwater in the Konya Closed Basin, central Anatolia, Turkey*. Hydrogeology Journal 17: 347-365.

Cendon, D.I., C. Ayora, J.J. Pueyo, C. Taberner and M.-M. Blanc-Valleron, 2008. *The chemical and hydrological evolution of the Mulhouse potash basin (France): Are "marine" ancient evaporates always representative of synchronous seawater chemistry?* Chemical Geology 252: 109-124.

Cendon, D.I., T.M. Peryt, C. Ayora, J.J. Pueyo and C. Taberner, 2004. *The importance of recycling processes in the Middle Miocene Badenian evaporite basin (Carpathian foredeep): paleoenvironmental implications*. Palaeogeography, Palaeoclimatology, Palaeoecology 212: 141-158.

Collerson, K.D., W.J. Ullman and T. Torgersen, 1988. *Ground waters with unradiogenic $^{87}Sr/^{86}Sr$ ratios in the Great Artesian Basin, Australia*. Geology 16: 59–63.

Eggenkamp, H.G.M. and M.L. Coleman, 2000. *Rediscovery of classical methods and their application to the measurement of stable bromine isotopes in natural samples*. Chemical Geology 167 (3): 393-402.

Farber, E., A. Vengosh, I. Gavrieli, A. Marie, T.D. Bullen, B. Mayer, A. Polak and U. Shavit, 2007. *The geochemistry of groundwater resources in the Jordan Valley: the impact of the Rift Valley brines*. Applied Geochemistry 22 (3): 494–514.

Faure, G., 1986. *Principles of Isotope Geology 2nd edition*. New York, John Wiley & Sons. 589 pp. ISBN 0-471-86412-9.

Fontes, J.C. and J.M. Garnier, 1979. *Determination of the initial C-14 activity of the total dissolved carbon - review of the existing models and a new approach*. Water Resources Research 15: 399-413.

Grasby, S.E. and Z. Chen, 2005. *Subglacial recharge into the Western Canada Sedimentary Basin-impact of Pleistocene glaciation on basin hydrodynamics*. GSA Bulletin 117: 500-514.

Hein, F.J., C.W. Langenberg, C. Kidston, H. Berhane, T. Berezniuk and D.K. Cotterill, 2001. *A comprehensive field guide for facies characterization of the Athabasca Oil Sands, Northeast Alberta*. Alberta Energy and Utilities Board Special Report 13. 415 pp.

Hitchon, B., S. Bachu, C.M. Ing, A. Lytviak and J.R. Underschultz, 1989. *Hydrogeological and Geothermal Regimes in the Phanerozoic Succession, Cold Lake Area, Alberta and Saskatchewan*. Alberta Research Council, Bulletin 59. 84 pp.

Hitchon, B., S. Bachu and J.R. Undershultz, 1990. *Regional subsurface hydrogeology, Peace River arch area, Alberta and British Columbia*. Bull. Canadian Petroleum Geology 38: 196-217.

Hughey, C.A., C.L. Hendriksen, R.P. Rodgers, A.G. Marshall and K. Qian, 2001. *Kendrick Mass Defect Spectrum: A compact visual analysis for the Ultrahigh-resolution broadband mass spectra*. Analytical Chemistry 73: 4676-4681.

Kloppmann, W., L. Dever and W.M. Edmunds, 1998. *Residence time of Chalk groundwaters in the Paris Basin and the North German Basin: a geochemical approach*. Applied Geochemistry 13(5): 593–606.

Light, T.S., 1972. *Standard solution for redox potential measurements*. Analytical Chemistry 44: 1038-1039.

McMahon, P.B., J.K. Böhlke and S.C. Christenson, 2008. *Geochemistry, radiocarbon ages, and paleorecharge conditions along a transect in the central High Plains aquifer, southwestern Kansas, USA*. Applied Geochemistry 19: 1655-1686.

Moldovanyi, E.P., L.M. Walter and L.S. Land, 1993. *Strontium, boron, oxygen, and hydrogen isotope geochemistry of brines from basal strata of the Gulf Coast sedimentary basin, USA*. Geochimica et Cosmochimica Acta 57: 2083–2099.

Nakai, N. and M.L. Jensen, 1964. *The kinetic isotope effect in the bacterial reduction and oxidation of sulfur*. Geochimica et Cosmochimica Acta 28: 1893-1912.

Nordstrom, D.K., 1977. *Thermochemical redox equilibria in Zobell's solution*. Geochimica et Cosmochimica Acta 41: 1835-1841.

Papelis, C., K.F. Hayes and J.O. Leckie, 1988. *HYDRAQL: A program for the computation of chemical equilibrium composition of aqueous batch systems including surface-complexation modeling of ion adsorption at the oxide/solution interface*. Stanford University, Palo Alto, California. Technical Report 306.

Parkhurst, D.L. and S.R. Charlton, 2008. *NetpathXL – an Excel interface to the program NETPATH*. U.S. Geological Survey Techniques and Methods 6-A26. 11 pp.

Peterman, Z.E. and J.S. Stuckless, 1992. *Application of strontium and other radiogenic tracer isotopes to paleohydrologic studies in Paleohydrological methods and their applications*. IN: Proceedings of an NEA Workshop, Paris, France, November 9–10. Nuclear Energy Agency, Organization for Economic Co-Operation and Development. pp. 59–84.

Plummer, L.N., E.C. Prestemon and D.L. Parkhurst, 1991. *An interactive code (NETPATH) for modeling NET geochemical reactions along a flow PATH*. U.S. Geological Survey Water-Resources Investigations Report 91-4078. 227 pp.

Plummer, L.N., E.C. Prestemon and D.L. Parkhurst, 1994. *An interactive code (NETPATH) for modeling NET geochemical reactions along a flow PATH, version 2.0*. U.S. Geological Survey Water-Resources Investigations Report 94-4169. 130 pp.

Plummer, L.N. and C.L. Sprinkle, 2001. *Radiocarbon dating of dissolved inorganic carbon in groundwater from confined parts of the Upper Floridan aquifer, Florida, USA*. Hydrogeology Journal 9: 127-150.

Ptacek, C.J., 1992. *Experimental determination of siderite solubility in high ionic-strength solutions*. Ph.D. Thesis. University of Waterloo, Waterloo, Ontario.

Ptacek, C.J. and D.W. Blowes, 1994. *Influence of siderite on the pore-water chemistry of inactive mine-tailings impoundments*. IN: Environmental Geochemistry of Sulfide Oxidation (C.N. Alpers and D.W. Blowes, eds.). American Chemical Society, Washington, DC. Volume 550, Chapter 13. pp. 172-189.

Shouakar-Stash, O., S.K. Frape and R.J. Drimmie, 2005. *Determination of bromine stable isotopes using continuous-flow isotope ratio mass spectrometry*. Analytical Chemistry 77: 4027–4033.

Swihart G.H., P.B. Moore and E.L. Callis, 1986. *Boron isotopic composition of marine and nonmarine evaporite borates*. Geochimica et Cosmochimica Acta 50: 1297–1301.

Thode, H.G. and J. Monster, 1965. *Sulfur-isotope geochemistry of petroleum, evaporites, and ancient seas*. AAPG Memoir 4: 363-373.

van der Kemp, W.J.M., C.A. Appelo, C.A. and K. Walraevens, 2000. *Inverse chemical modeling and radiocarbon dating of palaeogroundwaters: The Tertiary Ledo-Paniselian aquifer in Flanders, Belgium*. Water Resources Research 36: 1277-1287.

Wightman, D.M., M.N. Attalla, A.W. Desmond, R.S. Strobl, B. Habtemicael, D.K. Cotterill and T. Berezsniuk, 1995. *Resource characterization of the McMurray/Wabiskaw Deposit on the Athabasca Oil Sands Area: A synthesis*. Alberta Research Council, AOSTRA Technical Publication Series 10. 142 pp.

WorleyParsons, 2010. *2009 Athabasca River Geophysical Survey on a 125 km Reach of the Athabasca River. Fort McMurray to the Confluence of the Athabasca and Firebag River*.

9 ACRONYMS USED IN THIS REPORT

AMS	Accelerator Mass Spectrometry
AITF	Alberta Innovates – Technology Futures
CLW	Clearwater (formation)
CNRL	Canadian Natural Resources Limited
Dev	Devonian (formation)
EC	Electrical Conductivity
EM	Electromagnetic
EPP	Extractable Priority Pollutants
Fm	Formation
FT-ICR MS	Fourier Transform Ion Cyclotron Resonance Mass Spectrometry
GCMS	Gas Chromatograph Mass Spectrometry
GOWN	Groundwater Observation Well Network
HDPE	High Density Polyethylene
IRMS	Isotope Ratio Mass Spectrometry
KMD	Kendrick Mass Defects
Lat	Latitude
LEL	Local Evaporation Line
LMWL	Local Meteoric Water Line
Long	Longitude
McM	McMurray (formation)
NA	Naphthenic Acid
NOC	Natural Organic Compounds
OSRIN	Oil Sands Research and Information Network
PAH	Polycyclic Aromatic Hydrocarbon
PAW	Process Affected Water
PCA	Principle Components Analysis
pMC	Percentage Modern Carbon
scint.	Scintillation
SEE	School of Energy and the Environment

Shell	Shell Albian Sands
Syncrude	Syncrude Canada Ltd.
TOC	Total Organic Carbon
TU	Tritium Units
V-CDT	Vienna Canyon Diablo Troilite
V-SMOW	Vienna Standard Mean Ocean Water
V-PDB	Value per mL Pee Dee Belemnite
VPP	Volatile Priority Pollutants
WCSB	Western Canadian Sedimentary Basin
yBP	Years Before Present

APPENDIX 1: Isotopic and geochemical results.

Key:

DNS – did not submit

x – submitted, results unavailable

BDL – below detection limit

BQL – below quantification limit

NA – not available, not measured

Sample ID	Sampling Dates	Lat (N)	Long (W)	Location
River Water (near bed interface)				
S01	Jun-09	57.67	111.42	Dev (Waterways)
S02	Jun-09	57.59	111.51	Dev (Waterways)
S03	Jun-09	57.53	111.53	McM
S04	Jun-09	57.51	111.55	McM
S05	Jun-09	57.35	111.67	McM
S06	Jun-09	57.02	111.48	Dev (Waterways)
S07	Jun-09	57.01	111.47	Dev (Waterways)
S08	Jun-09	57.00	111.45	Dev (Waterways)
S09	Jun-09	56.77	111.39	Dev (Waterways)
S10	Jun-09	57.09	111.56	Dev (Waterways)
River Bed Seeps (below sediment interface)				
S01A	13-Aug-09	57.67	111.42	Dev (Waterways)
S01N	05-Nov-09	57.67	111.42	Dev (Waterways)
S02N	05-Nov-09	57.59	111.51	Dev (Waterways)
S03A	13-Aug-09	57.53	111.53	McM
S07A	14-Aug-09	57.01	111.47	Dev (Waterways)
SO8A	14-Aug-09	57.00	111.45	Dev (Waterways)
S09A	14-Aug-09	56.77	111.39	Dev (Waterways)
S10A	14-Aug-09	57.09	111.56	Dev (Waterways)
Process-Affected Water				
PAW 001	18-Aug-09	57.24	111.56	tailings pond- albian
PAW 002	18-Aug-09	57.30	111.51	coarse tailings- albian
PAW 003	19-Aug-09	57.04	111.62	tailings pond-syncrude
PAW 004	19-Aug-09	57.04	111.62	tailings pond- syncrude
PAW 005	19-Aug-09	57.04	111.62	coarse tailings- syncrude
PAW 006	20-Aug-09	57.24	111.56	tailings seepage- albian
PAW 007	04-Nov-09	57.34	111.88	coarse tailings- cnrl
PAW 008	04-Nov-09	57.34	111.78	recycled tailings-cnrl
PAW 009				DI Blank
Athabasca River Water (mid-channel, mid-depth)				
PAW N	21-Sep-09	57.67	111.42	river beginning of survey
PAW N 2	05-Nov-09	57.67	111.42	river beginning of survey
PAW S	21-Sep-09	56.77	111.40	river end of survey
PAW S 2	05-Nov-09	56.77	111.40	river end of survey
Groundwater Wells				
BAS 25	Sep-09	54.26	111.27	McM
BAS 25 A	Sep-09	54.26	111.27	McM
BAS 26	Sep-09	57.24	111.45	McM
CRW 1	Sep-09	57.18	111.13	CLW
SS 19	Sep-09	57.18	111.13	surficial
SS 22	Sep-09	57.18	111.13	surficial
Other Surface Waters				
NE7-09	Sep-09	57.15	-110.86	Lake
McClelland-09	Sep-09	57.47	-111.35	Wetland
AthaR-09	Sep-09	56.74	-111.39	River

Sample ID	pH	EC	T	Eh	Alk	H_2S
River Water		(uS/cm)	deg C	mV	mg/L	
S01	7.76	245	14.6	201.2	92	DNS
S02	7.58	242	13.5	198.2	100	DNS
S03	7.71	235	13.8	198.3	84	DNS
S04	7.67	245	13.3	199.7	88	DNS
S05	7.85	281	13.9	348.7	92	DNS
S06	7.69	265	13.4	308.7	112	DNS
S07	7.8	226	13.3	326	88	DNS
S08	7.57	212	13.9	314.6	68	DNS
S09	7.62	196	14	196.3	88	DNS
S10	7.9	255	15.7	212.3	96	DNS
River Bed Seeps						
S01A	7.06	2670	14.9	101	184	0
S01N	7.26	3090	2.8	-145	920	0.065
S02N	7.48	3710	4.4	46	376	0.019
S03A	7.25	1008	13.7	-40	228	0.01
S07A	7.02	4600	16.7	-128	540	0.029
SO8A	7.39	977	15.4	-141	156	0.005
S09A	8.42	1096	13.8	-31	248	NA
S10A	7.05	8180	16.3	-149	396	0.007
Process-Affected Water						
PAW 001	7.78	2530	19.3	258.5	324	DNS
PAW 002	7.4	1535	10.6	261.3	300	DNS
PAW 003	8.23	3880	10.6	237.8	580	DNS
PAW 004	8.24	3780	11.3	233.5	544	DNS
PAW 005	NA	NA	NA	NA	DNS	DNS
PAW 006	7.87	1668	9	224.2	432	DNS
PAW 007	7.65	2325	10	196.1	932	DNS
PAW 008	7.15	1001	10.6	215.6	352	DNS
PAW 009	NA	NA	NA	NA	DNS	DNS
Athabasca River Water						
PAW N	7.48	328	13	230.4	96	DNS
PAW N 2	8.11	653	1.1	142.5	128	DNS
PAW S	NA	NA	NA	NA	NA	DNS
PAW S 2	8.51	655	0.2	306	160	DNS
Groundwater Wells						
BAS 25	7.34	2865	NA	213.2	1056	DNS
BAS 25 A	7.7	2872	NA	211.2	1008	DNS
BAS 26	7.16	601	NA	325.8	304	DNS
CRW 1	7.77	2522	NA	219.2	1036	DNS
SS 19	8.49	609	NA	265.2	320	DNS
SS 22	7.96	896	NA	NA	476	DNS
Other Surface Waters						
NE7-09	5.04	24.7	12.7	NA	252	DNS
McClelland-09	7.99	231.9	NA	NA	156	DNS
AthaR-09	7.86	242.5	NA	NA	44	DNS

Sample ID	$\delta^{2}H$	$\delta^{18}O$	$\delta^{13}C$ DIC	$\delta^{13}C$ DOC	$\delta^{37}Cl$	$\delta^{81}Br$
River Water	$^{0}/_{00}$	$^{0}/_{00}$	$^{0}/_{00}$	PDB	SMOC	
S01	-145.54	-18.4	-7.11	-26.82	-3.25	DNS
S02	-145.87	-18.5	-7.16	-26.85	-0.05	DNS
S03	-145.11	-18.3	-6.87	-26.92	0.08	DNS
S04	-146.96	-18.7	-7.31	-26.86	-0.04	DNS
S05	-147.98	-18.9	-7.26	-26.89	0.41	DNS
S06	-150.47	-19.4	-6.60	-26.38	0.07	DNS
S07	-150.53	-19.2	-6.00	-26.28	0.18	DNS
S08	-138.33	-17.3	-8.70	-27.47	0.50	DNS
S09	-131.60	-16.5	-9.66	-27.64	-0.10	DNS
S10	-149.92	-19.3	-5.76	-26.34	0.49	DNS
River Bed Seeps						
S01A	-143.51	-18.1	-15.21	-28.21	-0.71	x
S01N	-140.26	-17.6	-19.67	-26.71	-0.93	x
S02N	-144.31	-18.0	-16.47	-27.00	-1.62	x
S03A	-138.96	-17.3	-15.74	-29.31	0.02	x
S07A	-143.77	-17.9	-2.35	-27.71	1.02	x
SO8A	-138.35	-17.3	-14.78	-26.72	-0.33	x
S09A	-141.86	-18.2	-10.85	-26.92	-0.88	x
S10A	-146.00	-18.4	-8.26	-28.91	0.50	x
Process-Affected Water						
PAW 001	-130.07	-14.5	-4.60	-29.47	0.39	x
PAW 002	-130.48	-14.7	-2.23	DNS	DNS	DNS
PAW 003	-113.71	-12.4	-1.41	-29.49	0.32	x
PAW 004	-113.87	-12.4	-1.38	-29.89	0.75	x
PAW 005	-115.44	-12.8	DNS	DNS	DNS	DNS
PAW 006	-133.59	-15.7	-6.49	-28.88	0.21	x
PAW 007	-130.06	-15.63	-21.1	x	x	x
PAW 008	-131.44	-15.44	-12.0	x	x	x
PAW 009	DNS	DNS	DNS	DNS	DNS	DNS
Athabasca River Water						
PAW N	-134.17	-16.9	DNS	-27.64	0.13	x
PAW N 2	-138.50	-17.2	-6.20	-26.84	0.49	x
PAW S	-139.96	-17.8	DNS	-27.02	0.58	x
PAW S 2	-141.62	-17.9	-5.56	-26.8	-0.85	x
Groundwater Wells						
BAS 25	-171.56	-22.2	-2.61	-28.3	0.19	x
BAS 25 A	-170.89	-22.2	-2.56	-28.7	0.13	x
BAS 26	-147.91	-19.2	-7.36	-27.7	NA	x
CRW 1	-154.13	-19.9	4.05	DNS	DNS	DNS
SS 19	-141.41	-18.3	-12.78	-28.0	-0.98	x
SS 22	-148.89	-19.2	-11.93	-28.0	0.28	x
Other Surface Waters						
NE7-09	-130.5	-16.44	-21.58	-27.54	NA	NA
McClelland-09	-97.2	-9.52	NA	NA	NA	NA
AthaR-09	-137.9	-17.65	NA	NA	NA	NA

Sample ID	$^{87}Sr/86Sr$	^{34}S	^{14}C		$E^{3}H$	± 1σ
River Water	NIST987	$^{0}/_{00}$	pMC	(+/-)	T.U.	
S01	0.71063	6.85	88.5	0.4	10.8	1.1
S02	0.71071	6.51	88.6	0.4	10.9	1.1
S03	0.71081	6.89	88.7	0.4	10.5	1.1
S04	0.71055	-1.54	88.0	0.4	11.2	1.1
S05	0.71074	5.77	88.0	0.4	9.6	1.0
S06	0.71118	7.78	86.3	0.4	13.0	1.0
S07	0.71103	7.12	85.9	0.4	9.2	1.0
S08	0.71072	2.45	86.1	0.4	12.3	1.1
S09	0.71038	-2.83	NA		13.1	1.2
S10	0.71097	7.06	84.8	0.4	8.7	1.0
River Bed Seeps						
S01A	0.71025	-3.67	84.8	0.4	10.6	1.1
S01N	x	-14.31	94.5	0.5	7.7	0.7
S02N	x	11.34	84.7	0.4	8.1	1.0
S03A	0.71059	9.61	87.5	0.4	10.3	1.0
S07A	0.71033	5.48	74.1	0.2	11.1	1.0
SO8A	0.71000	5.23	87.1	0.4	9.8	1.0
S09A	0.70849	-22.50	98.0	0.4	12.2	1.1
S10A	0.70909	5.84	62.7	0.4	11.8	1.1
Process-Affected Water						
PAW 001	0.71217	14.16	37.3	0.3	9.2	1.0
PAW 002	DNS	DNS	36.1	0.3	DNS	DNS
PAW 003	0.70823	8.06	17.2	0.2	12.8	1.1
PAW 004	0.70824	7.84	17.1	0.2	11.7	1.0
PAW 005	DNS	DNS	DNS	DNS	DNS	DNS
PAW 006	0.70909	17.04	39.3	0.3	7.8	0.7
PAW 007	x	x	x	x	x	x
PAW 008	x	x	x	x	x	x
PAW 009	DNS	DNS	DNS	DNS	DNS	DNS
Athabasca River Water						
PAW N	0.71066	10.09	DNS	DNS	DNS	DNS
PAW N 2	0.71038	8.09	87.3	0.4	9.4	0.8
PAW S	0.71072	9.08	DNS	DNS	DNS	DNS
PAW S 2	0.71022	8.61	89.5	0.4	7.9	0.9
Groundwater Wells						
BAS 25	0.70943	BQL	2.6	0.1	<0.8	0.6
BAS 25 A	0.70946	BQL	2.4	0.1	<0.8	0.7
BAS 26	0.71002	9.78	75.6	0.4	7.4	0.9
CRW 1	DNS	DNS	DNS	DNS	DNS	DNS
SS 19	0.71121	BQL	55.0	0.3	1.6	0.7
SS 22	0.71040	29.49	74.8	0.4	5.3	0.6
Other Surface Waters						
NE7-09	NA	NA	NA	NA	NA	NA
McClelland-09	NA	NA	NA	NA	NA	NA
AthaR-09	NA	NA	NA	NA	NA	NA

Sample ID	Li	Na	NH4	Mg	K	Ca
River Water	mg/L	mg/L	mg/L	mg/L	mg/L	mg/L
S01	DNS	DNS	DNS	DNS	DNS	DNS
S02	DNS	DNS	DNS	DNS	DNS	DNS
S03	DNS	DNS	DNS	DNS	DNS	DNS
S04	DNS	DNS	DNS	DNS	DNS	DNS
S05	DNS	DNS	DNS	DNS	DNS	DNS
S06	DNS	DNS	DNS	DNS	DNS	DNS
S07	DNS	DNS	DNS	DNS	DNS	DNS
S08	DNS	DNS	DNS	DNS	DNS	DNS
S09	DNS	DNS	DNS	DNS	DNS	DNS
S10	DNS	DNS	DNS	DNS	DNS	DNS
River Bed Seeps						
S01A	0.009	105.994	1.540	28.148	2.750	106.352
S01N	0.010	25.141	4.685	61.740	3.277	224.029
S02N	0.009	260.962	3.233	32.901	4.758	119.222
S03A	0.007	22.281	3.415	19.567	2.824	68.983
S07A	0.029	394.423	6.882	48.095	6.980	161.257
SO8A	0.009	66.762	3.364	11.803	1.922	39.723
S09A	0.019	42.318	0.152	27.283	2.551	57.688
S10A	0.059	530.060	5.879	83.021	7.447	293.677
Process-Affected Water						
PAW 001	0.106	263.879	1.065	12.421	14.970	20.572
PAW 002	0.150	253.437	2.820	20.000	20.616	29.442
PAW 003	0.154	708.524	35.702	12.004	15.029	19.018
PAW 004	0.151	709.422	35.474	11.905	14.947	18.704
PAW 005	DNS	DNS	DNS	DNS	DNS	DNS
PAW 006	0.111	206.469	2.243	34.531	13.584	83.539
PAW 007	x	x	x	x	x	x
PAW 008	x	x	x	x	x	x
PAW 009	DNS	DNS	DNS	DNS	DNS	DNS
Athabasca River Water						
PAW N	0.004	24.095	0.109	8.762	1.132	31.337
PAW N 2	0.005	25.322	0.106	10.841	1.308	36.550
PAW S	0.004	9.458	0.030	10.059	1.182	36.512
PAW S 2	0.005	15.249	0.057	13.094	1.667	46.448
Groundwater Wells						
BAS 25	0.213	532.719	8.378	32.602	21.390	31.502
BAS 25 A	0.212	525.938	8.314	32.160	21.272	31.259
BAS 26	0.013	8.836	0.270	21.984	0.524	81.386
CRW 1	0.072	562.819	4.579	1.937	2.459	2.569
SS 19	0.008	117.977	1.884	9.051	2.706	7.920
SS 22	0.047	47.198	4.308	65.732	4.877	41.407
Other Surface Waters						
NE7-09	BDL	0.4	0.28	1.1	0.1	3.5
McClelland-09	0.0209	5.0	0.12	17.4	2.7	23.5
AthaR-09	0.0065	10.3	0.06	9.0	1.4	33.1

Sample ID	Fluoride	Sulphate	Nitrite	Bromide	Nitrate	Phosphate	TOC
River Water	mg/L	mg/L	mg/L	mg/L	mg/L	mg/L	mg/L
S01	DNS	DNS	DNS	DNS	DNS	DNS	DNS
S02	DNS	DNS	DNS	DNS	DNS	DNS	DNS
S03	DNS	DNS	DNS	DNS	DNS	DNS	DNS
S04	DNS	DNS	DNS	DNS	DNS	DNS	DNS
S05	DNS	DNS	DNS	DNS	DNS	DNS	DNS
S06	DNS	DNS	DNS	DNS	DNS	DNS	DNS
S07	DNS	DNS	DNS	DNS	DNS	DNS	DNS
S08	DNS	DNS	DNS	DNS	DNS	DNS	DNS
S09	DNS	DNS	DNS	DNS	DNS	DNS	DNS
S10	DNS	DNS	DNS	DNS	DNS	DNS	DNS
River Bed Seeps							
S01A	0.102	84.505	0.561	BDL	BDL	BDL	10.865
S01N	x	x	x	x	x	x	16.435
S02N	x	x	x	x	x	x	15.460
S03A	0.094	21.883	BDL	BDL	5.568	BDL	14.015
S07A	0.082	15.795	BDL	BDL	BDL	BDL	21.455
SO8A	0.121	14.063	6.491	BDL	BDL	BDL	15.055
S09A	0.156	91.323	BDL	BDL	BDL	BDL	17.645
S10A	0.177	260.048	BDL	BDL	BDL	BDL	6.208
Process-Affected Water							
PAW 001	3.458	144.799	BDL	BDL	BDL	BDL	43.735
PAW 002	3.870	152.630	BDL	0.150	0.287	BDL	58.585
PAW 003	3.445	518.443	BDL	BDL	BDL	BDL	62.720
PAW 004	3.605	519.076	BDL	BDL	BDL	BDL	63.045
PAW 005	DNS	DNS	DNS	DNS	DNS	DNS	DNS
PAW 006	1.387	236.087	BDL	BDL	BDL	BDL	33.245
PAW 007	x	x	x	x	x	x	x
PAW 008	x	x	x	x	x	x	x
PAW 009	DNS	DNS	DNS	DNS	DNS	DNS	DNS
Athabasca River Water							
PAW N	0.103	25.406	BDL	BDL	BDL	BDL	7.663
PAW N 2	x	x	x	x	x	x	7.971
PAW S	0.085	31.313	BDL	BDL	BDL	BDL	4.049
PAW S 2	x	x	x	x	x	x	5.159
Groundwater Wells							
BAS 25	1.065	BDL	BDL	0.477	BDL	BDL	18.450
BAS 25 A	1.074	BDL	BDL	BDL	BDL	BDL	17.985
BAS 26	0.113	10.923	BDL	BDL	BDL	BDL	10.265
CRW 1	1.191	2.583	BDL	1.683	BDL	BDL	19.230
SS 19	0.126	0.109	BDL	BDL	BDL	BDL	13.680
SS 22	0.248	0.993	BDL	0.212	BDL	BDL	13.200
Other Surface Waters							
NE7-09	0.02	0.21	BDL	BDL	BDL	NA	35.6
McClelland-09	0.21	0.11	BDL	BDL	BDL	NA	12.4
AthaR-09	0.10	25.50	BDL	BDL	BDL	NA	9.0

Sample ID	Li	Si	Ti	V	Cr	Mn
River Water	ug/L	ug/L	ug/L	ug/L	ug/L	ug/L
S01	DNS	DNS	DNS	DNS	DNS	DNS
S02	DNS	DNS	DNS	DNS	DNS	DNS
S03	DNS	DNS	DNS	DNS	DNS	DNS
S04	DNS	DNS	DNS	DNS	DNS	DNS
S05	DNS	DNS	DNS	DNS	DNS	DNS
S06	DNS	DNS	DNS	DNS	DNS	DNS
S07	DNS	DNS	DNS	DNS	DNS	DNS
S08	DNS	DNS	DNS	DNS	DNS	DNS
S09	DNS	DNS	DNS	DNS	DNS	DNS
S10	DNS	DNS	DNS	DNS	DNS	DNS
River Bed Seeps						
S01A	19.24	9780.25	1.61	1.77	0.63	1998.98
S01N	x	x	x	x	x	x
S02N	x	x	x	x	x	x
S03A	16.83	14244.07	3.45	2.31	0.85	3292.19
S07A	53.32	14110.45	2.27	6.02	0.96	16293.89
SO8A	15.50	9956.21	1.46	2.24	0.60	2731.49
S09A	37.00	7005.33	1.08	0.65	0.73	42.90
S10A	100.05	13563.78	1.82	4.39	0.80	1257.65
Process-Affected Water						
PAW 001	169.60	6220.55	1.00	6.00	0.66	65.27
PAW 002	194.26	22103.79	79.82	89.86	59.40	2678.50
PAW 003	227.76	4927.61	1.04	9.04	0.66	54.47
PAW 004	230.05	4994.23	1.01	9.36	0.91	53.64
PAW 005	DNS	DNS	DNS	DNS	DNS	DNS
PAW 006	171.73	10855.36	2.20	1.36	0.62	1242.54
PAW 007	x	x	x	x	x	x
PAW 008	x	x	x	x	x	x
PAW 009	DNS	DNS	DNS	DNS	DNS	DNS
Athabasca River Water						
PAW N	9.15	4038.42	0.86	1.00	0.78	11.47
PAW N 2	x	x	x	x	x	x
PAW S	8.32	2178.74	0.66	0.61	0.51	1.12
PAW S 2	x	x	x	x	x	x
Groundwater Wells						
BAS 25	317.56	5897.52	0.94	1.44	0.44	27.99
BAS 25 A	320.86	6172.08	1.01	1.20	0.92	28.48
BAS 26	27.32	7644.65	0.86	0.63	0.60	681.80
CRW 1	119.42	5368.27	22.50	15.39	1.54	4.62
SS 19	19.35	916.36	0.14	0.07	0.47	9.11
SS 22	85.52	9505.27	1.22	0.42	0.42	102.46
Other Surface Waters						
NE7-09	BDL	1649.00	0.87	0.71	0.58	88.14
McClelland-09	20.86	8110.38	0.45	0.11	0.29	0.49
AthaR-09	6.45	900.38	0.40	0.25	0.36	3.71

Sample ID	Fe	Co	Ni	Cu	Zn	As
River Water	ug/L	ug/L	ug/L	ug/L	ug/L	ug/L
S01	DNS	DNS	DNS	DNS	DNS	DNS
S02	DNS	DNS	DNS	DNS	DNS	DNS
S03	DNS	DNS	DNS	DNS	DNS	DNS
S04	DNS	DNS	DNS	DNS	DNS	DNS
S05	DNS	DNS	DNS	DNS	DNS	DNS
S06	DNS	DNS	DNS	DNS	DNS	DNS
S07	DNS	DNS	DNS	DNS	DNS	DNS
S08	DNS	DNS	DNS	DNS	DNS	DNS
S09	DNS	DNS	DNS	DNS	DNS	DNS
S10	DNS	DNS	DNS	DNS	DNS	DNS
River Bed Seeps						
S01A	252.56	2.15	4.3371	BDL	1.3275	7.5361
S01N	x	x	x	x	x	x
S02N	x	x	x	x	x	x
S03A	1074.35	4.72	6.5669	0.8376	3.1276	6.7013
S07A	19058.27	17.41	17.0379	1.1062	2.0580	16.4323
SO8A	3080.54	1.86	1.9956	0.7889	1.6723	7.3392
S09A	158.99	0.51	3.3332	3.3238	1.5560	4.0665
S10A	33004.31	0.69	3.2236	BDL	1.2380	41.3680
Process-Affected Water						
PAW 001	47.63	6.47	10.0651	0.7026	1.3876	4.5922
PAW 002	72528.08	42.41	74.3755	8.2487	111.4716	17.5505
PAW 003	71.17	2.93	11.4603	BDL	2.1709	7.2497
PAW 004	60.88	2.96	11.6107	BDL	1.8201	6.9821
PAW 005	DNS	DNS	DNS	DNS	DNS	DNS
PAW 006	123.49	35.80	48.0864	BDL	1.4219	5.4600
PAW 007	x	x	x	x	x	x
PAW 008	x	x	x	x	x	x
PAW 009	DNS	DNS	DNS	DNS	DNS	DNS
Athabasca River Water						
PAW N	268.17	0.16	1.2174	1.0152	4.3527	2.3363
PAW N 2	x	x	x	x	x	x
PAW S	81.67	0.13	1.1218	1.0851	3.9700	2.5270
PAW S 2	x	x	x	x	x	x
Groundwater Wells						
BAS 25	76.24	0.21	1.0939	BDL	6.2881	1.9941
BAS 25 A	73.81	0.25	0.8298	BDL	5.7798	1.9308
BAS 26	5565.01	14.04	32.0471	BDL	33.9870	4.8523
CRW 1	355.75	0.82	15.4388	2.0738	51.0135	1.6453
SS 19	26.64	0.16	11.6660	0.3548	53.9833	0.7043
SS 22	3330.31	0.40	2.1452	BDL	9.6987	4.0400
Other Surface Waters						
NE7-09	497.70	0.26	0.4100	0.1000	12.1200	0.3800
McClelland-09	41.08	0.02	0.1240	0.1007	2.6279	1.0662
AthaR-09	219.58	0.12	1.0616	0.7375	2.4569	2.3411

Sample ID	Se	Rb	Sr	Y	Zr	Nb
River Water	ug/L	ug/L	ug/L	ug/L	ug/L	ug/L
S01	DNS	DNS	DNS	DNS	DNS	DNS
S02	DNS	DNS	DNS	DNS	DNS	DNS
S03	DNS	DNS	DNS	DNS	DNS	DNS
S04	DNS	DNS	DNS	DNS	DNS	DNS
S05	DNS	DNS	DNS	DNS	DNS	DNS
S06	DNS	DNS	DNS	DNS	DNS	DNS
S07	DNS	DNS	DNS	DNS	DNS	DNS
S08	DNS	DNS	DNS	DNS	DNS	DNS
S09	DNS	DNS	DNS	DNS	DNS	DNS
S10	DNS	DNS	DNS	DNS	DNS	DNS
River Bed Seeps						
S01A	0.7372	4.4509	1005.5732	0.1367	0.3893	BDL
S01N	x	x	x	x	x	x
S02N	x	x	x	x	x	x
S03A	0.5515	5.4850	538.3161	0.4764	1.1479	0.0103
S07A	2.3526	8.7126	1587.6559	0.4085	2.9368	0.0166
SO8A	0.6231	3.1986	320.2749	0.2024	0.8807	0.0050
S09A	0.4054	1.5389	371.8275	0.1271	0.4325	0.0039
S10A	2.9591	8.6485	2316.0159	0.1455	0.4009	0.0044
Process-Affected Water						
PAW 001	1.9518	23.8019	620.7584	0.0497	0.7342	0.0045
PAW 002	3.1512	58.0311	917.2691	51.3795	16.1543	0.7326
PAW 003	2.8466	37.1817	846.5113	0.0712	3.4888	0.0098
PAW 004	2.8690	37.7059	858.5467	0.0619	2.8999	0.0062
PAW 005	DNS	DNS	DNS	DNS	DNS	DNS
PAW 006	1.1903	20.0896	1324.2481	0.0468	0.4595	BDL
PAW 007	x	x	x	x	x	x
PAW 008	x	x	x	x	x	x
PAW 009	DNS	DNS	DNS	DNS	DNS	DNS
Athabasca River Water						
PAW N	0.3038	0.8284	231.6584	0.1053	0.0997	BDL
PAW N 2	x	x	x	x	x	x
PAW S	0.3536	0.8327	287.4499	0.0553	BDL	BDL
PAW S 2	x	x	x	x	x	x
Groundwater Wells						
BAS 25	2.4542	26.9546	1489.4263	0.0083	0.7653	BDL
BAS 25 A	2.4503	26.9948	1496.6398	0.0068	0.8176	0.0044
BAS 26	0.3703	0.6862	280.8074	0.0104	0.2070	BDL
CRW 1	6.2233	3.2555	201.0567	2.2433	4.6579	0.0203
SS 19	0.1284	0.7626	88.5400	0.0050	0.0533	0.0007
SS 22	0.4664	1.4655	543.5874	0.0089	0.1204	0.1027
Other Surface Waters						
NE7-09	0.0600	0.1400	6.7000	0.0320	0.1500	0.0070
McClelland-09	0.0920	2.6307	140.0732	0.0040	BDL	BDL
AthaR-09	0.3797	0.6763	226.3441	0.1658	0.1708	0.0021

Sample ID	Mo	Ag	Ba	La	Ce	Pr
River Water	ug/L	ug/L	ug/L	ug/L	ug/L	ug/L
S01	DNS	DNS	DNS	DNS	DNS	DNS
S02	DNS	DNS	DNS	DNS	DNS	DNS
S03	DNS	DNS	DNS	DNS	DNS	DNS
S04	DNS	DNS	DNS	DNS	DNS	DNS
S05	DNS	DNS	DNS	DNS	DNS	DNS
S06	DNS	DNS	DNS	DNS	DNS	DNS
S07	DNS	DNS	DNS	DNS	DNS	DNS
S08	DNS	DNS	DNS	DNS	DNS	DNS
S09	DNS	DNS	DNS	DNS	DNS	DNS
S10	DNS	DNS	DNS	DNS	DNS	DNS
River Bed Seeps						
S01A	1.4141	BDL	268.4521	0.0321	0.0809	0.0099
S01N	x	x	x	x	x	x
S02N	x	x	x	x	x	x
S03A	1.6088	BDL	206.6892	0.2651	0.6259	0.0823
S07A	2.5567	0.0062	862.3870	0.0870	0.2388	0.0304
SO8A	2.8314	0.0202	169.5808	0.0572	0.1354	0.0182
S09A	0.4994		43.3425	0.0419	0.0714	0.0140
S10A	0.4342	BDL	330.5039	0.0324	0.0615	0.0070
Process-Affected Water						
PAW 001	63.1842	0.0061	293.8089	0.0432	0.1042	0.0138
PAW 002	35.5045	0.0222	341.1614	68.8250	195.3652	22.4821
PAW 003	142.8278	0.0061	217.4209	0.0574	0.1475	0.0169
PAW 004	143.8713	0.0066	273.2064	0.0298	0.0755	0.0087
PAW 005	DNS	DNS	DNS		DNS	DNS
PAW 006	6.7526	BDL	193.1187	0.0080	0.0188	0.0030
PAW 007	x	x	x	x	x	x
PAW 008	x	x	x	x	x	x
PAW 009	DNS	DNS	DNS	DNS	DNS	DNS
Athabasca River Water						
PAW N	0.7286	BDL	59.0476	0.0526	0.0978	0.0151
PAW N 2	x	x	x	x	x	x
PAW S	0.7835	BDL	68.7561	0.0156	0.0300	0.0056
PAW S 2	x	x	x	x	x	x
Groundwater Wells						
BAS 25	0.8063	BDL	153.5649	BDL	BDL	BDL
BAS 25 A	0.7094	BDL	148.2805	0.0030	BDL	BDL
BAS 26	5.1564	BDL	125.9627	0.0035	BDL	BDL
CRW 1	6.3261	0.0117	119.5081	3.0214	6.5004	0.8788
SS 19	56.9196	0.0007	28.6064	0.0029	0.0070	0.0006
SS 22	3.3716	BDL	60.2196	0.0035	BDL	BDL
Other Surface Waters						
NE7-09	0.1100	BDL	16.7000	0.0240	0.0680	0.0080
McClelland-09	BDL	BDL	66.8015	0.0022	0.0034	0.0005
AthaR-09	0.6359	0.0035	82.6202	0.0698	0.1258	0.0241

Sample ID	Nd	Sm	Eu	Gd	Tb	Dy
River Water	ug/L	ug/L	ug/L	ug/L	ug/L	ug/L
S01	DNS	DNS	DNS	DNS	DNS	DNS
S02	DNS	DNS	DNS	DNS	DNS	DNS
S03	DNS	DNS	DNS	DNS	DNS	DNS
S04	DNS	DNS	DNS	DNS	DNS	DNS
S05	DNS	DNS	DNS	DNS	DNS	DNS
S06	DNS	DNS	DNS	DNS	DNS	DNS
S07	DNS	DNS	DNS	DNS	DNS	DNS
S08	DNS	DNS	DNS	DNS	DNS	DNS
S09	DNS	DNS	DNS	DNS	DNS	DNS
S10	DNS	DNS	DNS	DNS	DNS	DNS
River Bed Seeps						
S01A	0.0553	0.0147	0.0191	0.0209	0.0027	0.0165
S01N	x	x	x	x	x	x
S02N	x	x	x	x	x	x
S03A	0.3731	0.0961	0.0319	0.1081	0.0143	0.0788
S07A	0.1513	0.0381	0.0555	0.0558	0.0082	0.0492
SO8A	0.0965	0.0248	0.0164	0.0332	0.0040	0.0283
S09A	0.0709	0.0132	0.0070	0.0224	0.0027	0.0175
S10A	0.0376	0.0094	0.0199	0.0115	0.0022	0.0112
Process-Affected						
PAW 001	0.0598	0.0098	0.0196	0.0126	0.0017	0.0101
PAW 002	94.7491	20.2506	4.6087	19.3991	2.4176	12.4583
PAW 003	0.0737	0.0130	0.0180	0.0165	0.0019	0.0169
PAW 004	0.0386	0.0091	0.0155	0.0107	0.0013	0.0107
PAW 005	DNS	DNS	DNS	DNS	DNS	DNS
PAW 006	0.0099	0.0043	0.0121	0.0042	0.0010	0.0078
PAW 007	x	x	x	x	x	x
PAW 008	x	x	x	x	x	x
PAW 009	DNS	DNS	DNS	DNS	DNS	DNS
Athabasca River						
PAW N	0.0757	0.0152	0.0071	0.0185	0.0023	0.0136
PAW N 2	x	x	x	x	x	x
PAW S	0.0253	0.0038	0.0053	0.0067	0.0013	0.0085
PAW S 2	x	x	x	x	x	x
Groundwater Wells						
BAS 25	BDL	BDL	0.0094	0.0015	BDL	BDL
BAS 25 A	BDL	BDL	0.0104	BDL	BDL	BDL
BAS 26	BDL	BDL	0.0083	BDL	BDL	0.0015
CRW 1	3.6974	0.7594	0.1798	0.7268	0.0891	0.4756
SS 19	0.0033	0.0007	0.0017	0.0008	0.0001	0.0007
SS 22	0.0051	BDL	0.0042	BDL	BDL	0.0010
Other Surface Waters						
NE7-09	0.0360	0.0070	0.0028	0.0080	0.0011	0.0070
McClelland-09	0.0024	0.0008	0.0038	0.0007	0.0001	0.0004
AthaR-09	0.1170	0.0290	0.0116	0.0333	0.0046	0.0296

Sample ID	Cd	Sn	Sb	Cs	Ho	Er
River Water	ug/L	ug/L	ug/L	ug/L	ug/L	ug/L
S01	DNS	DNS	DNS	DNS	DNS	DNS
S02	DNS	DNS	DNS	DNS	DNS	DNS
S03	DNS	DNS	DNS	DNS	DNS	DNS
S04	DNS	DNS	DNS	DNS	DNS	DNS
S05	DNS	DNS	DNS	DNS	DNS	DNS
S06	DNS	DNS	DNS	DNS	DNS	DNS
S07	DNS	DNS	DNS	DNS	DNS	DNS
S08	DNS	DNS	DNS	DNS	DNS	DNS
S09	DNS	DNS	DNS	DNS	DNS	DNS
S10	DNS	DNS	DNS	DNS	DNS	DNS
River Bed Seeps						
S01A	0.0148	1.6492	0.1735	0.0251	0.0039	0.0130
S01N	x	x	x	x	x	x
S02N	x	x	x	x	x	x
S03A	0.0155	1.7653	0.1504	0.0413	0.0166	0.0446
S07A	0.0058	1.6210	0.1794	0.0431	0.0122	0.0359
SO8A	0.0071	1.5790	0.1131	0.0166	0.0064	0.0194
S09A	0.0064	1.7929	0.4039	0.0066	0.0048	0.0147
S10A	0.0042	1.6733	0.0277	0.0164	0.0034	0.0113
Process-Affected Water						
PAW 001	0.0500	BDL	3.1515	0.1473	0.0022	0.0066
PAW 002	1.1110	1.9711	1.0888	1.3905	2.2636	5.3972
PAW 003	0.1047	BDL	4.6310	0.8981	0.0020	0.0085
PAW 004	0.1023	BDL	4.4677	0.9254	0.0022	0.0076
PAW 005	DNS	DNS	DNS	DNS	DNS	DNS
PAW 006	0.0119	BDL	0.0432	0.0592	0.0018	BDL
PAW 007	x	x	x	x	x	x
PAW 008	x	x	x	x	x	x
PAW 009	DNS	DNS	DNS	DNS	DNS	DNS
Athabasca River Water						
PAW N	0.0140	BDL	0.1182	0.0039	0.0032	0.0092
PAW N 2	x	x	x	x	x	x
PAW S	0.0265	1.7563	0.1284	0.0054	0.0018	0.0051
PAW S 2	x	x	x	x	x	x
Groundwater Wells						
BAS 25	0.0058	1.4715	0.0543	0.1182	BDL	BDL
BAS 25 A	0.0056	1.8244	0.0608	0.1191	BDL	BDL
BAS 26	0.0074	1.4009	0.3383	0.0053	0.0004	BDL
CRW 1	0.0107	2.2217	1.4013	0.0712	0.0859	0.2181
SS 19	0.0443	0.3422	0.3813	0.0024	0.0002	0.0005
SS 22	0.0076	1.4509	0.3350	0.0077	0.0005	BDL
Other Surface Waters						
NE7-09	0.0495	BDL	0.0100	BDL	0.0012	0.0033
McClelland-09	0.0148	BDL	0.0317	0.0041	0.0001	BDL
AthaR-09	0.0193	0.1445	0.0800	0.0028	0.0053	0.0165

Sample ID	Tm	Yb	Lu	Pb	Th	U
River Water	ug/L	ug/L	ug/L	ug/L	ug/L	ug/L
S01	DNS	DNS	DNS	DNS	DNS	DNS
S02	DNS	DNS	DNS	DNS	DNS	DNS
S03	DNS	DNS	DNS	DNS	DNS	DNS
S04	DNS	DNS	DNS	DNS	DNS	DNS
S05	DNS	DNS	DNS	DNS	DNS	DNS
S06	DNS	DNS	DNS	DNS	DNS	DNS
S07	DNS	DNS	DNS	DNS	DNS	DNS
S08	DNS	DNS	DNS	DNS	DNS	DNS
S09	DNS	DNS	DNS	DNS	DNS	DNS
S10	DNS	DNS	DNS	DNS	DNS	DNS
River Bed Seeps						
S01A	0.0019	0.0102	0.0019	1.2195	BDL	0.6329
S01N	x	x	x	x	x	x
S02N	x	x	x	x	x	x
S03A	0.0062	0.0433	0.0064	1.9045	BDL	0.8494
S07A	0.0055	0.0349	0.0060	1.1688	BDL	2.0579
SO8A	0.0026	0.0181	0.0032	1.5201	BDL	0.4267
S09A	0.0020	0.0118	0.0019	1.1722	BDL	0.7664
S10A	0.0017	0.0087	0.0011	1.0620	BDL	0.2648
Process-Affected Water						
PAW 001	0.0008	0.0044	0.0010	1.1274	BDL	2.7885
PAW 002	0.7177	4.1683	0.5697	29.9449	80.2435	9.1828
PAW 003	0.0009	0.0105	0.0018	1.1310	0.2339	7.3774
PAW 004	0.0012	0.0081	0.0019	1.1207	BDL	7.3807
PAW 005	DNS	DNS		DNS	DNS	DNS
PAW 006	0.0008	0.0044	0.0009	1.1388	BDL	1.6094
PAW 007	x	x	x	x	x	x
PAW 008	x	x	x	x	x	x
PAW 009	DNS	DNS	DNS	DNS	DNS	DNS
Athabasca River Water						
PAW N	0.0013	0.0085	0.0012	1.2305	BDL	0.3201
PAW N 2	x	x	x	x		x
PAW S	0.0008	0.0038	0.0007	1.2704	BDL	0.4296
PAW S 2	x	x	x	x		x
Groundwater Wells						
BAS 25	BDL	0.0005	BDL	1.1729	BDL	BDL
BAS 25 A	BDL	BDL	BDL	1.1335	BDL	BDL
BAS 26	0.0003	0.0010	0.0003	1.1613	BDL	0.2869
CRW 1	0.0291	0.1691	0.0240	2.7930	3.5425	0.4837
SS 19	0.0001	0.0005	0.0001	0.0491	BDL	0.0053
SS 22	0.0002	0.0009	0.0002	1.1711	BDL	0.1871
Other Surface Waters						
NE7-09	0.0005	0.0030	0.0005	0.0700	0.0110	BDL
McClelland-09	0.0001	0.0003	0.0000	0.0072	BDL	0.0010
AthaR-09	0.0023	0.0141	0.0021	0.0509	BDL	0.3284

APPENDIX 2. Detected priority pollutants and naphthenic acids.

A complete list of scanned compounds, detection limits and uncertainties are given in APPENDIX 3.

Sample ID	Benzene ug/l	Chloroform ug/l	Ethyl benzene ug/l	isopropylbenzene ug/l	n-propylbenzene ug/l	m.p. Xylene ug/l	Trihalomethanes ug/l	Toluene ug/l	Xylenes ug/l	sec-Butylbenzene ug/l	Napthenic Acids mg/l	Unresolved Hydrocarbons ug/l	Unresolved Hydrocarbons ug/l (C12-C36)	Bis(2-ethylhexyl)phthalate ug/l	Di-n-butylphthalate ug/l	Phenanthrene ug/l	Acenaphthene ug/l	Chrysene ug/l	1.2.4 Trtimethylbenzene ug/l	1.3.5 Trtimethylbenzene ug/l	NOC analyses
River Bed Water																					
S01	DNS	DNS	DNS	DNS	DNS	DNS	DNS	DNS	DNS	DNS	DNS	DNS	DNS	DNS	DNS	DNS	DNS	DNS	DNS	DNS	DNS
S02	DNS	DNS	DNS	DNS	DNS	DNS	DNS	DNS	DNS	DNS	DNS	DNS	DNS	DNS	DNS	DNS	DNS	DNS	DNS	DNS	DNS
S03	DNS	DNS	DNS	DNS	DNS	DNS	DNS	DNS	DNS	DNS	DNS	DNS	DNS	DNS	DNS	DNS	DNS	DNS	DNS	DNS	DNS
S04	DNS	DNS	DNS	DNS	DNS	DNS	DNS	DNS	DNS	DNS	DNS	DNS	DNS	DNS	DNS	DNS	DNS	DNS	DNS	DNS	DNS
S05	DNS	DNS	DNS	DNS	DNS	DNS	DNS	DNS	DNS	DNS	DNS	DNS	DNS	DNS	DNS	DNS	DNS	DNS	DNS	DNS	DNS
S06	DNS	DNS	DNS	DNS	DNS	DNS	DNS	DNS	DNS	DNS	DNS	DNS	DNS	DNS	DNS	DNS	DNS	DNS	DNS	DNS	DNS
S07	DNS	DNS	DNS	DNS	DNS	DNS	DNS	DNS	DNS	DNS	DNS	DNS	DNS	DNS	DNS	DNS	DNS	DNS	DNS	DNS	DNS
S08	DNS	DNS	DNS	DNS	DNS	DNS	DNS	DNS	DNS	DNS	DNS	DNS	DNS	DNS	DNS	DNS	DNS	DNS	DNS	DNS	DNS
S09	DNS	DNS	DNS	DNS	DNS	DNS	DNS	DNS	DNS	DNS	DNS	DNS	DNS	DNS	DNS	DNS	DNS	DNS	DNS	DNS	DNS
S10	DNS	DNS	DNS	DNS	DNS	DNS	DNS	DNS	DNS	DNS	DNS	DNS	DNS	DNS	DNS	DNS	DNS	DNS	DNS	DNS	DNS
River Bed Seepage																					
S01A	BDL	BDL	BDL	BDL	BDL	BDL	BDL	BDL	BDL	BDL	0.08	BDL	BDL	0.4	BDL	BDL	BDL	BDL	BDL	BDL	y
S01N	BDL	BDL	BDL	BDL	BDL	BDL	BDL	BDL	BDL	BDL	0.07	BDL	BDL	1	BDL	BDL	BDL	BDL	BDL	BDL	y
S02N	BDL	BDL	BDL	BDL	BDL	BDL	BDL	BDL	BDL	BDL	0.04	BDL	BDL	0.5	BDL	BDL	BDL	BDL	BDL	BDL	y
S03A	BDL	BDL	BDL	BDL	BDL	BDL	BDL	BDL	BDL	BDL	0.07	BDL	BDL	0.3	0.2	BDL	BDL	BDL	BDL	BDL	y
S07A	BDL	BDL	BDL	BDL	BDL	BDL	BDL	BDL	BDL	BDL	0.14	BDL	BDL	0.6	0.2	BDL	BDL	BDL	BDL	BDL	y
SO8A	BDL	BDL	BDL	BDL	BDL	BDL	BDL	BDL	BDL	BDL	0.05	BDL	BDL	0.4	0.2	BDL	BDL	BDL	BDL	BDL	y
S09A	BDL	BDL	BDL	BDL	BDL	BDL	BDL	BDL	BDL	BDL	0.29	BDL	BDL	0.3	0.2	BDL	BDL	BDL	BDL	BDL	y
S10A	BDL	BDL	BDL	BDL	BDL	BDL	BDL	0.2	BDL	BDL	0.2	BDL	BDL	0.3	0.2	BDL	BDL	BDL	BDL	BDL	y

Sample ID	Benzene ug/l	Chloroform ug/l	Ethyl benzene ug/l	isopropylbenzene ug/l	n-propylbenzene ug/l	m.p. Xylene ug/l	Trihalomethanes ug/l	Toluene ug/l	Xylenes ug/l	sec-Butylbenzene ug/l	Napthenic Acids mg/l	Unresolved Hydrocarbons ug/l	Unresolved Hydrocarbons ug/l (C12-C36)	Bis(2-ethylhexyl)phthalate ug/l	Di-n-butylphthalate ug/l	Phenanthrene ug/l	Acenaphthene ug/l	Chrysene ug/l	1.2.4 Trtimethylbenzene ug/l	1.3.5 Trtimethylbenzene ug/l	NOC analyses
Processed Water																					
PAW 001	BDL	0.2	BDL	BDL	BDL	BDL	0.2	BDL	BDL	BDL	4.26	11	9600	0.7	BDL	BDL					y
PAW 002	BDL	88.2	68.7	BDL	BDL	632	88.2	BDL	919	BDL	2.71	128600	BDL	BDL	BDL	35.3	8.5	15.2	BDL	BDL	y
PAW 003	BDL	BDL	BDL	BDL	BDL	BDL	BDL	BDL	BDL	BDL	11.4	70	23000	BDL	BDL	BDL	BDL	BDL	BDL	BDL	y
PAW 004	BDL	BDL	BDL	BDL	BDL	BDL	BDL	BDL	BDL	BDL	16.5	86	17000	BDL	BDL	BDL	BDL	BDL	BDL	BDL	y
PAW 005	31.4	70.9	67.4	BDL	BDL	614	70.9	47.7	883	BDL	1.84	144900	BDL	17.8	BDL	6.3	BDL	BDL	BDL	BDL	
PAW 006	BDL	BDL	BDL	BDL	BDL	0.1	BDL	BDL	0.1	BDL	9.4	74	BDL	BDL	BDL	BDL	BDL	BDL	BDL	BDL	y
PAW 007	295	BDL	1270	246	453	3530	BDL	3310	5160	112	168	268000	BDL	BDL	BDL	BDL	BDL	BDL	1330	773	y
PAW 008	BDL	BDL	BDL	BDL	BDL	17.5	BDL	BDL	53.7	BDL	29.5	10700	BDL	BDL	BDL	41	5.5	BDL	5.8	99	y
PAW 009	BDL	BDL	BDL	BDL	BDL	BDL	BDL	BDL	BDL	BDL	BDL	BDL	BDL	0.5	BDL	BDL	BDL	BDL	BDL	BDL	y
River Water																					
PAW N	BDL	BDL	BDL	BDL	BDL	BDL	BDL	BDL	BDL	BDL	0.4	BDL	BDL	BDL	BDL	BDL	BDL	BDL	BDL	BDL	y
PAW N 2	BDL	BDL	BDL	BDL	BDL	BDL	BDL	BDL	BDL	BDL	0.9	BDL	BDL	0.9	BDL	BDL	BDL	BDL	BDL	BDL	
PAW S	BDL	BDL	BDL	BDL	BDL	BDL	BDL	BDL	BDL	BDL	0.4	BDL	BDL	BDL	BDL	BDL	BDL	BDL	BDL	BDL	y
PAW S 2	BDL	BDL	BDL	BDL	BDL	BDL	BDL	BDL	BDL	BDL	0.5	BDL	BDL	0.7	BDL	BDL	BDL	BDL	BDL	BDL	
Ground Water																					
BAS 25	DNS	DNS	DNS	DNS	DNS	DNS	DNS	DNS	DNS	DNS	DNS	DNS	DNS	DNS	DNS	DNS	DNS	DNS	DNS	DNS	y
BAS 25 A	DNS	DNS	DNS	DNS	DNS	DNS	DNS	DNS	DNS	DNS	DNS	DNS	DNS	DNS	DNS	DNS	DNS	DNS	DNS	DNS	y
BAS 26	DNS	DNS	DNS	DNS	DNS	DNS	DNS	DNS	DNS	DNS	DNS	DNS	DNS	DNS	DNS	DNS	DNS	DNS	DNS	DNS	y
CRW 1	DNS	DNS	DNS	DNS	DNS	DNS	DNS	DNS	DNS	DNS	DNS	DNS	DNS	DNS	DNS	DNS	DNS	DNS	DNS	DNS	y
SS 19	DNS	DNS	DNS	DNS	DNS	DNS	DNS	DNS	DNS	DNS	DNS	DNS	DNS	DNS	DNS	DNS	DNS	DNS	DNS	DNS	y
SS 22	DNS	DNS	DNS	DNS	DNS	DNS	DNS	DNS	DNS	DNS	DNS	DNS	DNS	DNS	DNS	DNS	DNS	DNS	DNS	DNS	
Other Surface Water																					
NE7-09	DNS	DNS	DNS	DNS	DNS	DNS	DNS	DNS	DNS	DNS	DNS	DNS	DNS	DNS	DNS	DNS	DNS	DNS	DNS	DNS	y
McClelland-09	DNS	DNS	DNS	DNS	DNS	DNS	DNS	DNS	DNS	DNS	DNS	DNS	DNS	DNS	DNS	DNS	DNS	DNS	DNS	DNS	y
AthaR-09	DNS	DNS	DNS	DNS	DNS	DNS	DNS	DNS	DNS	DNS	DNS	DNS	DNS	DNS	DNS	DNS	DNS	DNS	DNS	DNS	y

APPENDIX 3: Detection limits and uncertainties for major ion and trace elements.

Parameter	Units	Minimum Detection Limit	+/-
Balance		0.01	NA
Cations	meq/L	0.01	NA
Anions	meq/L	0.01	NA
Conductivity	uS/cm	1	0.5
Solids, Total Dissolved (Calculated)	mg/L	0.001	NA
PH	units	N/A	0.07
Alkalinity, Total	mgCaCO3/L	1	0
Alkalinity, Partial	mgCaCO3/L	1	NA
Bicarbonate	mg/L	1	NA
Carbonate	mg/L	1	NA
Calcium	mg/L	0.4	0.21
Magnesium	mg/L	0.01	0.062
Hardness, Total	mgCaCO3/L	0.01	NA
Sodium	mg/L	1	0.3
Potassium	mg/L	0.4	0
Nitrate+Nitrite	mg/L	0.005	NA
Nitrite-N	mg/L	0.002	NA
Silica	mg/L	0.1	0.5
Chloride	mg/L	0.3	0.2
Sulfate	mg/L	3	3
Fluoride	mg/L	0.02	0.01
Iron	ug/L	2	0.4
Carbon, Diss Organic	mg/L	0.2	0.4
Nitrate-N Calculated	mg/L	0.005	NA
Aluminum	ug/L	0.2	0.34
Antimony	ug/L	0.0005	0.0022
Arsenic	ug/L	0.002	0.017
Barium	ug/L	0.4	0.35
Beryllium	ug/L	0.003	0.0027
Bismuth	ug/L	0.001	NA
Boron	ug/L	3	0.15
Cadmium	ug/L	0.002	0.0005
Chlorine	mg/L	10	0.016
Chromium	ug/L	0.03	0.014
Cobalt	ug/L	0.001	0.0018
Copper	ug/L	0.05	0.017
Lead	ug/L	0.001	NA
Lithium	ug/L	2	0.2
Manganese	ug/L	0.003	0.021
Mercury	ug/L	0.01	NA

Parameter	Units	Minimum Detection Limit	+/-
Molybdenum	ug/L	0.001	0.011
Nickel	ug/L	0.005	0.0066
Phosphorus	ug/L	0.8	NA
Potassium	mg/L	0.002	0.0037
Selenium	ug/L	0.04	0.03
Silicon	mg/L	0.01	0.012
Silver	ug/L	0.0005	NA
Sodium	mg/L	0.2	0.067
Strontium	ug/L	0.4	2.2
Sulfur	mg/L	20	0.11
Thallium	ug/L	0.0003	0.0006
Thorium	ug/L	0.0003	0.0008
Tin	ug/L	0.03	NA
Titanium	ug/L	0.04	0.04
Uranium	ug/L	0.0001	0.0044
Vanadium	ug/L	0.005	0.0047
Zinc	ug/L	0.05	0.01

APPENDIX 4: List of scanned organic compounds, with detection limits and uncertainties.

All compounds were undetected except as summarized in APPENDIX 2.

Compound Name	Detection Limit ug/L	+/- ug/L
Volatile Priority Pollutants		
1,1,1,2-Tetrachloroethane	0.1	0.1
1,1,2,2-Tetrachloroethane	0.1	0.1
1,1-Dichloroethane	0.1	0.1
1,1-Dichloropropylene	0.1	0.1
1,2,3-Trichloropropane	0.1	0.1
1,2,4-Trimethylbenzene	0.1	0.1
1,2-Dibromoethane	0.1	0.1
1,2-Dichloroethane	0.1	0.1
1,3,5-Trimethylbenzene	0.1	0.1
1,3-Dichloropropane	0.1	0.1
2,2-Dichloropropane	0.1	0.1
2-Chlorotoluene	0.1	0.1
Benzene	0.1	0.1
Bromodichloromethane	0.1	0.1
Bromomethane	0.1	0.1
Chlorobenzene	0.1	0.1
Chloroform	0.1	0.1
Dibromochloromethane	0.1	0.1
Ethyl benzene	0.1	0.1
Isopropylbenzene	0.1	0.1
Methylene chloride	2.0	0.1
Styrene	0.1	0.1
Tetrachloroethylene	0.3	0.1
Trichloroethylene	0.1	0.1
Vinyl chloride	0.5	0.1
cis-1,2-Dichloroethylene	0.1	0.1
m,p-Xylene	0.1	0.1
n-Propylbenzene	0.1	0.1
p-Isopropyltoluene	0.1	0.1
tert-Butylbenzene	0.1	0.1
trans-1,3-Dichloropropylene	0.3	0.1
1,1,1-Trichloroethane	0.1	0.1
1,1,2-Trichloroethane	0.1	0.1
1,1-Dichloroethylene	0.1	0.1
1,2,3-Trichlorobenzene	0.1	0.1
1,2,4-Trichlorobenzene	0.1	0.1
1,2-Dibromo-3-chloropropane	0.3	0.1
1,2-Dichlorobenzene	0.1	0.1
1,2-Dichloropropane	0.1	0.1

Compound Name	Detection Limit ug/L	+/- ug/L
Volatile Priority Pollutants		
1,3-Dichlorobenzene	0.1	0.1
1,4-Dichlorobenzene	0.1	0.1
2-Chloroethoxyethylene	0.4	0.1
4-Chlorotoluene	0.1	0.1
Bromobenzene	0.1	0.1
Bromoform	0.5	0.1
Carbon tetrachloride	0.1	0.1
Chloroethane	0.1	0.1
Chloromethane	0.5	0.1
Dibromomethane	0.1	0.1
Hexachlorobutadiene	0.3	0.1
MTBE	0.1	0.1
Naphthalene	0.1	0.1
TRIHALOMETHANES	0.1	0.1
Toluene	0.1	0.1
Trichlorofluoromethane	0.1	0.1
XYLENES	0.1	0.1
cis-1,3-Dichloropropylene	0.3	0.1
n-Butylbenzene	0.1	0.1
o-Xylene	0.1	0.1
sec-Butylbenzene	0.1	0.1
trans-1,2-Dichloroethylene	0.1	0.1
Unresolved Hydrocarbons	NA	NA
Extractable Priority Pollutants		
1,2,4-Trichlorobenzene	0.1	0.1
2,3,4,6-Tetrachlorophenol	0.1	0.2
2,4-Dichlorophenol	0.1	0.2
2,4-Dinitrophenol	0.1	0.2
2,6-Dinitrotoluene	0.1	0.1
2-Chlorophenol	0.2	0.2
2-Nitrophenol	0.1	0.2
4-Chloro-3-methylphenol	0.1	0.2
4-Nitrophenol	0.1	0.2
Acenaphthylene	0.1	0.1
Benzidine	0.2	0.2
Benzo(a)pyrene	0.1	0.2
Benzo(ghi)perylene	0.2	0.1
Bis(2-chloroethoxy)methane	0.1	0.1
Bis(2-chloroisopropyl)ether	0.1	0.1
Butylbenzylphthalate	0.1	0.1
Di-n-butylphthalate	0.1	0.1
Dibenzo(ah)anthracene	0.5	0.1

Compound Name	Detection Limit ug/L	+/- ug/L
Volatile Priority Pollutants		
Dimethyl phthalate	0.1	0.1
Fluorene	0.1	0.1
Hexachlorobutadiene	0.5	0.1
Hexachloroethane	0.5	0.1
Isophorone	0.1	0.1
N-Nitrosodiphenylamine	0.1	0.1
Nitrobenzene	0.1	0.1
Phenanthrene	0.1	0.1
Pyrene	0.1	0.1
1,2-Diphenylhydrazine	0.1	0.1
2,4,6-Trichlorophenol	0.1	0.2
2,4-Dimethylphenol	0.2	0.2
2,4-Dinitrotoluene	0.1	0.1
2-Chloronaphthalene	0.1	0.1
2-Methyl-4,6-dinitrophenol	0.1	0.2
4-Bromophenyl phenyl ether	0.1	0.1
4-Chlorophenyl phenyl ether	0.1	0.1
Acenaphthene	0.1	0.1
Anthracene	0.1	0.1
Benzo(a)anthracene	0.1	0.1
Benzo(b)fluoranthene	0.1	0.1
Benzo(k)fluoranthene	0.1	0.1
Bis(2-chloroethyl)ether	0.1	0.1
Bis(2-ethylhexyl)phthalate	0.1	0.1
Chrysene	0.1	0.1
Di-n-octyl phthalate	0.1	0.1
Diethyl phthalate	0.1	0.1
Fluoranthene	0.1	0.1
Hexachlorobenzene	0.1	0.1
Hexachlorocyclopentadiene	0.1	0.1
Indeno(1,2,3-cd)pyrene	0.1	0.1
N-Nitroso-di-n-propylamine	0.2	0.1
Naphthalene	0.1	0.1
Pentachlorophenol	0.1	0.2
Phenol	0.1	0.2
Unresolved Hydrocarbons (C12-C36)	NA	NA
Naphthenic Acids		
Naphthenic Acids	0.2	3.0

APPENDIX 5. Notes on FT-ICR-MS protocol for analysis used for oil sands fingerprinting at University of Victoria proteomics laboratory.

Protocol 1: direct infusion (DI) – FTICR MS of water samples without organic solvent liquid-liquid extraction

- 1 mL of each water sample was mixed with 2 mL of acetonitrile, vortexed and then centrifuged at 2,500 x g for 10 min. 1 mL of the supernatant was carefully pipetted out and spiked with 4 μL of Agilent 'ES tuning mix" standard solution as the mass references for internal calibration during and post data acquisitions.
- This solution was then made into 0.2% formic acid and directly infused into a Bruker apex-Qe 12-Tesla hybrid quadrupole-Fourier transform ion cyclotron resonance mass spectrometry (FTICR MS) instrument through an atmospheric pressure nebulizing-assisted electrospray ionization source.
- Within a mass range of 200 to 1200 Th, data were acquired from an accumulation of 500 scans per spectrum with an FT transient size of 1024 kilobytes per second.

APPENDIX 6: FT-ICR-MS results for selected samples, including Kendrick plots and statistical analysis of slope patterns in Kendrick plots.

SO1A

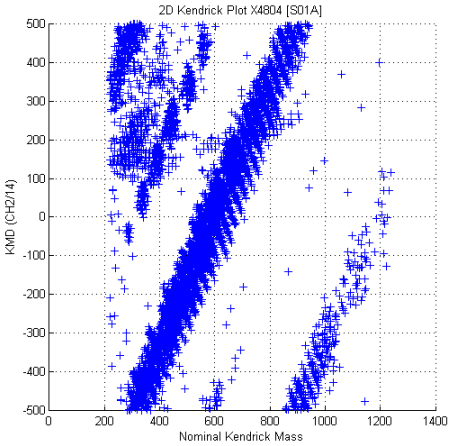

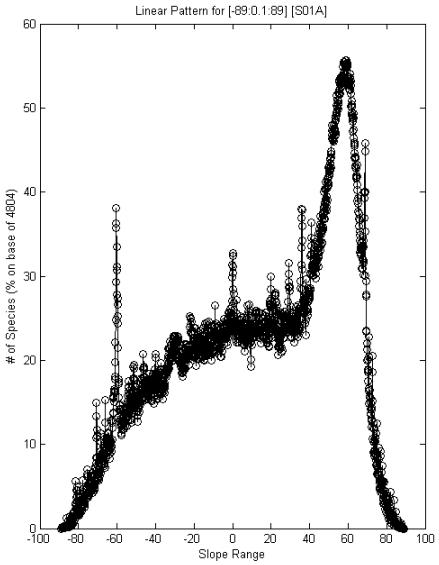

S01N

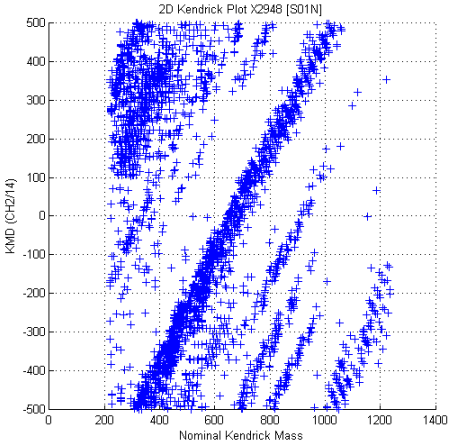

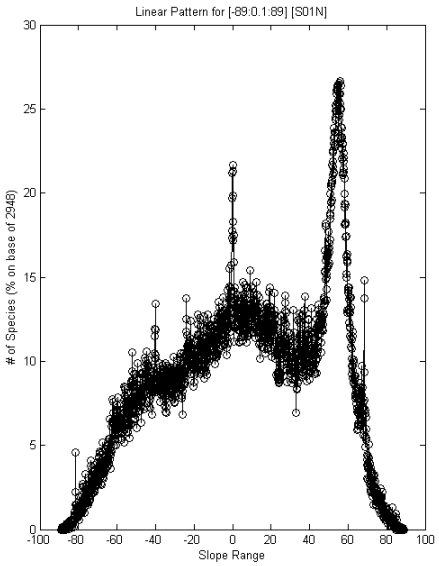

S02A

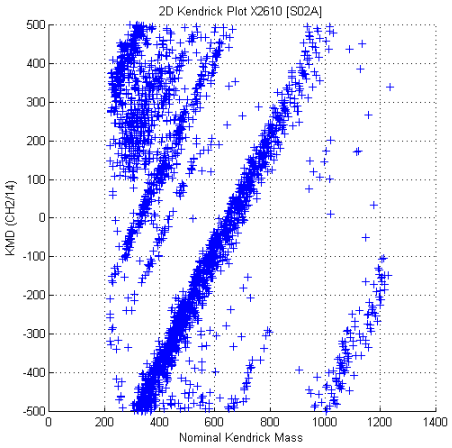
2D Kendrick Plot X2610 [S02A]
KMD (CH2/14)
Nominal Kendrick Mass

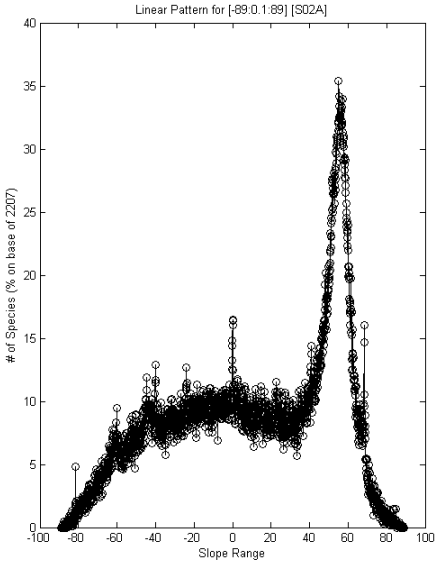
Linear Pattern for [-89:0.1:89] [S02A]
# of Species (% on base of 2207)
Slope Range

S02N

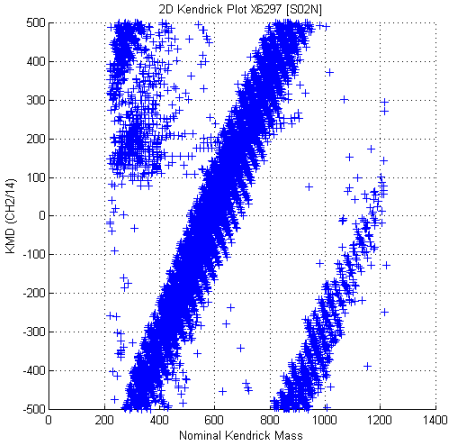
2D Kendrick Plot X6297 [S02N]
KMD (CH2/14)
Nominal Kendrick Mass

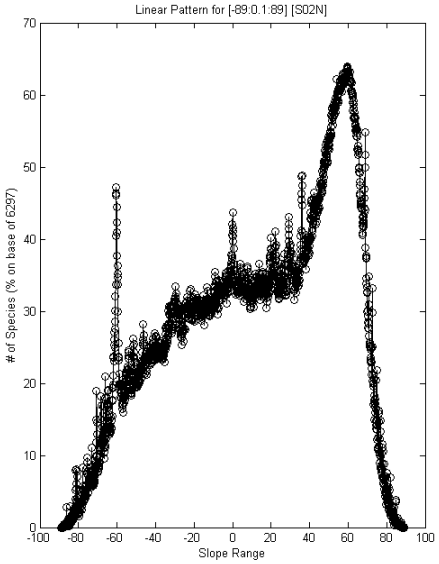
Linear Pattern for [-89:0.1:89] [S02N]
# of Species (% on base of 6297)
Slope Range

S07A

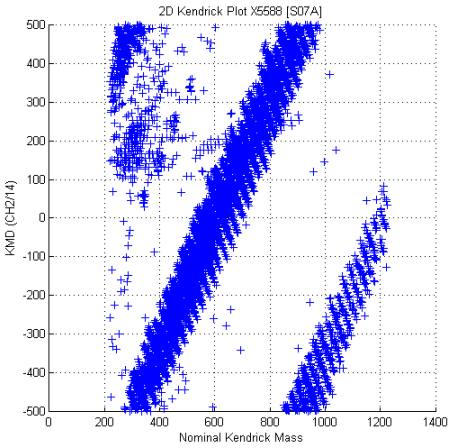
2D Kendrick Plot X5588 [S07A]
KMD (CH2/14)
Nominal Kendrick Mass

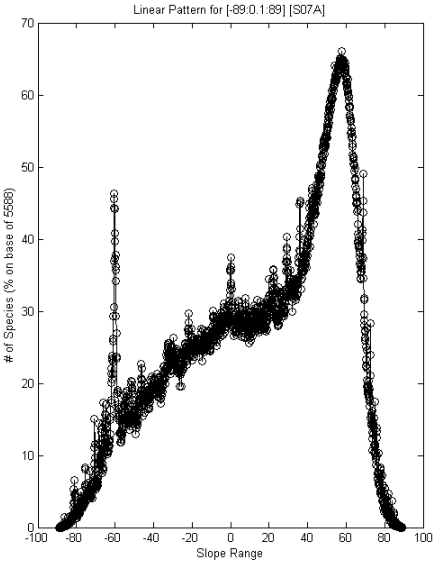
Linear Pattern for [-89:0.1:89] [S07A]
# of Species (% on base of 5588)
Slope Range

S08A

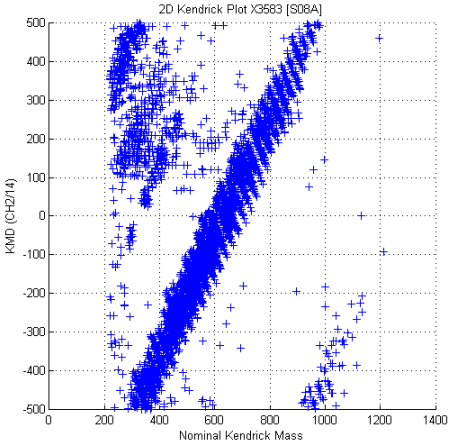
2D Kendrick Plot X3583 [S08A]
KMD (CH2/14)
Nominal Kendrick Mass

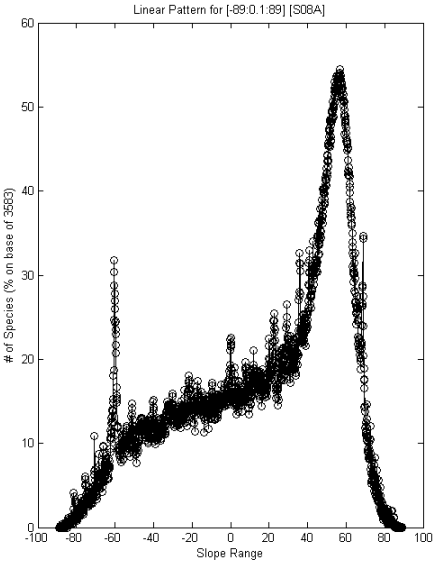
Linear Pattern for [-89:0.1:89] [S08A]
# of Species (% on base of 3583)
Slope Range

S09A

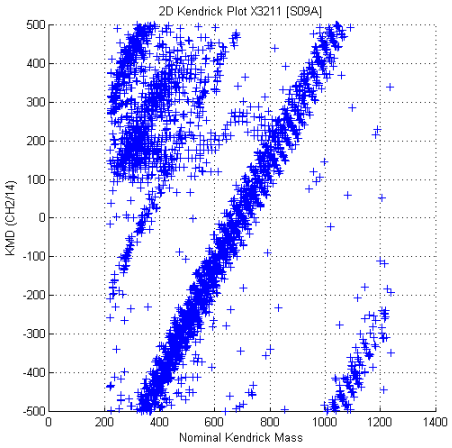
2D Kendrick Plot X3211 [S09A]
KMD (CH2/14)
Nominal Kendrick Mass

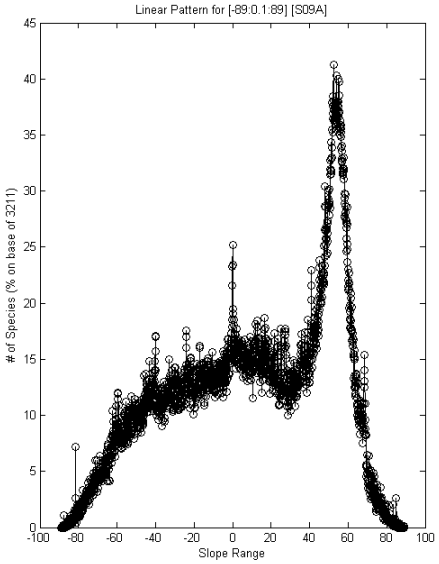
Linear Pattern for [-89:0.1:89] [S09A]
# of Species (% on base of 3211)
Slope Range

S10A

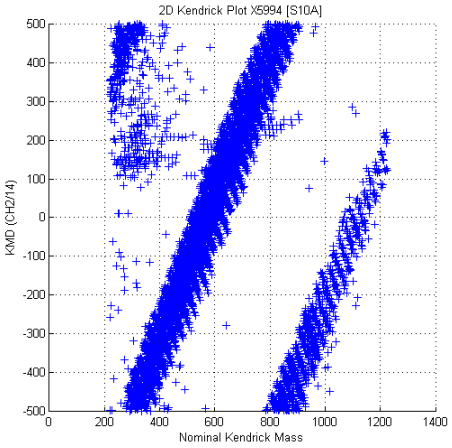
2D Kendrick Plot X5994 [S10A]
KMD (CH2/14)
Nominal Kendrick Mass

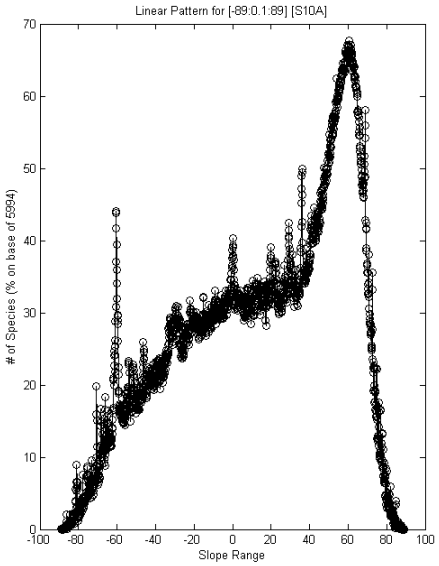
Linear Pattern for [-89:0.1:89] [S10A]
# of Species (% on base of 5994)
Slope Range

PAW001

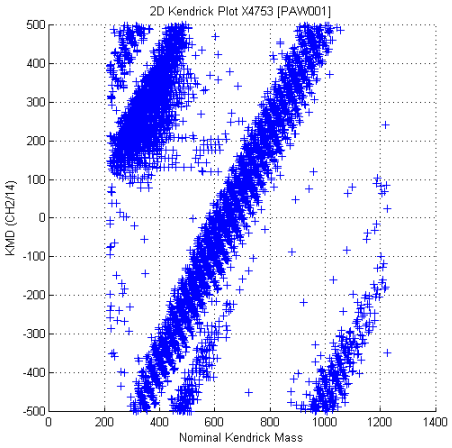

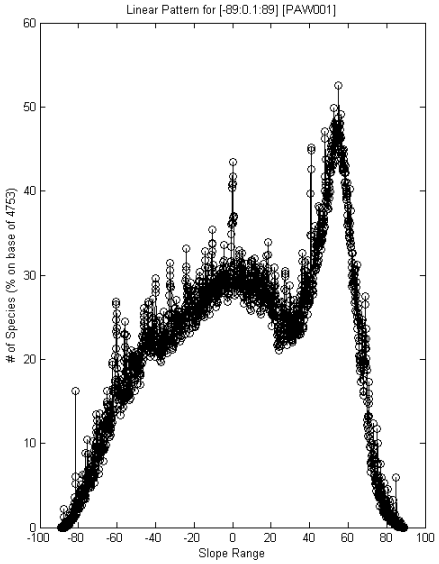

PAW002

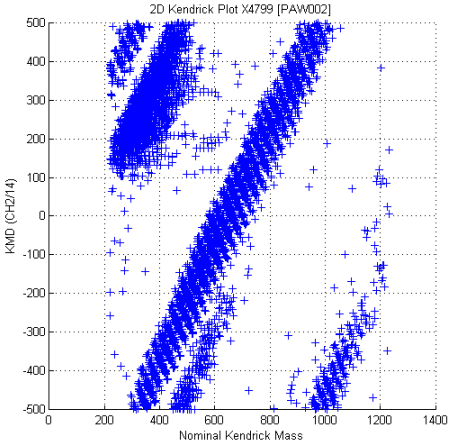

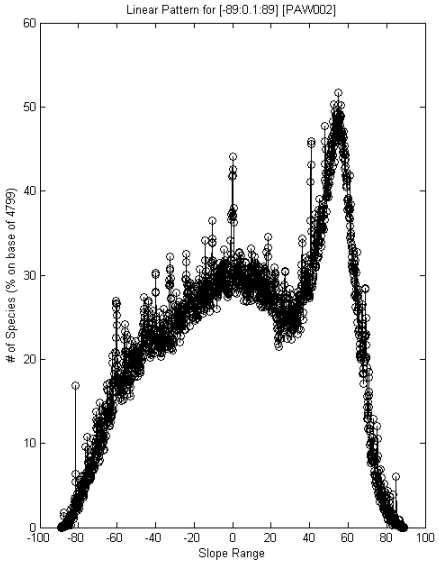

PAW003

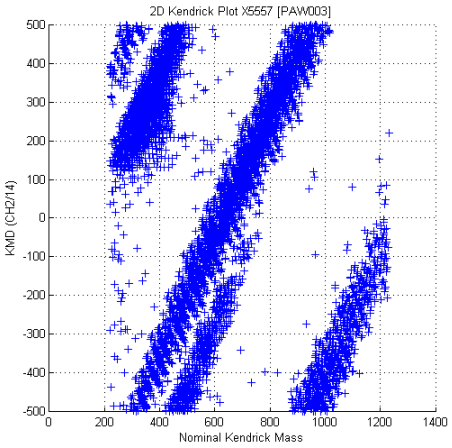

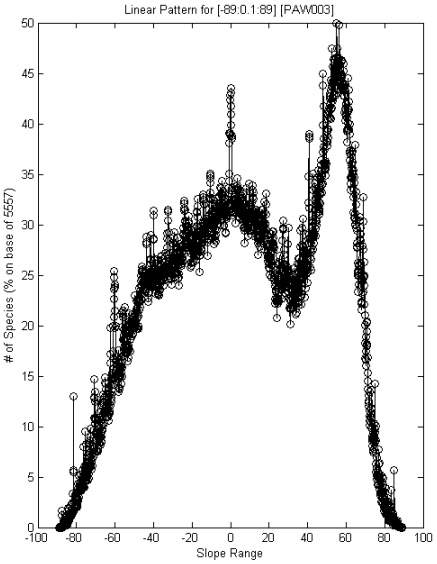

PAW004

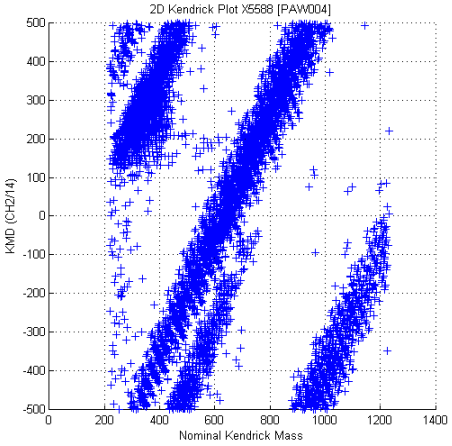

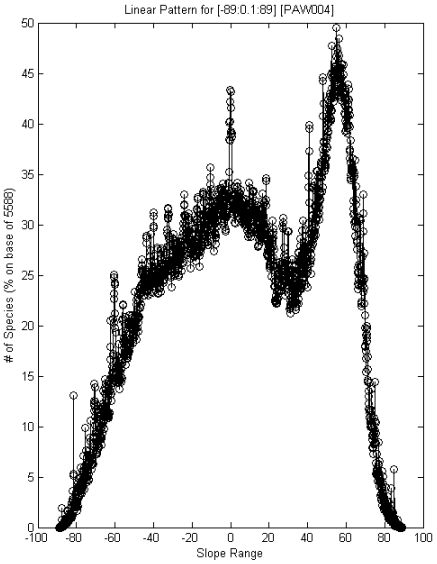

PAW006

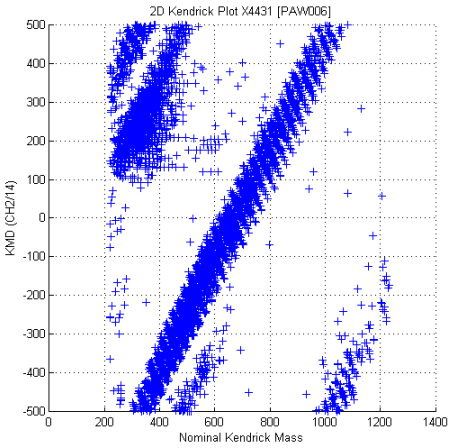

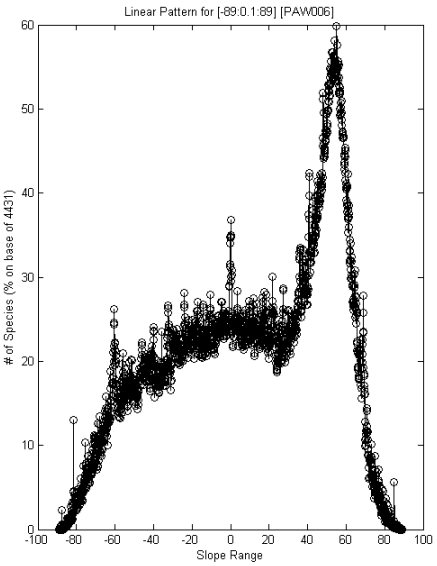

PAW007

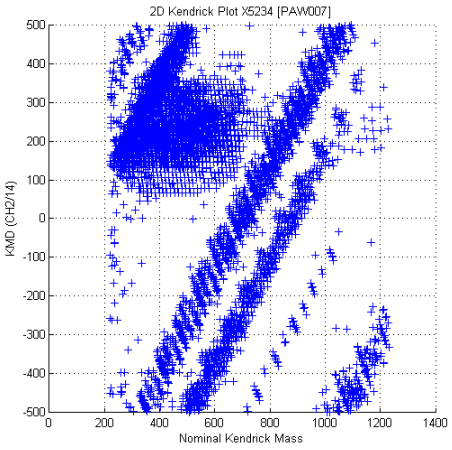

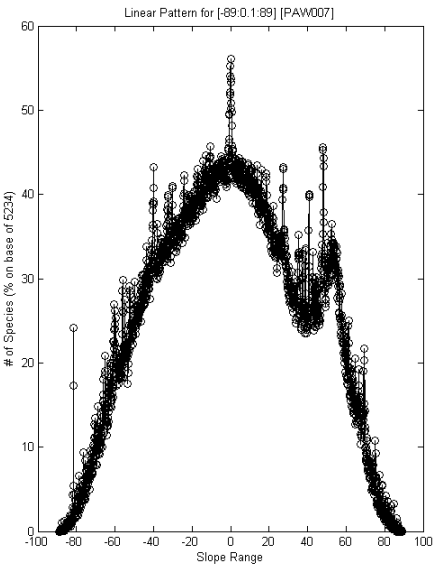

PAW008

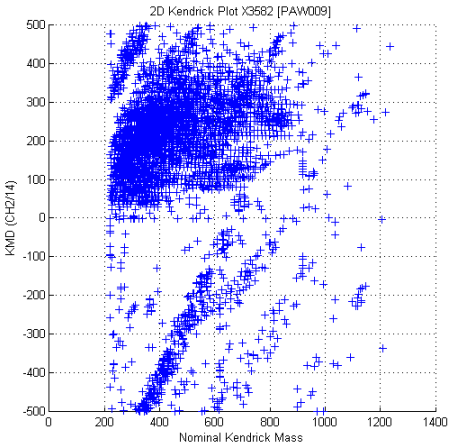

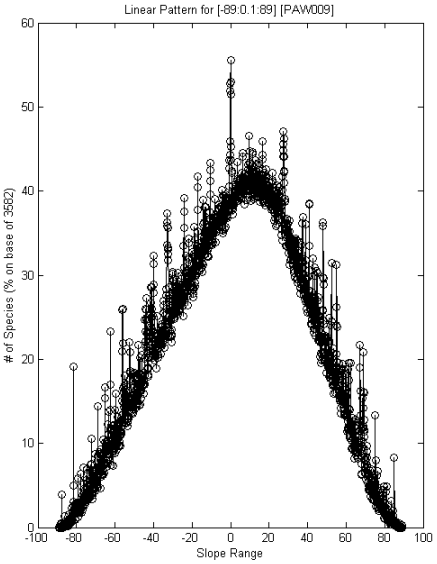

PAW009

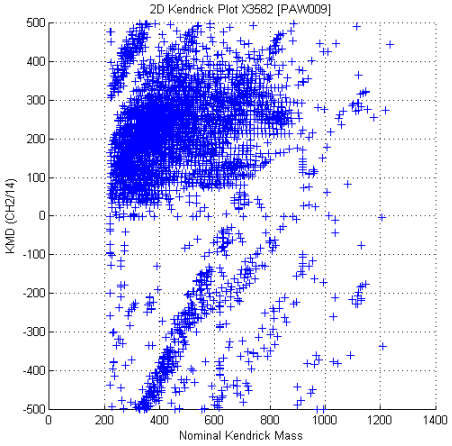

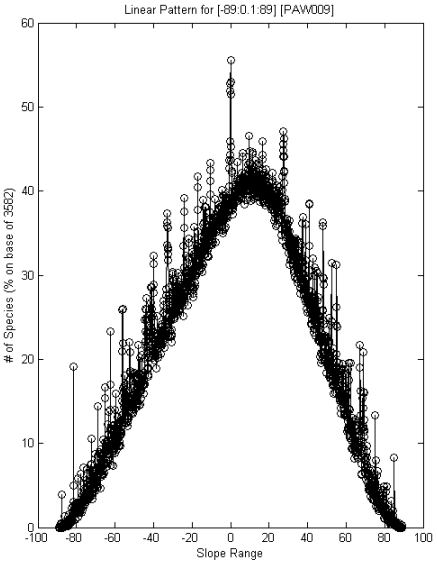

PAW N

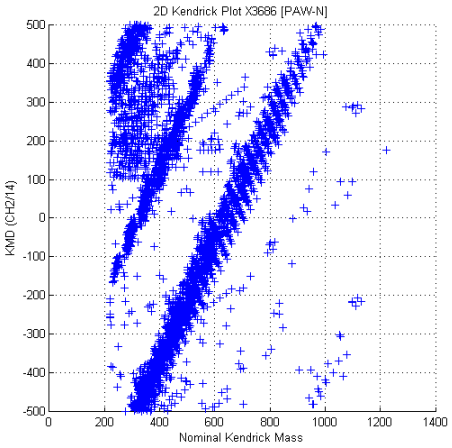
2D Kendrick Plot X3686 [PAW-N]
KMD (CH2/14)
Nominal Kendrick Mass

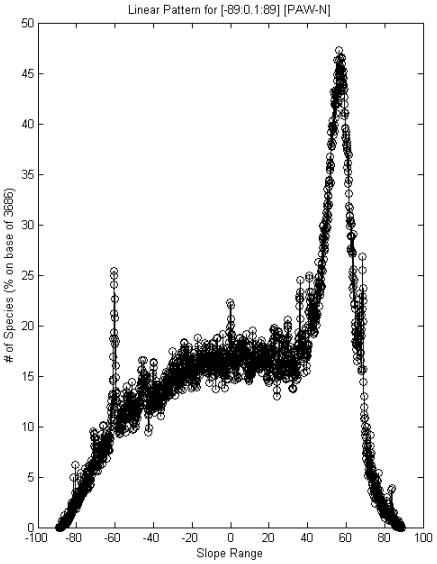
Linear Pattern for [-89:0.1:89] [PAW-N]
# of Species (% on base of 3686)
Slope Range

PAW S

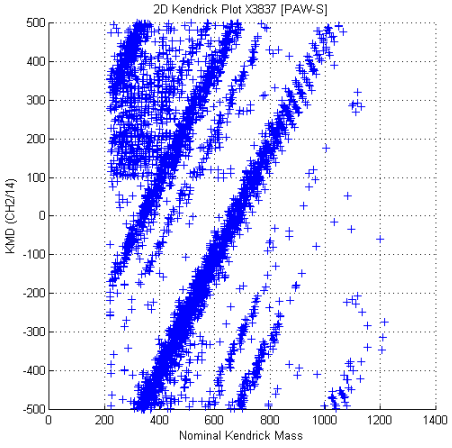
2D Kendrick Plot X3837 [PAW-S]
KMD (CH2/14)
Nominal Kendrick Mass

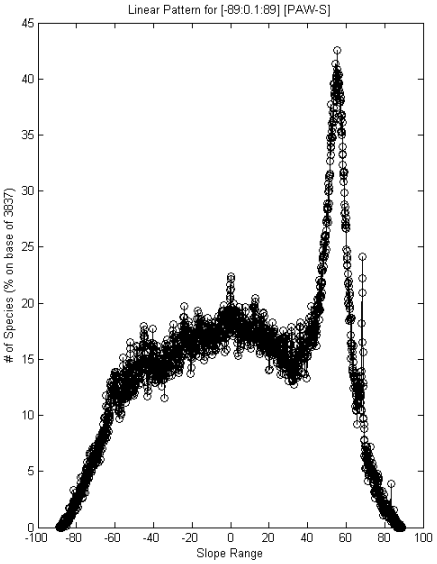
Linear Pattern for [-89:0.1:89] [PAW-S]
# of Species (% on base of 3837)
Slope Range

BAS 25

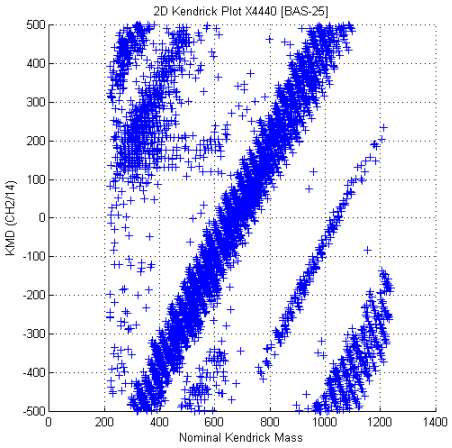
2D Kendrick Plot X4440 [BAS-25]
KMD (CH2/14)
Nominal Kendrick Mass

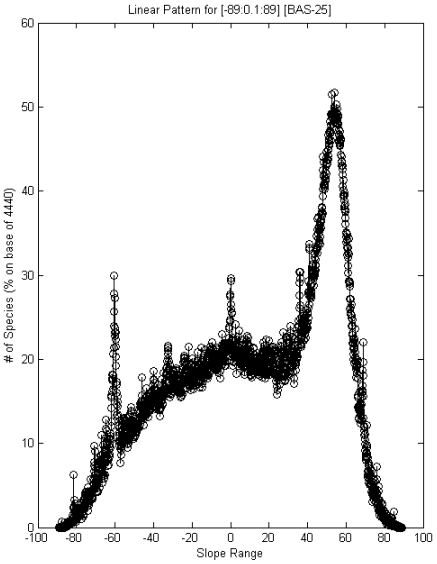
Linear Pattern for [-89:0.1:89] [BAS-25]
# of Species (% on base of 4440)
Slope Range

BAS 26

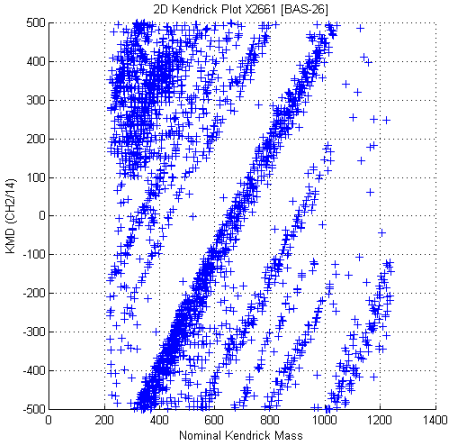
2D Kendrick Plot X2661 [BAS-26]
KMD (CH2/14)
Nominal Kendrick Mass

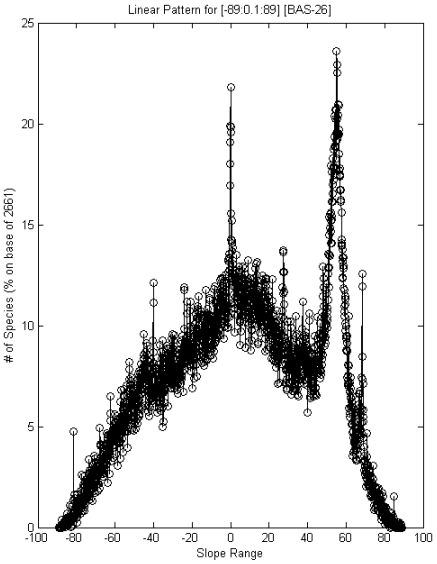
Linear Pattern for [-89:0.1:89] [BAS-26]
# of Species (% on base of 2661)
Slope Range

CRW1

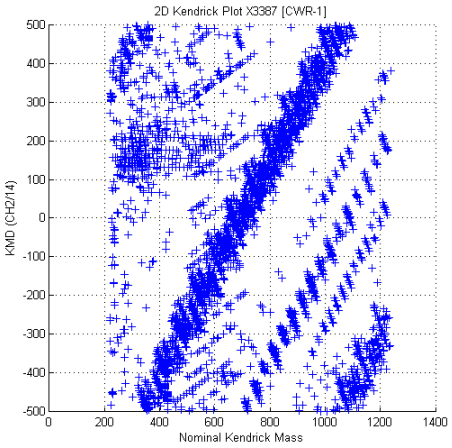
2D Kendrick Plot X3387 [CWR-1]
KMD (CH2/14)
Nominal Kendrick Mass

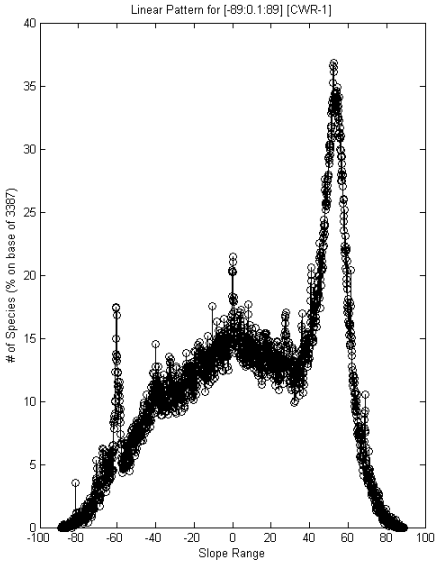
Linear Pattern for [-89:0.1:89] [CWR-1]
# of Species (% on base of 3387)
Slope Range

SS19

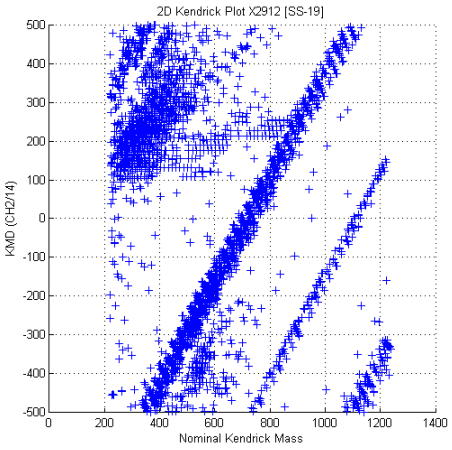
2D Kendrick Plot X2912 [SS-19]
KMD (CH2/14)
Nominal Kendrick Mass

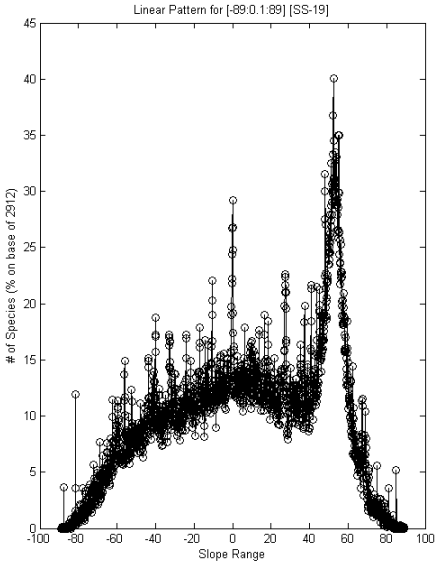
Linear Pattern for [-89:0.1:89] [SS-19]
# of Species (% on base of 2912)
Slope Range